Understanding and Estimating Travel Times of Overland Flows on Planes

by

Manoj KC

A dissertation submitted to the Graduate Faculty of
Auburn University
in partial fulfillment of the
requirements for the Degree of
Doctor of Philosophy

Auburn, Alabama
May 04, 2014

Keywords: Time of Concentration, Travel Time, Overland Flow Modeling, Impervious Surface, Particle Tracking

Approved by

Xing Fang, Chair, Professor of Civil Engineering
T. Prabhakar Clement, Professor of Civil Engineering
Jose G. Vasconcelos, Assistant Professor of Civil Engineering
Jeyhoon (Jay) M. Khodadadi, Professor of Mechanical Engineering

Abstract

Estimating travel time of overland flow is one of the important studies in hydrology. A quasi-two-dimensional overland flow model (OFM) with the options of dynamic, diffusion, and kinematic wave approximation integrated with particle tracking model and rainfall loss models for both impervious and pervious surfaces (planes) was developed to study flow travel times. There are many formulas for estimating time of concentration (T_c) of overland flows, but these formulas predict large unrealistic T_c as the topographic slope (S_o) approaches zero. Based on numerical modeling and a review of relevant literature, a lower bound for slope (S_{lb}) of 0.1% was identified as a threshold below which traditional T_c estimation formulas become unreliable. The rainfall-runoff data collected in a relatively low slope field were used for model validation. The validated model was used to generate 750 T_c data using diverse combinations of the four physically based input variables: length (L), slope, roughness coefficient (n) of the surfaces, and effective rainfall intensity (i). The dataset of 750 T_c for a range of slopes was used to develop T_c regression formulas for standard slopes ($S_o \geq 0.1\%$) and low slopes ($S_o < 0.1\%$).

The OFM was also used for numerical study of travel times of overland flow using particle tracking model. Although T_c is commonly defined as the time for the runoff to travel to the outlet from the most remote part of the catchment, most researchers have used an indirect method such as hydrograph analysis to estimate T_c. Travel times for 85%, 95% and 100% of particles arrival at the outlet of impervious surfaces (i.e., T_{t85},

T_{t95}, and T_{t100}) were calculated from 530 model runs directly tracking both slow and fast moving particles on the flow plane. Regression equations of T_{t85}, T_{t95}, and T_{t100} were developed using the four physically based input variables (L, S_o, n, and i).

Stormwater with velocity equal or close to equilibrium velocity (V_{eq}) can cause more soil erosion on pervious surfaces and transport significant amounts of dissolved and particulate materials on impervious surfaces to downstream receiving waters. The diffusion wave approximation of OFM was used to simulate V_{eq} of impervious overland flows using diverse combinations of the four physically based input variables. A dataset of 530 V_{eq} estimates was developed and the relation between V_{eq} and input variables was developed.

Acknowledgements

I would like to express my deepest sense of gratitude to my academic advisor, Dr. Xing Fang, for his valuable guidance, support and encouragement throughout the work. He is an excellent professional researcher as well a very good human being and he will always remain as an inspiration to me throughout my life.

I am also equally thankful to my committee members; Dr. T. Prabhakar Clement, Dr. Jose G. Vasconcelos and Dr. Jay Khodadadi for their valuable time to review my proposal and dissertation, their encouragements, insights and suggestions that have helped to improve the research. I am also thankful to Dr. Yanzhao Cao for being my dissertation reader to review my dissertation.

I am grateful to Dr. Young-Jae Yi and Dr. Ming-Han Li of Texas A&M University for their data collection. I am grateful to Dr. Theodore G. Cleveland of the Texas Tech University and Dr. David B. Thompson of R. O. Anderson Engineering, Inc. for their support and input to the study. I am thankful to Dr. A. Ben-Zvi of Israel Hydrological Service and Dr. C. Mugler of Climate and Environment Sciences Laboratory, France for their data inputs to the study. I am also thankful to anonymous reviewers for their valuable comments for journal papers that are presented in Chapters two to four.

The financial supports of Department of Civil Engineering at Auburn University and Texas Department of Transportation (TxDOT) are gratefully acknowledged. The project advising members at TxDOT Research Project 0–6382 are also acknowledged for

their guidance and support for the experimental field study in Texas. This study was partially supported by TxDOT Research Projects 0–6382 and partially by Auburn University Teaching Assistantship.

I am also thankful to my colleagues Dr. Nirajan Dhakal, Janesh Devkota, Dr. Shoeb Alam, Gang Chen, Liping Jiang and Thomas Hatcher for the help during my study in Auburn. Finally, I am thankful to my parents for their continuous love, support and sacrifice.

Table of Contents

List of Tables

List of Figures

List of Abbreviations

ASCE	American Society of Civil Engineers
DEM	Digital Elevation Model
DHM	Diffusion Hydrodynamic Model
DWM	Diffusion Wave Model
DWMPT	Diffusion Wave Model with Particle Tracking
FRAC	Fractional Loss Model
GAIL	Green-Ampt Infiltration Loss Model
GIS	Geographic Information System
HEC	Hydrologic Engineering Center
HMS	Hydrologic Modeling System
HSJ	Hydrological Sciences Journal
NRCS	Natural Resources Conservation Service
OFM	Overland Flow Model
PTM	Particle Tracking Model
Q2DWM	Quasi 2D Dynamic Wave Model
SGAIL	Simplified Green-Ampt Infiltration Loss Model
SWMM	Storm Water Management Model
TFO	Taylor & Francis Online
TxDOT	Texas Department of Transportation

USEPA	United States Environmental Protection Agency
USGS	U.S. Geological Survey

Chapter 1 Introduction

1.1 Background

Each year, billions of dollars are spent on new construction on highway related drainage structures (e.g., culverts, drainage channels, bridges, detention and retention basins) based on design discharges from hydrologic analysis and modeling. Traditional hydrologic methods used for design such as the modified rational method, unit hydrographs, as well as modeling tools such as HEC-HMS (USACE 2000), NRCS TR-55 (NRCS 1986), EPA-SWMM (Huber et al. 1988), etc. rely on an estimate of the time response characteristics of the watershed or time of concentration . McCuen et al. (1984) stated that almost all hydrologic analyses require the value of a time response characteristics as input, and time of concentration (T_c) is the most commonly used. The concept was first presented by Mulvany (1851) as the time at which discharge is the highest for a uniform rate of rainfall as the runoff from every portion of the catchment arrives at the outlet and similarly defined by Kuichling (1889b). Figure 1.1 shows the conceptual representation of T_c for overland flow with the four physically based input variables: length (L), slope (S_o), Manning's roughness coefficient (n) of the surfaces, and effective rainfall intensity (i) that are responsible for the effect on T_c. Bondelid et al. (1982) demonstrated that as much as 75% of the total error in an estimate of the peak discharge can result from errors in the T_c estimation.

Recognizing its importance, a number of empirical formulas (Kirpich 1940;

Kerby 1959; Graf et al. 1982; Thomas et al. 2000) were developed to estimate T_c, but the applicability of any particular formula for general use is constrained by lack of diversity in the data used to develop the formula (McCuen et al. 1984). Therefore, the empirical estimation method should be used with considerable caution for watersheds different from those used for development and calibration of the method. This cautionary warning implies analyst knowledge of development of the method used. Sheridan (1994) indicated that after more than a century of development and evolution in hydrologic design concepts and procedures, the end-user is still constrained by confusing choices of empirical relationship for estimating T_c for ungaged watersheds.

Moreover this uncertainty increases as the topographic slope (S_o) of the overland flow decreases. It should be acknowledged that energy slope and not topographic slope control flow in a flat or zero slopes, however physical measurement of energy slope is difficult. T_c is inversely proportional to the topographic slope in most of these empirical equations. As S_o approaches zero in regions such as in the coastal plains of the southeastern U.S., the resulting prediction of T_c is unreasonably larger than expected estimate.

The effect of the topographic slope on the runoff generation is illustrated in Fig. 1.2. The equilibrium S-hydrographs are generated using the diffusion wave model DWM (KC and Fang 2014) for different topographic slopes for L = 305 m (1000 ft), n = 0.02, and i = 88.9 mm/hr (3.5 in/hr). T_c derived from simulated S-hydrograph increases from 6.9 to 48.6 minutes as S_o decreases from 10% to 0.05%. T_c estimated using formula from Morgali and Linsley (1965) is 8.1 and 61.9 minutes for S_o = 10% and 0.05%, respectively. The error of estimated T_c increases as the slope decreases. Hence,

underestimation of peak discharge in both impervious and pervious surfaces may occur in the hydrological design due to use of unreasonably longer estimates of T_c for a low slope. A design based on under-estimated discharge is more prone to failure by hydraulic overloading. However, over-estimation using arbitrary T_c values is also possible, leading to costly over-design. Therefore, appropriate estimation of T_c for low-slope terrains is necessary and will increase the confidence in design discharges for those regions. This will assist in better designs and corresponding costs, efficient use of resources, and appropriate structure sizes for the required level of risk.

However, the development of method for estimating T_c for low-slope planes requires identification of a threshold below which slope can be defined as "low." Such a boundary, S_{lb}, represents a threshold below which traditional relations become unreliable and the hydraulic behavior deviates from the assumptions (Morgali and Linsley 1965) used in the development of the relations. In this study, a slope S_o less than S_{lb} is referred as low slope for which alternate methods for T_c estimation should be considered. The slope S_o greater than S_{lb} is referred as non-low slope (or standard slope) where current traditional T_c estimation formulas are appropriate.

Another complication in T_c study is lack of universally accepted definition and method to quantify it. Several definitions of T_c can be found in the literature along with several related estimation methods for each definition (McCuen 2009). Grimaldi et al. (2012), using their case studies, have demonstrated that available approaches for the estimation of T_c may yield numerical predictions that differ from each other by up to 500%. Even though T_c is commonly defined as the time it takes runoff to travel from the most distant point along a hydraulic pathway in the watershed to the outlet, many

researchers have used the indirect method such as hydrograph analysis to estimate T_c instead of measuring or determining travel time for particles to reach the outlet. Hence, a direct approach of determining travel time of both fast and slow moving particles to reach the outlet of impervious surfaces would assist designer to better estimate travel times on ungaged catchments and watersheds.

1.2 Research Objectives

The specific objectives of the research are:

1. Extension of research database for low-slope study, either by collection of existing data from various smaller watersheds, or by field data collection of hydrologic responses of low-slope watersheds in selected locations in Texas, to provide a research database to investigate hydrologic behavior on different slopes. The database may be analyzed in a variety of fashions by the researchers; if generic modeling is determined to be useful such a database should be used to support model results. Development of hydrodynamic wave model for overland flow with appropriate rainfall loss models for impervious and pervious surfaces is required. Identification, from literature and numerical modeling, an effective lower bound of the topographic slope at which the traditional hydrologic timing relationships become unreliable. And finally identification, suggestion, and development of alternate methods for T_c estimation in low-slope regions.
2. Use of particle tracking based on numerical modeling study for the determination of hydrologic timing response of watershed including on impervious surface and thus development of direct estimating equation for determining travel time of both

fast and slow moving particles to reach the outlet of impervious surfaces.

3. Development of direct estimation equation for equilibrium velocity (V_{eq}) and time to equilibrium velocity (T_{veq}) for the overland flow on an impervious surface under specific rainfall event based on physically based input parameters using numerical modeling study. The equilibrium velocity is defined as the maximum velocity attained under a constant effective rainfall over an impervious plane.

The focus of proposed study deals with travel time of runoff generated from a rainfall event. The first objective is related to the Texas Department of Transportation (TxDOT) Research Project 0–6382 "Establish effective lower bounds of watershed slope for traditional hydrologic methods" funded by the TxDOT through a sub-contract from Texas Tech University. The project was in cooperation with Dr. Theodore G. Cleveland at Texas Tech University, Dr. William A. Asquith at USGS Texas Water Science Center, Dr. Ming-Han Li at Texas A&M University, and Dr. David B. Thompson at R.O. Anderson Engineering, Inc. The study on travel time of runoff, especially T_c, has been investigated by many researchers over many years. The focus of proposed research is for low-slope planes of overland flow when current and traditional formulas of T_c in current textbooks and journal publications do not work well and produce unreasonably large estimation on T_c.

1.3 Methodology

1.3.1 Collection of Rainfall-Runoff Data for Impervious Surface from Published Sources

One of the first objectives of this project is the extension of research database for

non-low and low-slope study, either by collection of existing data from various smaller watersheds, not necessarily in Texas or by field data collection of hydrologic responses of low-slope watersheds in selected locations in Texas, to provide a research database to investigate hydrologic behavior on different slopes. Hence, several published data from Izzard (1946), Yu and McNown (1964), Emmett (1970a), Chow (1967), Ben-zvi (1984) and Mügler et al. (2011) were collected from literature for the project. Most of these studies were conducted on laboratory and small-scale field studies to investigate travel time and runoff characteristics of overland flow of non-low slope and few were conducted for relatively-low slope. The details of the studies and data used for validation are given in Chapters two to four.

1.3.2 Collection of Rainfall-Runoff Data for Low-Slope Study on Impervious Surface from Field Study

I also used field data collected by Dr. Ming-Han Li and his student at Texas A&M University, who cooperatively worked on TxDOT Research Project 0–6382, to examine hydrologic responses of low-slope overland flow planes. Since there were very few studies done on the low-slope, researchers at Texas A&M University (Dr. Ming-Han Li and his student, Dr. Young-Jae Yi) conducted the field study on a concrete surfaced watershed with slope of 0.25% to extend research database for relatively low-slope watersheds. Researchers at Texas A&M University instrumented a concrete plot to record rainfall and runoff. The plot is located at the Texas A&M University Riverside campus on an abandoned airstrip taxiway (Fig. 2.1A). The plot is surrounded by soil berms of 178 mm (7 in) tall to form a watershed boundary. Figure 2.1A is an image of

the concrete plot looking upslope along the greater diagonal. The details of the field study are given in Chapter two.

1.3.3 Collection of Rainfall-Runoff Data for Low-Slope Study on Pervious Surface from Indoor Laboratory Study

Researchers at Texas A&M University (Dr. Ming-Han Li and his student, Dr. Young-Jae Yi) instrumented an indoor plot on clay surface to investigate travel time and runoff characteristics of overland flow on pervious surface. This task also falls under the Objective 1 of the project to extend research database for low-slope study by field data collection of hydrologic responses of low-slope watersheds in selected locations in Texas, to provide a research database to investigate hydrologic behavior on different slopes. The indoor tests data consists of discharge rate and surface runoff depth under varying rainfall intensity and slope. The tests were conducted on a steel-framed bed of 6 ft wide, 30 ft long and 14 in deep (Fig. 1.4). The test bed was filled with clay and compacted with a lawn roller and left outdoors for over a month for natural compaction. The experiment was conducted using a rainfall simulator with a maximum capacity up to 4.5 in./hr. The tests used two samplers equipped with bubbler flow modules to collect discharge depths and surface runoff depths (near outlet) with 0.001 ft resolution every minute. The discharge flow depth was measured with a 22.5º V-notch weir box. The equipment setting can be seen in Fig. 1.4. The rainfall intensity was monitored using an inline flow meter connected to the rainfall simulator. The tipping bucket rain gauge was also used to double check the rainfall depth. The rainfall was stopped about 10 minutes after the peak discharge was attained and the discharge measurement was done until the

runoff ceased. The slope of test bed ranges from 0.02% to 1.04%. The control of the slope of overland flow was done by raising or lowering of the steel-framed bed. However the control of test bed was challenging due to sagging of the bed and difficulty of surface leveling on clay surface. Therefore, the slope was controlled based on the steel frame and the sagging was minimized by using steel blocks or jacks underneath the test bed. The slope of the bed was surveyed at eight grid points on the steel frame.

During the study period, 30 rainfall events were recorded at the experimental watershed, with 6 events for each slope. The numerical modeling study using the data collected through these indoor test experiments is a logical extension of the current study and will be published in the near future.

1.3.4 Development of Overland Flow Model

An Overland Flow Model (OFM) integrated with Particle Tracking Model (PTM), impervious rainfall loss (Fractional Loss Model) and pervious rainfall loss model (Green-Ampt Infiltration Loss Model) and Time of Concentration Model in Fortran Programming language was developed. The OFM is an extension of a previous model, DHM by Hromadka and Yen (1986). The OFM solves the momentum and continuity equations for overland flows (Akan and Yen 1984). The flowchart algorithm of the OFM code is given in Fig 1.4. The main routine in OFM code has the option of running either dynamic wave model, diffusion wave model or kinematic wave model. When the dynamic wave approximation of momentum equation is used, the model becomes a quasi-2D dynamic wave model (Q2DWM) used for the study in Chapter two. The details of the governing equations and modifications to original DHM are given in

Chapter two. When the diffusion wave approximation of momentum equation is used, the model becomes a diffusion wave model (DWM) which is used for numerical modeling in Chapters three and four. DWM integrated with Particle Tracking Model (DWMPT) that is used and explained in detail in Chapter three.

First, the model uses respective rainfall loss models based on the user input whether the surface is impervious or pervious. The description of each rainfall loss models are given in subsequent sections. After the effective rainfall depth is calculated using appropriate rainfall loss model, the code chooses either dynamic or diffusion or kinematic wave approximation as specified by the user. Chapter two uses dynamic wave approximation while Chapters three and four applies diffusion wave approximation in this study. After that the code calculates velocity and flow depth by numerically solving flow equations and checks the stability criteria by using Courant condition (Courant et al. 1967), the details of which is presented in Chapter two. Next the code checks if there is outflow at the outlet and then outputs outflow by user specified outflow boundary condition if there is any. If the particle tracking model is turned on, the code tracks the particles and outputs appropriate results. The code marches forward from one time step to another up to the user specified simulation time. The code also outputs appropriate time of concentration results if specified by the user (Fig. 1.4).

Rainfall Loss Model for Impervious Surface

An initial abstraction was used to remove an absolute depth of rainfall at or near the beginning of a rainfall event that does not produce runoff, and then the fractional loss model (FRAC) (McCuen 1998) was used and implemented in OFM. The FRAC

(Thompson et al. 2008) assumes that the watershed converts a constant fraction (proportion) of each rainfall input into an excess rainfall, and the constant runoff fraction used was a volumetric runoff coefficient (Dhakal et al. 2012). Even on a completely impervious surface some rainfall input is still lost to evaporation, interception, wind, absorption by the surface, depression storage on the surface, etc. The loss due to these factors is also influenced by the temperature and wind speed at the site where observation is done. Evaporation and transpiration during a rain event play minor roles and are commonly neglected in event-based considerations (Niemelä et al. 2011). Since interception and depression storage mainly occur at the beginning of a rainfall event, both are often lumped together as an initial abstraction loss (Niemelä et al. 2011). The runoff coefficient in FRAC is calculated from the volume ratio of observed discharge volume and rainfall input (Dhakal et al. 2012). The runoff coefficient indirectly considers some of these rainfall losses during the rainfall event and is only used in model validation using observed data. However, the rainfall input used for the parametric study is the effective rainfall input.

Rainfall Loss Model for Pervious Surface

Infiltration is the primary rainfall loss in pervious surface. Ferguson (1994) defined infiltration as the movement of water which forces runoff away from surface discharge into the underlying soil. Green-Ampt Infiltration Loss model (GAIL) (Green and Ampt 1911) was implemented in OFM for rainfall loss modeling of pervious surfaces because it is a valid and simple physics-based model (Rubin et al. 1976; Hillel 2004). Chow et al. (1988) stated that even though it is an approximate model, it is a physics-based model

with acceptable accuracy. The GAIL model in the OFM is implemented based on two approaches for the calculation of excess rainfall; one with detailed GAIL model which is comprehensive model considering all the conditions for ponded and non-ponded conditions for steady (Mein and Larson 1973) and non-steady rainfall (Chu 1978); and the other with simplified approach in which the model assumes that the watershed has some capacity to absorb rainfall depth and runoff occurs only when the rainfall input exceeds the absorption rate (Thompson et al. 2008). More information and further discussion of the detailed and simplified GAIL models are given in Appendix A and will be published in future studies.

1.3.5 Mass Conservation Validation of Overland Flow Model

The OFM was checked for mass conservation error along with comprehensive validation from observed discharge, velocity and depth hydrographs from different published and field studies. An example observation from Yu and McNown (1963) was used in mass conservation validation. Yu and McNown (1963) measured runoff and depth hydrographs for different combinations of slope, roughness, and rainfall intensity at the airfield drainage in Santa Monica, California. The detail of their study is provided in Chapters two and three. Figure 1.5(a) shows mass conservation error during simulation time of 20 minutes for a concrete surface (n = 0.011) plot of 500 ft long and 3 ft wide with slope of 2% and rainfall of 7.44 in./hr from case 1 of Yu and McNown (1963). Similarly, Fig. 1.5(b) shows inflow (rainfall), simulated storage and outflow, and observed outflow volume variations during the same simulation period for the same plot. Simulated storage is the water remained on the overland flow plane during the simulation

as function of simulated water depths at all cells at each time step. Spatial discretization of the model run was 0.5 ft by 0.5 ft. It can be seen from the Fig. 1.5, that the mass is well conserved and the mass conservation error is very low (0.08%). The simulated outflow volume matched well with observed outflow volume. The Table 1.1 shows the total mass conservation error (%) for different spatial discretization for the same concrete surface from Yu and McNown (1963) for the simulation period of 8 minutes. It can be seen from the Table 1.1 that even for very large discretization the total mass conservation is not large. However, this may be misleading if only total mass conservation error is checked as shown in Figs. 1.6 and 1.7. Figure 1.6 shows mass conservation error (%) for different spatial discretization for the same concrete surface as above. It can be seen from Fig. 1.6 that the mass conservation error for larger discretization is very high (more than 20%) at the initial simulation period. The large error leads incorrect output for the simulation, and such large discretization should be avoided in the simulation. However, the mass conservation error decreases with the discretization. For discretization of 0.5 ft, the error reduces to 0.08%. Similarly, normalized discharge hydrographs for different spatial discretizations for the same plot are shown in Fig. 1.7. Discharge was normalized by respective peak discharge, i.e., normalized discharge $Q_n = Q/Q_p$ where Q is the discharge at time t and Q_p is the peak discharge. It can be seen that the larger discretization under-predicts the observed discharge due to mass conservation error. Simulation with finer discretization matched well with the observed discharge. The details about the discretization used in the simulations are given in respective Chapters.

1.4 Organization of Dissertation

The dissertation is organized into five chapters. Chapter one discusses the background, research objectives, methodology of data collection and model development, and organization of the dissertation. Chapters two to four are organized in journal paper format prepared for the American Society of Civil Engineers (ASCE) and the International Association of Hydrological Sciences (IAHS) journal publications, respectively. Chapter two (Paper 1) has already been published in ASCE's Journal of Hydrologic Engineering and Chapter three (Paper 2) has already been accepted for publication in IAHS's Hydrological Sciences Journal (HSJ) by the time this dissertation was written. Chapter four (Paper 3) has been submitted to HSJ and is under journal external review by the time this dissertation was written. Literature review for the study is given in Chapters two to four for corresponding journal papers. References for all three papers were combined, sorted, and listed at the end of the dissertation.

Chapter two deals with the estimation of improved T_c for overland flows on impervious surfaces for both non-low and low slopes. A quasi-two-dimensional dynamic wave model, Q2DWM was developed to simulate runoff hydrographs for standard ($S_o \geq 0.1\%$) and low-sloped planes ($S_o < 0.1\%$). The validated Q2DWM model was used in a parametric study to generate 750 T_c data for a range of slopes and other input variables (length L, roughness coefficient n, and rainfall intensity i) that were used to develop T_c regression formulas for standard and low slopes.

The work of this chapter has been published as:

Paper 1: **KC, Manoj,** Fang, Xing, Yi, Young-Jae., Li, Ming-Han., Thompson, David. B., and Cleveland, Theodore. G. (2014). "Improved time of concentration estimation on

overland flow surfaces including low-sloped planes." *Journal of Hydrologic Engineering*, 19(3), 495-508, DOI:10.1061/(ASCE)HE.1943-5584.0000830.

A part of the work has also been published as a conference paper:

KC, Manoj, Fang, Xing, Yi, Young-Jae., Li, Ming-Han., Thompson, David. B., and Cleveland, Theodore. G. (2012). "Estimating time of concentration on low-slope planes using diffusion hydrodynamic model." World Environmental & Water Resources Congress 2012, ASCE/EWRI, Albuquerque, New Mexico.

Chapter three deals with the estimation of travel time parameters of overland flow on impervious surface by the particle tracking method. A quasi-two dimensional diffusion wave model with particle tracking, DWMPT was developed for calculating travel time of all the particles in the discretized domain of the impervious overland surface. Based on the percentage of particles that have arrived at the outlet, travel times for 85%, 95% and 100% particles arrival at the outlet were defined as T_{t85}, T_{t95}, and T_{t100}, respectively. A total of 530 DWMPT runs were performed to generate a dataset for developing estimation equations for T_{t85}, T_{t95} and T_{t100}.

The work of this chapter has been accepted for publication:

Paper 2: **KC, Manoj** and Fang, Xing (2014). "Estimating time parameters of overland flow on impervious surfaces by particle tracking method." *Hydrological Sciences Journal*, In press, DOI:10.1080/02626667.2014.889833.

A part of the work has also been accepted as extended abstract and poster presentation:

KC, Manoj and Fang, Xing (2014). "Estimating time of concentration of overland flow on impervious surface using particle tracking model." World Environmental and Water

Resources Congress 2014, ASCE/EWRI, Portland, OR.

Chapter four deals with the estimation of the equilibrium velocity of overland flows induced by constant rainfalls on impervious surfaces. A quasi-two dimensional diffusion wave model (DWM) was used to determine 530 equilibrium velocity (V_{eq}) estimates on impervious surfaces using diverse combinations of the four physically based input variables: L, S_o, n, and i. Regression formulas for estimating V_{eq} and time to equilibrium velocity (T_{veq}) using the input variables was developed for the overland flow on impervious surface.

The work of this chapter is a journal paper submitted to *Hydrological Sciences Journal* under review:

Paper 3: **KC, Manoj** and Fang, Xing "Estimation of the equilibrium velocity of overland flows induced by constant rainfalls on impervious surfaces." *Hydrological Sciences Journal*.

A part of the work has been accepted as extended abstract and poster presentation: **KC, Manoj** and Fang, Xing (2014). "Estimating maximum velocity of overland flow on impervious surface using diffusion wave model." World Environmental and Water Resources Congress 2014, ASCE/EWRI, Portland, OR.

Chapter five summarizes the study as conclusions and provides limitations of the study and recommends future study in this area.

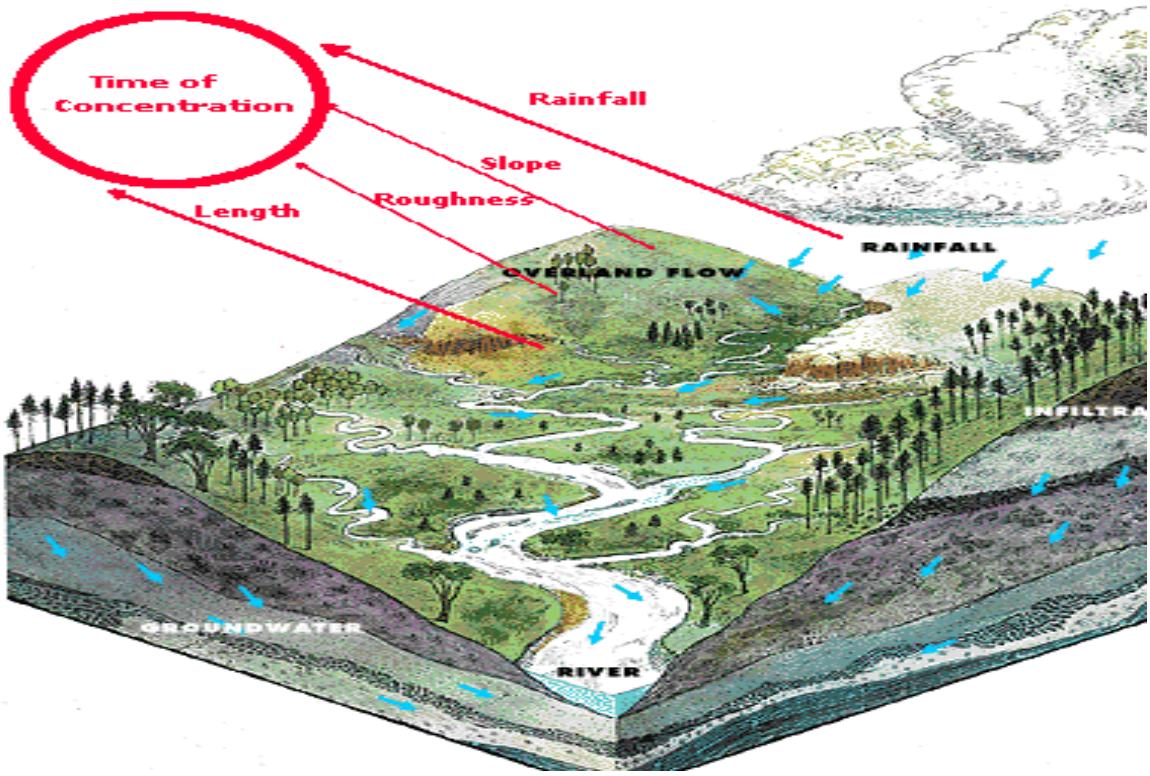

Fig. 1.1. Conceptual representation of time of concentration (T_c) for overland flow surfaces

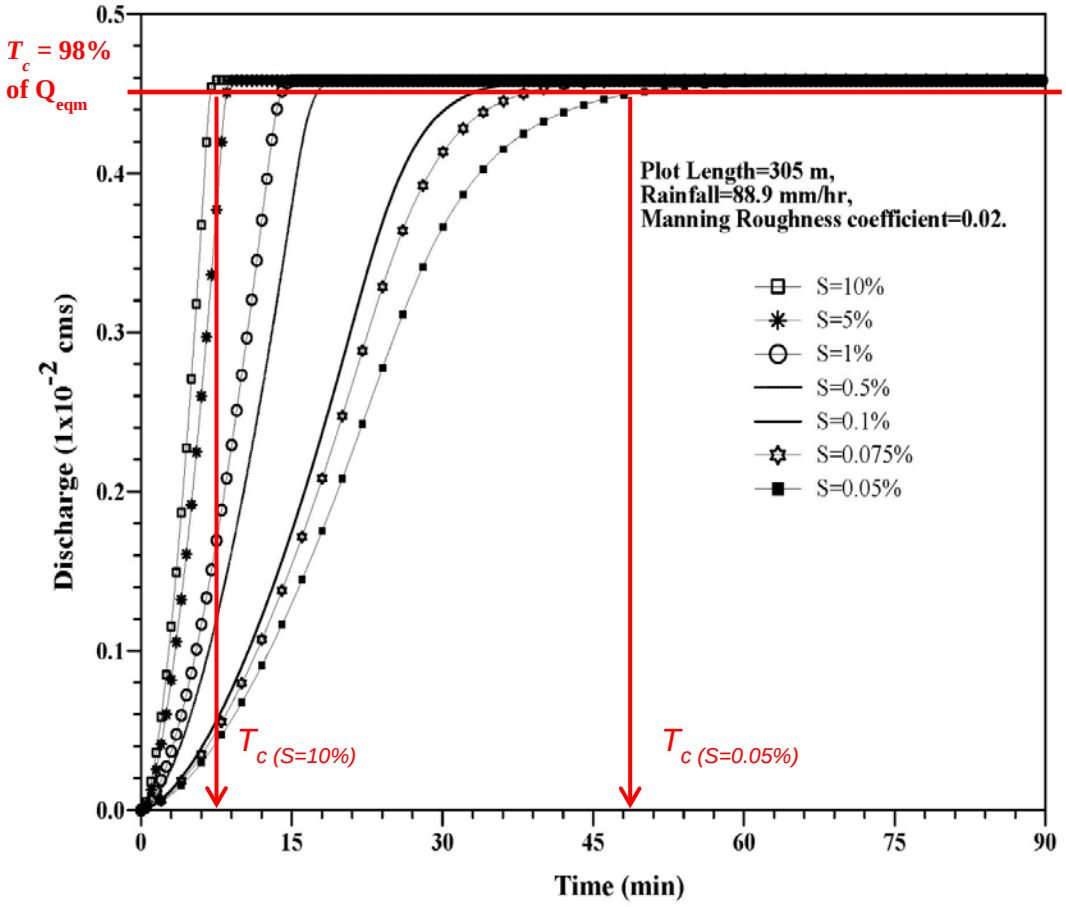

Fig. 1.2. Equilibrium S-hydrographs generated using diffusion wave model (DWM) for different topographic slopes for L = 305 m (1000 ft), n = 0.02, and i = 88.9 mm/hr (3.5 in/hr)

Fig. 1.3. Equipment setting for indoor laboratory study for rainfall-runoff data collection at Texas A&M University that provides the data for numerical model development and applications in the study.

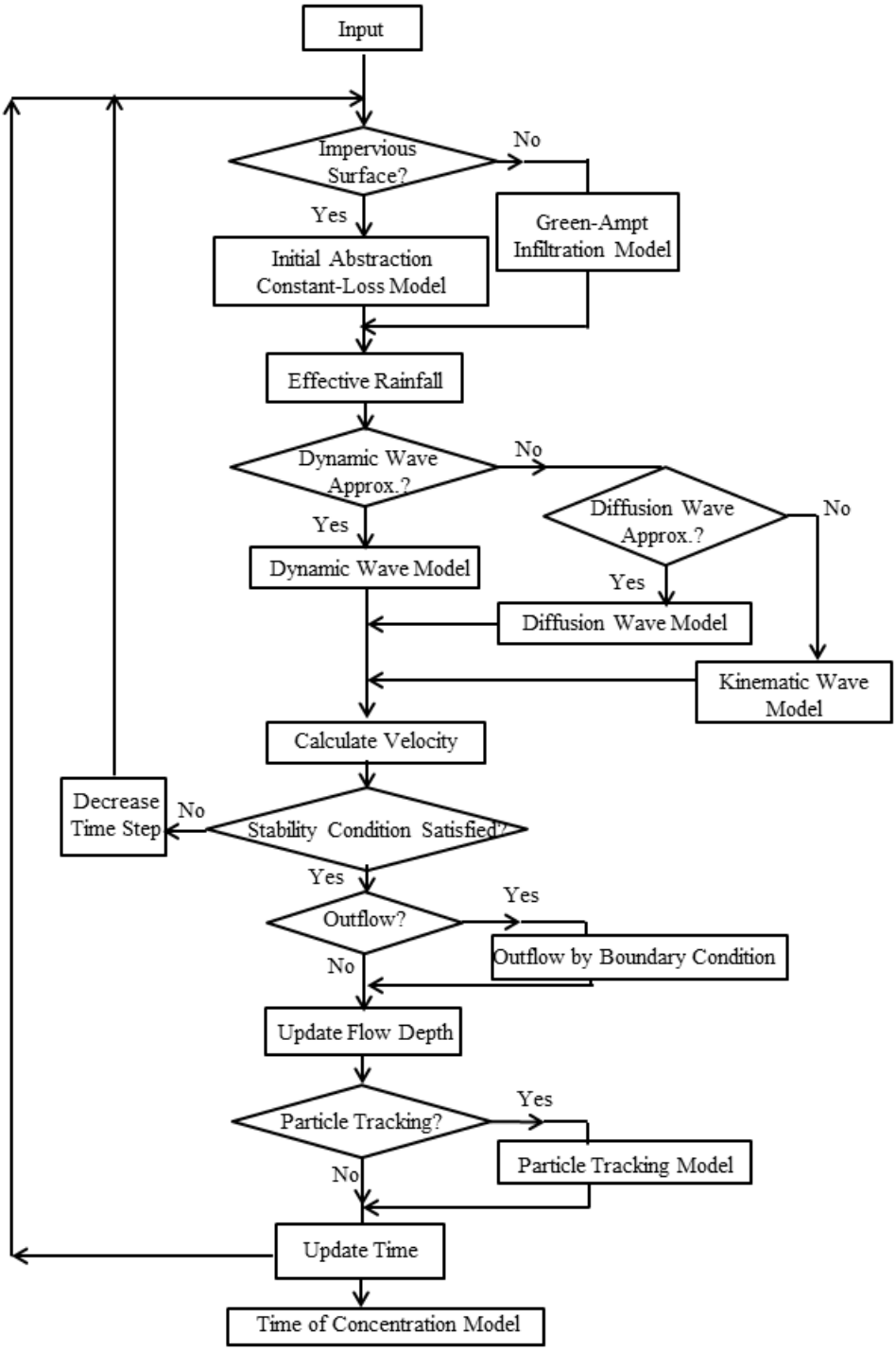

Fig. 1.4. Flowchart showing computation algorithm of Overland Flow Model (OFM) with rainfall loss model, different wave approximation models, and particle tracking model

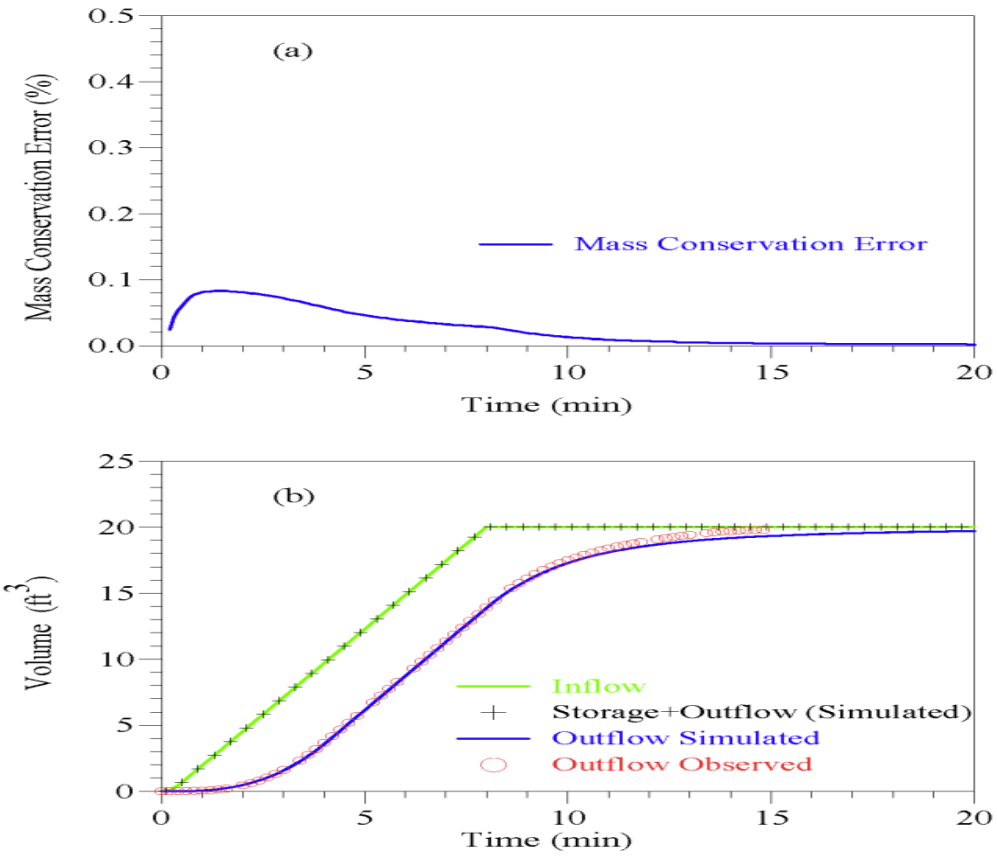

Fig. 1.5 (a) Mass conservation error during simulation time for a concrete surface (n = 0.011) plot of 500 ft long and 3 ft wide with slope of 2% and rainfall of 7.44 in./hr from the case 1 of Yu and McNown (1963), (b) Inflow (rainfall), simulated storage and outflow, and observed outflow volume variations during the simulation. Spatial discretization was 0.5 ft by 0.5 ft

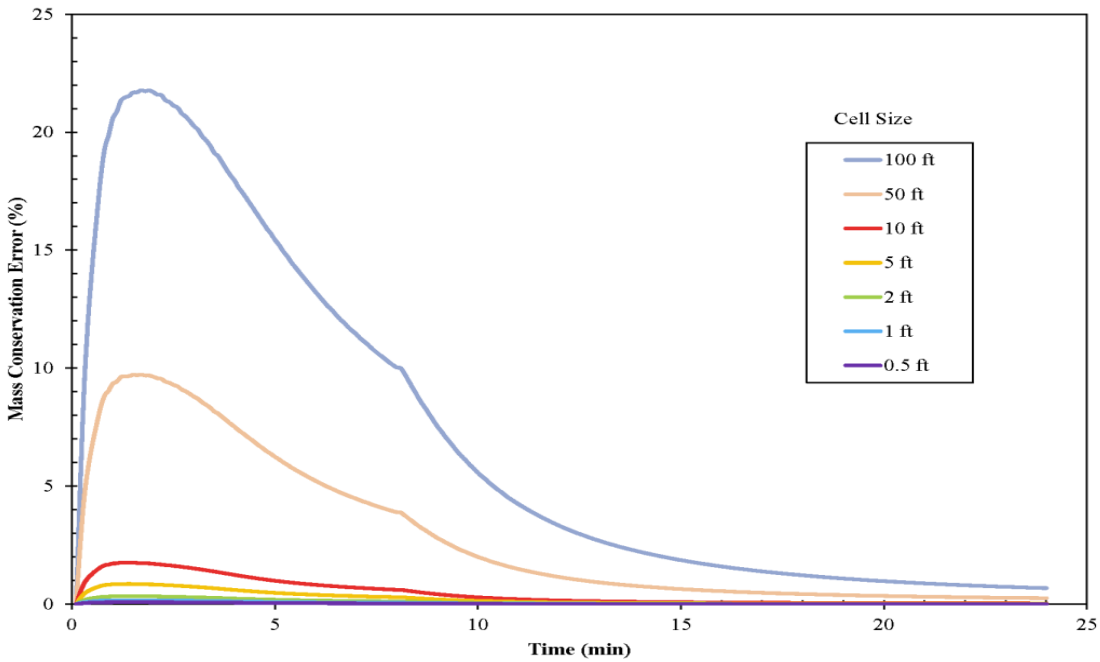

Fig. 1.6. Mass conservation error (%) for different spatial discretization for a concrete surface (n = 0.011) plot of 500 ft long and 3 ft wide with slope of 2% and rainfall of 7.44 in./hr from the case 1 of Yu and McNown (1963)

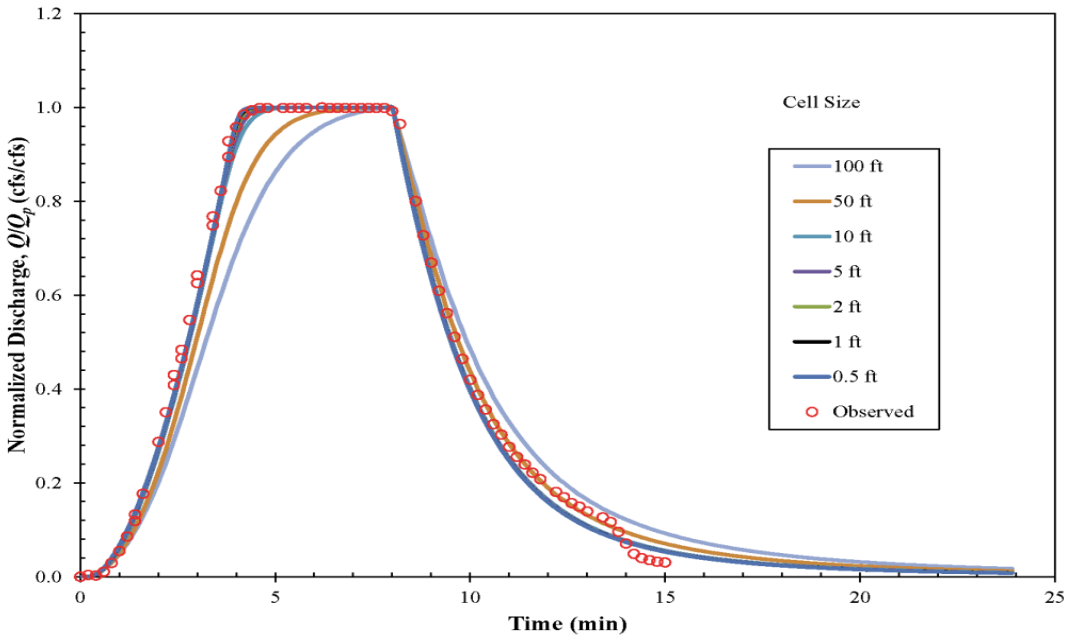

Fig. 1.7. Normalized discharge hydrograph for different spatial discretization for a concrete surface (n = 0.011) plot of 500 ft long and 3 ft wide with slope of 2% and rainfall of 7.44 in./hr from case1 of Yu and McNown (1963). The normalized discharge Q_n = Q/Q_p where Q is the discharge at time t and Q_p is the peak discharge

Table 1.1. Total Mass Conservation Error (%) for Different Spatial Discretization for a Concrete Surface (n=0.011) Plot of 500 ft long and 3 ft wide with Slope of 2% and Rainfall of 7.44 in/hr for a Simulation Period of 8 minutes from Case 1 of Yu and McNown (1963)

Test No.	Discretization Δx (ft)	No. of Cells (L = 500 ft)	Inflow (ft^3)	Storage (ft^3)	Outflow (ft^3)	Mass Conservation Error (%)
1	0.5	1000	20.02	0.21	19.81	0.001
2	1	500	40.05	0.42	39.62	0.002
3	2	250	80.09	0.86	79.23	0.004
4	5	100	200.23	2.26	197.99	0.013
5	10	50	400.30	4.87	395.55	0.032
6	50	10	1999.29	38.60	1965.71	0.251
7	100	5	3998.57	122.90	3902.60	0.674

Chapter 2 Improved Time of Concentration Estimation on Overland Flow Surfaces Including Low-Sloped Planes

2.1 Abstract

Time of concentration (T_c) is one of the most used time parameters in hydrologic analyses. As topographic slope (S_o) approaches zero, traditional T_c estimation formulas predict large T_c. Based on numerical modeling and a review of relevant literature, a lower bound for slope (S_{lb}) of 0.1% was identified as a threshold below which traditional T_c estimation formulas become unreliable and alternate methods should be considered. In this study, slopes less than S_{lb} are defined as low slopes. Slopes equal to or exceeding S_{lb} are defined as standard slopes where traditional T_c estimation formulas are appropriate. A field study was conducted on a concrete plot with a topographic slope of 0.25% to collect rainfall and runoff data between April 2009 and March 2010 to support numerical modeling of overland flows on low-sloped planes. A quasi-two-dimensional dynamic wave model (Q2DWM) was developed for overland flow simulation and validated using published and observed data. The validated Q2DWM model was used in a parametric study to generate T_c data for a range of slopes that were used to develop T_c regression formulas for standard slopes ($S_o \geq 0.1\%$) and low slopes ($S_o < 0.1\%$).

2.2 Introduction

Without actually using the term “time of concentration” (T_c), the concept was first presented by Mulvany (1851) as the time at which discharge is the highest for a uniform

rate of rainfall as the runoff from every portion of the catchment arrives at the outlet. It is the time needed for rain that falls on the most remote part of the catchment to travel to the outlet (Kuichling 1889b). McCuen et al. (1984) stated that almost all hydrologic analyses require the value of a time parameter as input, and T_c is the most commonly used.

Even though T_c is a fundamental time parameter, the practical measurement of the time required to travel the entire flow path in a watershed was seldom attempted except by Pilgrim (1966). Because field measurement of the travel time is labor, time, and cost intensive, hydrograph analysis of observed or simulated discharges is often used to determine T_c.

Determination of T_c using hydrograph analysis dates from , (Kuichling 1889b)who stated "discharge from a given drainage area increases directly with the rainfall intensity until it reaches T_c." Hicks (1942b) analyzed hydrographs from laboratory watersheds and computed T_c as the time from the beginning of rainfall to the time of equilibrium discharge. Izzard (1946) defined T_c from the beginning of a rainfall until the runoff reaches 97% of the input rate. Muzik (1974) defined T_c as the time to equilibrium discharge for his laboratory watersheds. Su and Fang (2004) and KC et al. (2012) determined T_c as the time from the beginning of effective rainfall to the time when flow reaches 98% of the equilibrium discharge. Wong (2005) considered T_c as the time from the beginning of effective rainfall to the time when flow reaches 95% of the equilibrium discharge.

A number of empirical formulas were developed to estimate T_c, but the applicability of any formula for general use is constrained by lack of diversity in the data used to develop the formula (McCuen et al. 1984). Sheridan (1994) indicated that, after more than a century of development and evolution in hydrologic design concepts and

procedures, the end-user is constrained by confusing choices of empirical formulas for estimating T_c for ungaged watersheds.

Most of the empirical formulas to estimate T_c use the reciprocal of topographic slope S_o. As S_o approaches zero (such as in the coastal plains of the southeastern U.S., the Texas Gulf Coast, and the High Plains), the resulting prediction of T_c approaches infinity. If used in hydrologic design, such estimates result in underestimation of peak discharge. A hydrologic design based on under-estimated discharge is prone to failure by hydraulic overloading. In the absence of proper estimates of time of concentration, analysts frequently choose arbitrary values that are based on local rules of thumb or engineering judgment. If the estimate is less than the actual time of concentration, then the resulting estimate of peak discharge will be greater than the correct value (over-estimated), resulting in costly over-design. However, under-estimation of peak discharge resulting in under-design is also possible if the analyst-selected time of concentration is less than the correct value. Such underestimates can result in failure of the drainage system, loss of lives, etc., with costs that exceed those of the over-designed system. Therefore, appropriate estimation of T_c for low-sloped terrains is required and will increase confidence in design discharge estimate for those regions.

The development of a method for estimating T_c for low-sloped planes requires identification of a threshold, below which slope is defined as "low." Such a boundary (S_{lb}) represents a threshold below which traditional relations like Henderson and Wooding (1964) and Morgali and Linsley (1965) become unreliable when slope approaches zero. In this study, slopes less than S_{lb} (0.1%) are defined as low slopes for which alternate methods for T_c estimation should be considered. Slopes equal to or greater than S_{lb} are

defined as standard slopes ($S_o \geq 0.1\%$) where traditional T_c estimation formulas are appropriate.

Based on the literature review and the results of numerical modeling, an effective lower bound of the topographic slope was established. A field study was conducted to collect rainfall and runoff data on a concrete plot with an average slope of 0.25% to extend the research database for relatively low-sloped planes. A quasi-two-dimensional dynamic wave model (Q2DWM) for overland flows was developed and validated using published and observed data. Based on the results of the validation studies, T_c values were calculated as the time from the beginning of effective rainfall to the time when discharge reaches 98% of the peak discharge. The Q2DWM was used to conduct a parametric study to extend the project dataset. Relationships between T_c and physically based input variables were developed for overland flow planes of standard slopes ($S_o \geq 0.1\%$). In the final step, we developed a T_c estimation formula for overland flow planes with low slopes ($S_o < 0.1\%$) using an alternate slope ($S_o + S_{lb}$).

2.3 Field Study

Izzard (1946) and Yu and McNown (1964) conducted laboratory and field studies to investigate travel time and runoff characteristics of overland flow. Izzard used rectangular asphalt and turf surfaces 1.8 m (6 ft) wide, 3.7 to 21.9 m (12 to 72 ft) long, with slopes ranging from 0.1% to 4%. Rainfall was simulated using sprinklers that produced intensities from 41.9 to 104.1 mm/hr (1.65 to 4.10 in./h). Izzard used runoff hydrographs to find T_c as the time from the beginning of a rainfall until the runoff reaches 97% of the input rate. Yu and McNown (1963) reported runoff hydrographs measured

at an airfield watershed in Santa Monica, CA. Runoff was measured during simulated rainfall events with intensities varying from 6.4 to 254 mm/hr (0.25 to 10.0 in./h) from three concrete surfaces 152.4 m (500 ft) long and 0.9 m (3 ft) wide, with slopes of 0.5%, 1.0% and 2.0%. Li and Chibber (2008) conducted field experiments on five surfaces; bare clay, lawn, pasture, concrete, and asphalt using a rainfall simulator. The test watersheds were 9.1 m (30 ft) long and 1.8 m (6 ft) wide, with slopes ranging from 0.24% to 0.48%. T_c was defined as the time required for the runoff hydrograph to reach peak discharge. Fifty-three events (Li and Chibber 2008) were used to derive an estimation formula for T_c with S_o in the denominator.

For the study reported herein, a field study was conducted using a concrete plot with slope of 0.25% to extend the research database for relatively low-sloped planes. Researchers at Texas A&M University instrumented a concrete plot to record rainfall and runoff. The plot is located at the Texas A&M University Riverside campus on an abandoned airstrip taxiway (Fig. 2.1A). The plot is surrounded by soil berms of 178 mm (7 in) tall to form a watershed boundary. Figure 2.1A is an image of the concrete plot looking upslope along the greater diagonal. The tipping-bucket rain gauge and the 0.23 m (0.75 ft) H-flume located at the outlet are visible in the image. The plot survey was conducted by recording elevation differences every 3.80 m (12.50 ft) with a vertical resolution of 0.30 mm (0.001 ft) with respect to the outlet (Fig. 2.1B). The slope along the diagonal from the far corner to the outlet of the rectangular plot is 0.25%. Figure 2.1B is a digital elevation model (perspective view) of the plot where the scale in z-axis is magnified twenty times in comparison to the scale of x- or y- axis.

Stage (water-surface elevation) of flow in the H-flume (Fig. 2.1A) was measured using an ISCO bubbler flow module connected to an ISCO sampler (http://www.isco.com/). The flow module records a flow depth observation in the H-flume at 0.30 mm (0.001 ft) resolution every minute. The ISCO tipping-bucket rain gauge records rainfall depths at 0.25 mm (0.01 in) resolution once each minute. The instruments were manually connected and powered before each forecasted rainfall event. The ISCO sampler was triggered to store data when rainfall intensity exceeded 0.25 mm per hour (0.01 inch per hour) or the flow depth in H-flume was greater than 0.90 mm (0.003 ft).

During the study period, 27 rainfall events were recorded. The 24 events listed in Table 2.1 were used during the numerical model calibration and verification. Three events were excluded because outlet discharges exceeded what could be attributed to incoming rainfall. This mismatch was attributed to the sediment transported to the H-flume when the high-intensity rainfall eroded the boundary berm. Such sediment deposited in the H-flume increased the depth readings and introduced an uncorrectable bias.

Recorded flow depths were adjusted when the bubbler flow module read false initial flow depth. This false reading occurred during an initial dry period, or when two consecutive rainfall events occurred in a short interval of time. These initial readings were considered offsets and subtracted from subsequent depths. Adjusted depths in the H-flume were converted to discharges using the rating curve provided by the flume manufacturer, Free Flow, Inc. (http://freeflowinc.com/).

Total runoff volume for each event was computed from observed discharges and compared to total rainfall volume. Early in development of the dataset, it was discovered that recorded total rainfall volumes were less than observed total runoff volumes. Habib et al. (2001) found that the rainfall intensity measured by tipping-bucket rain gauge could be erroneous at the 1-min interval readings, but the errors were significantly reduced at the 5-min and 10-min interval readings. Therefore, rainfall data were adjusted. A total-catch (container) rain gauge was installed at the test plot to record total event rainfall depths at 1 mm resolution to confirm rainfall depths recorded using the tipping-bucket rain gauge. The readings from the tipping-bucket rain gauge were also compared to data from the weather station at Riverside, Bryan, TX (KTXBRYAN19), which is located about 1.6 km from the test site. The weather station uses Davis Vantage Pro2^{TM} to record cumulative rainfall volume every 10 minutes in real time. The comparison of rainfall data recorded using the tipping-bucket rain gauge, container rain gauge, and Davis Vantage Pro2^{TM} at the weather station indicated a systematic under-recording by the tipping-bucket rain gauge. The event-rainfall data collected at the container rain gauge matched the measurements from the weather station (coefficient of determination R^2 = 0.99 and the slope of the regression line is 0.98). The event-rainfall data recorded by tipping-bucket rain gauge correlated well with the data recorded from the weather station (R^2 = 0.96 and the slope of the regression line is 0.72). Therefore, rainfall data recorded with the tipping-bucket rain gauge were aggregated into 5-minute-interval data and then were adjusted by dividing the data by 0.72, the slope of the regression line.

Twenty-four rainfall-runoff events monitored and used during this study are summarized in Table 2.1. Total rainfall depths ranged from 6.0 to 76.2 mm (0.2 to 3.0 in) and rainfall durations ranged from 1 to 27 hours. Observed maximum 5-minute rainfall intensities varied from 4.3 to 102.4 mm/hr (0.2 to 4.0 in./h). Total runoff volume (Table 2.1) was computed from the runoff hydrograph. The volumetric runoff coefficient (Table 2.1), the total runoff divided by total rainfall (Dhakal et al. 2012) was computed. The effective rainfall depth, one of the input data to Q2DWM, is derived by multiplying volumetric runoff coefficient with the gross rainfall depth. Rainfall and runoff data collected during the field study were used to validate the performance of the Q2DWM for watersheds with low slopes as discussed below.

2.4 Quasi-Two-Dimensional Dynamic Wave Model

Overland flow has been simulated using one- and two-dimensional (1D or 2D) kinematic or diffusion wave models (Henderson and Wooding 1964; Woolhiser and Liggett 1967; Singh 1976; Yen and Chow 1983; Abbott et al. 1986; Chen and Wong 1993; Wong 1996; Jia et al. 2001; Ivanov et al. 2004) and dynamic wave models (Morgali and Linsley 1965; Yeh et al. 1998; Su and Fang 2004). Both kinematic and diffusion wave models have been used to simulate surface water movement (Kazezyılmaz-Alhan and Medina Jr. 2007a; López-Barrera et al. 2012b) in hydrologic-hydraulic models. The kinematic wave model is frequently used for the development of T_c formulas (Wong 2005). Woolhiser and Liggett (1967) introduced a kinematic wave number for evaluating the validity of the kinematic wave assumption for simulating flow over a sloping plane with lateral inflow. McCuen and Spiess (1995) suggested that the kinematic wave

assumption should be limited to kinematic wave number $nL/\sqrt{S_o}$ < 100 where n, L and S_o are Manning's roughness coefficient, length, and slope of the plane, respectively. Therefore, the kinematic wave model may not be suitable for overland flow planes with low slopes.

Hromadka and Yen (1986) developed a quasi-2D diffusion hydrodynamic model (DHM) to incorporate the pressure effects neglected by the kinematic approximation. Even though the diffusion wave approximation is fairly accurate for most overland flow conditions (Singh and Aravamuthan 1995; Moramarco and Singh 2002; Singh et al. 2005), it is inaccurate for cases in which the inertial terms play prominent roles such as when the slope of the surface is small (Yeh et al. 1998). In this study, a quasi-2D dynamic wave model, Q2DWM was developed by modifying the quasi-2D DHM for simulating overland flow on low-sloped planes. The local and convective acceleration terms neglected in DHM were included in Q2DWM because they can be significant for overland flow on low-sloped planes in comparison to other terms.

The governing equations of DHM (Hromadka and Yen 1986) and Q2DWM were solved using a two-dimensional square grid system (Fig. 2.2) and the integrated finite difference version of the nodal domain integration method (Hromadka and Yen 1986). Each cell has four inter-cell boundaries in the north, east, south, and west directions. Each cell is represented using bed elevation (z_p in Fig. 2.2), flow depth (h_p), and Manning's roughness coefficient n. The quasi-2D DHM (Hromadka and Yen 1986) and Q2DWM solve one-dimensional equation of motion, Eq. (2.1) along four directions in the east-west and north-south directions independently for each computation cell (Fig. 2.2) first and then solve the continuity Eq. (2.2):

$$\frac{\partial q_j}{\partial t} + \frac{\partial}{\partial j}\left(\frac{q_j^2}{h}\right) + gh\left(\frac{\partial H}{\partial j} + S_{fj}\right) = 0 \tag{2.1}$$

$$\sum \frac{\partial q_j}{\partial j} + \frac{\partial h}{\partial t} = i \tag{2.2}$$

where j varies from 1 to 4, 1 for north, 2 for east, 3 for south, and 4 for west direction, q_j is the flow rate per unit width in the j direction, i is the effective rainfall intensity as a source term, S_{fj} is the friction slope in j direction, g is the gravitational acceleration, H and h are the water-surface elevation and flow depth in each computational cell as functions of time t. The water surface elevation H is given by Eq. (2.3):

$$H = h + z \tag{2.3}$$

where z is the bottom elevation of the computational cell. Both h and z are defined at the cell center, and fluxes (q_j), and friction slopes (S_{fj}) are defined at the inter-cell boundaries (Fig. 2.2). Writing Eq. (2.1) in velocity form, we get:

$$\frac{\partial v_j}{\partial t} + v_j \frac{\partial v_j}{\partial j} + g\left(\frac{\partial H}{\partial j} + S_{fj}\right) = 0 \tag{2.4}$$

The friction slope (S_{fj}) in Eq. (2.4) is approximated from Manning's equation (Akan and Yen 1981):

$$v_j = \frac{k_n}{n} h^2 S_{fj}^{1/2} \quad or \quad S_{fj} = \left(\frac{v_j n}{k_n h^{2/3}}\right)^2 \tag{2.5}$$

where k_n = 1 (SI units) or 1.49 (USC units). The average values of h and n of the two adjacent cells in the j direction are used for Eq. (2.5).

Hromadka and Yen (1986) defined a dimensionless momentum factor, m_j, which represents the sum of first two acceleration terms in Eq. (2.4) after dividing by g:

$$m_j = \frac{1}{g}\left[\frac{\partial(v_j)}{\partial t} + v_j \frac{\partial v_j}{\partial j}\right] = a_{lj} + a_{cj} \tag{2.6}$$

where a_{lj} and a_{cj} are dimensionless local and convective accelerations, respectively. Using m_j from Eq. (2.6), Eq. (2.4) is written as:

$$S_{fj} = -\left(\frac{\partial H}{\partial j} + m_j\right) \tag{2.7}$$

Using Eq. (2.7) with Eq. (2.5), the velocity in each direction (j) can be calculated as:

$$v_j = -K_j\left(\frac{\partial H}{\partial j} + m_j\right) \tag{2.8}$$

where K_j is conduction parameter computed as (Hromadka and Yen 1986):

$$K_j = \frac{k_n}{n} h^{2/3} \frac{1}{\left(\frac{\partial H}{\partial j} + m_j\right)^{1/2}} \tag{2.9}$$

Richardson and Julien (1994) studied the acceleration terms of the Saint-Venant equations for overland flow under stationary and moving storms. The local acceleration during the rising limb of a hydrograph and the convective acceleration after equilibrium can be estimated as:

$$a_{lj} = \frac{\beta - 1}{g\ t^{(2-\beta)}} \alpha\ i^{(\beta-1)} \tag{2.10}$$

$$a_{cj} = \frac{\beta - 1}{\beta\, g\, X^{(2/\beta-1)}} \alpha^{2/\beta}\ i^{(2-2/\beta)} \tag{2.11}$$

where $\alpha = S_{fj}^{0.5} / n$, β = 5/3 (Richardson and Julien 1994), i is rainfall intensity in m/s, and X is the distance in m from its boundary along each j direction. During the rising limb of a hydrograph, the space derivatives are comparatively small, and the local

acceleration (Eq. 2.10) is dominant. As the time *t* increases or flow approaches equilibrium, time derivatives in Eq. (2.4) vanish, and the convective acceleration (Eq. 2.11) is dominant (Richardson and Julien 1994).

After the velocity or the flow rate in each *j* direction is solved, the flow depth is updated using continuity Eq. (2.2). The Eq. (2.2) was derived from the conservation of mass or volume in each cell, e.g., the cell *p* in Fig. 2.2. The difference form of Eq. (2.2) can be written as:

$$h_p^t = h_p^{t-1} - \Delta t(\sum \frac{q_j}{\Delta j}) + i\ \Delta t \qquad (2.12)$$

where superscripts *t-1* and *t* stand for the previous and new time step. The Eq. (2.12) was solved explicitly for each cell. Rainfall input (*i*) was converted from effective rainfall intensity (after removing any rainfall losses) to a depth change in each cell at each time step to model its contribution to the flow hydraulics. In Eq. (2.12), $\sum q_j$ is the sum of q_{east}, q_{west}, q_{south}, and q_{north} (Fig. 2.2). For quasi-2D DHM (Hromadka and Yen 1986) and Q2DWM, Δx (or Δj) is equal to Δy for each square cell (Fig. 2.2).

For the Q2DWM, the time step Δt is dynamically updated based on the minimum and the maximum time steps (Δt_{min} and Δt_{max}), where Δt_{min} is an input parameter and Δt_{max} is dynamic updated using Eq. (2.13). At each time step, after velocity and flow depth are solved for all cells in the simulation domain, the maximum velocity (v_{max}) of all the cells in the simulation domain and its corresponding flow depth (h_{vmax}) where v_{max} occurs are determined. Similarly, the maximum flow depth (h_{max}) of all the cells and its corresponding velocity (v_{hmax}) where h_{max} occurs are determined. v_{max} and v_{hmax} are calculated from the sum of average of east-west (x-velocity) and average of north-south

(y-velocity). Hence, the maximum time step Δt_{max} is computed as:

$$\Delta t_{\max} = Cr \times Min\left[\frac{\Delta x}{v_{\max} + \sqrt{gh_{v\max}}}, \frac{\Delta x}{v_{h\max} + \sqrt{gh_{\max}}}\right] \tag{2.13}$$

where Cr is the courant number (Courant et al. 1967), a numerical stability criterion, the limit of which is taken as 0.1 for our low-sloped study. The model starts with Δt_{min}, and increases at 5% of Δt_{min} at each computational cycle until the time step is just smaller than or equal to Δt_{max} calculated by Eq. (2.13).

The Q2DWM advances in time explicitly for all the cells in the domain until the specified simulation ending time is reached and simulates quasi-2D overland flow coupled with a simple rainfall loss model. For validation with the experimental data, an initial abstraction was used to remove rainfall at or near the beginning of rainfall event that did not produce runoff, and then the fractional loss model (FRAC) was used (McCuen 1998). The FRAC model (Thompson et al. 2008) assumes that the watershed converts a constant fraction (proportion) of each rainfall input into an excess rainfall. The constant runoff fraction used was a volumetric runoff coefficient (Dhakal et al. 2012). However, for parametric study effective rainfall is an input to the model.

2.4.1 Model Validation using Published Data from Previous Studies

The Q2DWM was first validated using published data. The Los Angeles District of the U.S. Army Corps of Engineers conducted an extensive experimental rainfall-runoff study on three separate concrete channels (Yu and McNown 1963). Yu and McNown (1963) reported runoff hydrographs from different combinations of slope, roughness, and rainfall intensity (using artificial rainfall simulator). Hydrographs simulated using Q2DWM

matched observed hydrographs well (Table 2.2). Two example comparisons are shown in Figs. 2.3A and 2.3B. Observed and simulated hydrographs from a concrete surface of 152.4 m (500 ft) by 0.3 m (1 ft) with a slope of 2% and of 76.8 m (252 ft) by 0.3 m (1 ft) with relative low slope of 0.5% are shown in Figs. 2.3A and 2.3B, respectively. The hyetograph for the experiment presented in Fig. 2.3A was a rainfall intensity of 189 mm/hr (7.44 in./h) with duration of 8 minutes. The hyetograph for the event depicted in Fig. 2.3B was a variable rainfall intensity of 43.2 mm/hr (1.70 in./h) for first 6 minutes, then 95.8 mm/hr (3.77 in./h) from 6 to 18 minutes, and finally 44.5 mm/hr (1.75 in./h) for the remaining portion of the storm with a total duration of 32 minutes.

Izzard and Augustine (1943) analyzed runoff data from paved and turf surfaces collected by the Public Roads Administration in 1942. Their objective was to study the hydraulics of overland flow using a rainfall simulator. The data were collected in three phases. The data used in Fig. 2.3 are from the first phase, which comprised smooth asphalt or concrete paved surfaces. Observed and simulated hydrographs for a 3.7 m (12 ft) long and 1.8 m (6 ft) wide asphalt pavement with slope of 2% for a 6 minutes uniform rainfall intensity of 49.0 mm/hr (1.93 in./h) and a 21.9 m (72 ft) long and 1.8 m (6 ft) wide concrete surface with slope of 0.1% for a variable rainfall intensity of 46.5 mm/hr (1.83 in./h) for 12 minutes, then 93.0 mm/hr (3.65 in./h) for 12 to 19 minutes are shown in Figs. 2.3C and 2.3D, respectively (Izzard and Augustine 1943).

Hydrographs were simulated using 1 ft by 1 ft cell size and Manning's roughness coefficient of 0.011 for concrete and 0.013 for asphalt surfaces. The Nash-Sutcliffe coefficient (*Ns*) and root mean square error (*RMSE*) were used to evaluate Q2DWM performance. Legates and McCabe (1999) demonstrated that *Ns* is a parameter to

measure goodness-of-fit between modeled and observed data. Bennis and Crobeddu (2007) concluded that, for a hydrograph simulation, a good agreement between the simulated and the measured data is achieved when *Ns* exceeds 0.7. Hydrographs simulated using Q2DWM were compared with eight experimental hydrographs from Izzard and Augustine (1943) and Yu and McNown (1963). The average *Ns* was 0.97 (ranged from 0.87 to 0.99 in Table 2.2), and average *RMSE* was 0.04×10^{-3} m^3/s (ranged from 0.008–0.116×10^{-3} m^3/s in Table 2.2). These statistics indicate close agreement between measured and simulated hydrographs.

2.4.2 Model Validation using Observations from Current Field Study

Measured rainfall-runoff data were used to validate the performance of the Q2DWM model for catchments with relatively low slope and with elevation variations in two dimensions. Simulated hydrographs matched observed hydrographs well (Table 2.3). Four example comparisons are shown in Fig. 2.4. Rainfall intensities measured from rainfall events (Fig. 2.4) were more variable comparing with the artificial rainfalls shown in Fig. 2.3. Both measured and simulated hydrographs showed response to rainfall intensity variation, for example, the event on September 11–12, 2009 (Fig. 2.4C). Simulated and measured peak discharges (Q_p) and time-to-peak (T_p) are listed in Table 2.3 and compared in Fig. 2.5 for all 24 events. There are two relatively large disagreements between simulated and measured T_p in Fig. 2.5 because the initial rainfall abstractions, used in the simple rainfall loss model for Q2DWM, were less than the actual initial abstractions for these events.

Q2DWM simulations were based on 3.81 m (12.5 ft) square cells (Fig. 2.1B) with

a Manning's roughness coefficient of 0.02. Cell sizes finer than 3.81 m were tested but did not improve model results. Aggregated observed hyetographs with a 5-minute interval were used as model input. The model boundary condition at the outlet is crucial to overland flow simulation. Su and Fang (2004) developed estimation formulas of T_c for low-sloped planes with 100% and 20% opening at the outlet boundary. In the field study, the surrounding boundaries of the rectangular plot were closed using soil berms (Fig. 2.1) except an opening through the 0.75 ft H-flume. The H-flume is a specially shaped open-channel flow section designed to restrict the channel width from 0.434 to 0.023 m (1.425 to 0.075 ft) and create a critical flow condition for flow measurement. Therefore, the boundary condition at the outlet was critical flow for a rectangular opening. A calibrated opening width of 0.122 m (0.4 ft) for the 3.81 m (12.5 ft) computational cell size was used.

The *Ns* and *RMSE* statistics developed for 24 simulated hydrographs are listed in Table 2.3. The average *Ns* was 0.81 and the average *RMSE* was 0.13×10^{-3} m^3/s. These results indicate an acceptable match between measured and simulated hydrographs; therefore, Q2DWM can be used to estimate response for watershed with standard ($S_o \geq 0.1\%$) and low slopes ($S_o < 0.1\%$) for uniform and variable rainfall intensities.

2.5 Estimation of Time of Concentration

There is no practical method to directly measure T_c in the field or laboratory. Therefore, the indirect approach of analyzing the discharge hydrograph is the viable method to estimate T_c. For the study reported herein, T_c is defined as the time from the beginning of effective rainfall to the point when the runoff reaches 98% of the peak discharge under

a constant rainfall rate. This approach is similar to those used by Izzard (1946), Su and Fang (2004), and Wong (2005). For the parametric study, the peak discharge was calculated using the rational formula (Kuichling 1889b). When the discharge approaches equilibrium from a constant rainfall supply, the time rate of change of discharge is nearly zero and could fluctuate (in response to numerical diffusion and unsteady flow nature), especially for low-sloped overland flows. This sensitivity at "computational equilibrium" makes the determination of the practical equilibrium time difficult (McCuen 2009) and prone to error. Therefore, T_c was not estimated as the equilibrium time, but the time to 98% of the peak discharge.

Peak discharges calculated using the rational formula, modeled using Q2DWM, and measured just before rainfall cessation are listed in Table 2.2. Peak discharges calculated from above three methods are almost the same (Table 2.2), and absolute relative difference between two peaks is less than 2%. T_c values were derived from Q2DWM simulated hydrographs for planes with slopes of 0.1%, 0.5% (relatively low slope), and 2% (standard slope), rainfall intensity from 21.6 to 189.3 mm/hr (0.85 to 7.45 in./h), roughness from 0.011 to 0.035, and plane length from 3.7 to 152.4 m (12 to 500 ft). T_c values extracted from Q2DWM simulated hydrographs agree well with T_c derived from published experimental hydrographs. The average error of T_c is 0.6 min with a standard deviation of 0.7 min. Therefore, Q2DWM produces T_c results that commensurate with observations and is considered valid for the subsequent parametric study.

2.6 Identification of Lower-Bound Slope (S_{lb})

Developing appropriate equations to estimate T_c for overland flow on low-sloped planes requires a definition of what constitutes "low-slope." Yates and Sheridan (1973) conducted one of the first studies on flow measurement techniques in low-sloped watersheds. They considered flow measurement in streams with slopes less than 0.1% to be difficult and discussed hydrologic methods for those slopes. Capece et al. (1988) reported that delineation of watersheds with topographic slope less than 0.5% was difficult. Both Capece et al. (1988) and Sheridan et al. (2002) suggested that present hydrologic methods require modifications to improve performance for such "flatland" watersheds because the "flatland" energy and flow velocities are relatively small. Sheridan (1994) concluded that flow length was sufficient to explain hydrograph time parameters and precluded the use of topographic slope for "flatland" in the time parameter estimates. Sheridan (1994) classified channel slopes of 0.1–0.5% as stream networks of low-sloped systems. Van der Molen et al. (1995) used numerical experiments to conclude that water depth at the upper boundary is finite when slope is 0.2%. More recently, Su and Fang (2004) used a two-dimensional numerical model to examine the variation of T_c with plot slope, length, roughness coefficient and rainfall and concluded that there is less variation of T_c for slopes less than 0.05%. Li et al. (2005) and Li and Chibber (2008) analyzed laboratory data and reported that the contribution of the slope to hydrograph time response is negligible for topographic slopes less than 0.5%. Cleveland et al. (2008) computed travel times using a particle tracking model based on an equation similar to Manning's equation. They reported that uncertainty in their prediction model increased substantially when they included watersheds of slopes of 0.02–0.2%. Cleveland et al. (2011) used the

variation of dimensionless water-surface slope with Manning's roughness coefficient, *n*, provided by Riggs (1976) to examine the relation between them. They concluded that the relation between *n* and water-surface slope changed when the slope is less than 0.3%. This result can be considered another source for the low-slope threshold. In summary, most of the researchers considered the low-slope threshold to be between 0.1%–0.5% (Table 2.4).

Related studies provide an insight into the definition of low slope. However, except for Su and Fang (2004), most evaluated the variation of slope with hydrologic variables other than T_c. To further examine the variation of T_c with slope, we conducted a series of Q2DWM numerical experiments to test the threshold slope for T_c estimations by varying S_o while retaining constant values of *n*, *i*, and *L* [n = 0.02, i = 88.9 mm/hr (3.5 in./h), and L = 305 m (1000 ft)]. Simulated Q2DWM hydrographs for varying topographic slopes are shown in Fig. 2.6D. Simulated hydrographs for slopes less than 0.1% are substantially different from those with greater slopes. Estimated T_c values versus S_o for two sets of numerical experiments are shown in Fig. 2.7: case (i) for L = 305 m (1000 ft), n = 0.02, i = 88.9 mm/hr (3.5 in./h); and case (ii) for L = 90 m (300 ft), n = 0.035, i = 25.4 mm/hr (1 in./h). The regression lines were derived for slopes greater than 0.1% (Fig. 2.7). When the slope is less than 0.1%, T_c values depart from the corresponding regression line ($S_o \geq 0.1\%$). Based on these numerical experiments, S_{lb}, a lower bound for topographic slope can be established at 0.1%, which agrees reasonably well with the values recommended by others (Table 2.4). Inappropriate estimates of T_c are likely to arise if T_c equations such as Henderson and Wooding (1964) or Morgali and Linsley (1965) are used where slope is less than 0.1%, as shown in Fig. 2.7. The T_c

equation commonly used in TR-55 by the Natural Resources Conservation Service (NRCS) for sheet flow (NRCS 1986) was derived from Morgali and Linsley (1965).

2.7 Parametric Study for the Time of Concentration of Overland Flow

Yen (1982) stated "overland and channel flows are in separate but connected hydraulic systems". Kibler and Aron (1983) reported that improved estimates of T_c are achieved if overland and channel flow are considered separately. Therefore, using the lower-bound slope (0.1%), a parametric study was conducted to develop estimating tools for standard ($S_o \geq 0.1\%$) and low-sloped ($S_o < 0.1\%$) overland flows where channel flows are negligible.

Development of empirical equations for T_c estimation dates from the 1940's, when Kirpich (1940) computed T_c for a watershed using channel length and average channel slope. For overland flows, Izzard (1946), Morgali and Linsley (1965), Woolhiser and Liggett (1967), and Su and Fang (2004) derived estimation formulas using length L, slope S_o, and Manning's roughness coefficient n of the overland flow plane, and rainfall intensity i as input variables.

More than 750 T_c values were estimated from hydrographs simulated using Q2DWM by varying the four physically based input variables, L, S_o, n, and i to extend the dataset available for analysis. The input variable L was varied from 5 to 305 m (16 to 1000 ft), S_o from 0.001% to 10%, n from 0.01 to 0.80, and i from 2.5 to 254 mm/hr (0.1 to 10.0 in./h). Hydrographs were simulated holding the three variables constant and varying the fourth by 10–20%. Example S-hydrographs from these simulations are displayed in Fig. 2.6. When n was varied from 0.01 to 0.30 for L = 305 m (1000 ft), S_o =

0.5%, and i = 88.9 mm/hr (3.5 in./h), T_c increased from 11.4 to 94.9 minutes (Fig. 2.6A). Similarly, T_c increases as L increases (Fig. 2.6B), decreases as i increases (Fig. 2.6C), and increases as S_o decreases (Fig. 2.6D).

Five hundred and fifty Q2DWM runs were conducted to obtain database for developing an estimation formula for standard slopes ($S_o \geq 0.1\%$). A generalized power relation (Eq. 2.14) was chosen for developing the regression equation,

$$T_c = C_1 \, L^{k_1} \, S_o^{k_2} \, n^{k_3} \, i^{k_4} \tag{2.14}$$

where L is in m, S_o is in m/m, i is in mm/hr, C_1, k_1, k_2, k_3, and k_4 are regression parameters. Eq. (2.14) was log-transformed and non-linear regression was used to estimate parameter values. The resulting equation is

$$T_c = 8.67 \frac{L^{0.541} n^{0.649}}{i^{0.391} S_o^{0.359}} \tag{2.15}$$

where T_c is in minutes, and other variables are as previously defined. Regression results are presented in Table 2.5. Statistical results indicate that the input variables L, S_o, n, and i have a high level of significance with p-value < 0.0001 (Table 2.5) and are critical variables in the determination of T_c. The regression parameters (C_1, k_1, k_2, k_3, and k_4) have less standard errors and small ranges of variation at the 95% confidence interval (Table 2.5).

Values predicted with Eq. (2.15) compare well with those from formulas developed by Henderson and Wooding (1964) and Morgali and Linsley (1965), as shown on Fig. 2.8. Furthermore, the predicted values compare well with estimates from Q2DWM numerical experiments (Fig. 2.8). The coefficients of determination R^2 and *RMSE* for Eq. (2.15), formulas of Henderson and Wooding (1964) and Morgali and

Linsley (1965) are similar (R^2 > 0.94, as shown in Table 2.6).

Three additional estimation formulas were explored and developed using combinations of input variables and compared with the formulas described above. One option for T_c estimation formula is to use the quotient $L/\sqrt{S_0}$ as a combined input variable. This combination was used for T_c formulas developed by Kirpich (1940), Johnstone and Cross (1949), and Linsley et al. (1958). The variable $L/\sqrt{S_0}$ is derived from application of Manning's equation for estimating overland flow velocity. The second option of combined variables considered is the product *nL* that is related to the total resistance length of the overland flow. The third option explored is to use the quotient $nL/\sqrt{S_0}$ that is related to Manning's equation. Estimation formulas of T_c using combined input variables were developed using non-linear regression and are presented in Table 2.6. Estimation formulas using the combined variables performed as well as Eq. (2.15) and had R^2 values greater than 0.94. The *p*-value reported in Table 2.6 was developed between T_c and all input variables in each regression equation. These formulas are highly significant because the *p*-value for each formula is less than 0.0001 (Table 2.6). The *p*-values for the correlation between T_c and each of above three combined variables were developed and are each less than 0.0001. Therefore, these combined variables can also be considered as critical input variables in the determination of T_c. Based on these results, the regression equations developed in this study and those of Henderson and Wooding (1964) and Morgali and Linsley (1965) are acceptable for estimating T_c of overland flow on planes with standard slope ($S_o \geq 0.1\%$).

2.8 Time of Concentration for Low-Sloped Overland Flow

Using the equations presented in Table 2.6, the resulting estimates of T_c grow without bound as topographic slope S_o approaches zero. Therefore, an alternate formulation, Eq. (2.16) using the combined slope ($S_o + S_{lb}$) was chosen for planes with $S_o < 0.1\%$,

$$T_c = C_2 \, L^{k_5} \left(S_o + S_{lb}\right)^{k_6} n^{k_7} i^{k_8} \tag{2.16}$$

where C_2, k_5, k_6, k_7, and k_8 are constants derived from non-linear regression. Using the Q2DWM dataset for low-sloped planes, the resulting regression equation is

$$T_c = \frac{L^{0.563} n^{0.612}}{11043.81 \; i^{0.304} (S_o + S_{lb})^{2.139}} \tag{2.17}$$

where T_c is in minutes, the low-slope threshold S_{lb} is 0.1%, and other variables in SI units are as previously defined.

Use of the offset S_{lb} in Eq. (2.17) allows computation of T_c in low- and zero-sloped conditions. For Eq. (2.17), the input variables L, ($S_o + S_{lb}$), n, and i are critical input variables for determination of T_c, presenting a high level of significance with p-value < 0.0001 (Table 2.7). R^2 and *RMSE* for Eq. (2.17) are 0.87 and 16.9 minutes, respectively, when results from Eq. (2.17) are compared to T_c dataset (Fig. 2.9). Normalized *RMSE* (RMSE divided by the range of T_c values) is 6% for Eq. (2.17). Comparing Eq. (2.15) for standard slopes with Eq. (2.17) for low slopes, regression constants or exponents of L, n, and i are similar, but the exponent of S_o (0.3–0.4 in Table 2.6) is much smaller than the exponent of ($S_o + S_{lb}$), which is 2.139 in Eq. (2.17). This is because a combined slope ($S_o + S_{lb}$) was used in Eq. (2.17) instead of topographic slope S_o. It is worth to note that Eq. (2.17) has a large coefficient in the denominator. The combination of large coefficient and large exponent for ($S_o + S_{lb}$) in the denominator

produces T_c values which are acceptable in low-sloped planes.

When topographic slope S_o is much smaller than S_{lb}, e.g., $S_o < 0.005\%$, predicted T_c using Eq. (2.17) changes only slightly as S_o approaches to zero, which is displayed on Fig. 2.7. This result also indicates that Eq. (2.17) agrees well with the data for two example cases in Fig. 2.7. Furthermore, this result corroborates those of previous studies (Sheridan 1994; Su and Fang 2004; Li et al. 2005; Li and Chibber 2008) concluding that negligible change occurs in T_c at low topographic slopes. Predicted T_c values from Eq. (2.17) correlated reasonably well with low-sloped T_c dataset ($R^2 = 0.87$, Fig. 2.9). However, T_c values predicted using Eq. (2.15) and formulas of Henderson and Wooding (1964) and Morgali and Linsley (1965) have very weak correlations with the same dataset, *i.e.*, R^2 varied from 0.17 to 0.23 and *RMSE* from 144 to 716 min, indicating less of the variance is captured by these formulas.

2.9 Summary and Conclusions

A combination of field monitoring and numerical studies was performed to develop an ancillary dataset to further evaluate time of concentration, T_c for overland flow, especially for low-sloped planes. The field study was conducted on a concrete plot with recording rain gauge and flow measurement equipment to extend the research database for relatively low-sloped planes of 0.25%. Rainfall and runoff data were recorded for 27 events from April 2009 to March 2010.

A quasi-two-dimensional dynamic wave model, Q2DWM was developed to simulate runoff hydrographs for standard ($S_o \geq 0.1\%$) and low-sloped planes ($S_o < 0.1\%$). Q2DWM was validated using data from published studies and collected at the

experimental watershed. The average Nash-Sutcliffe coefficients were 0.97 and 0.82 for published and field data, respectively. The validated Q2DWM model was used in a parametric study to generate T_c data for a range of slopes and other input variables (length L, roughness coefficient n, and rainfall intensity i) that were used to develop T_c regression formulas for standard and low slopes. In our parametric study, T_c was defined as the time from the beginning of effective rainfall to the time when the flow reaches 98% of peak discharge. Classical formulas like Henderson and Wooding (1964) and Morgali and Linsley (1965) for estimating T_c deviate from modeled values where the watershed topographic slope is less than about 0.1%. This value (0.1%) is termed the lower-bound slope, S_{lb}. Slopes less than S_{lb} are defined as low slopes; those equal to or greater than S_{lb} are defined as standard slopes ($S_o \geq 0.1\%$).

During the parametric study, n was varied from 0.01 to 0.80, L from 5 to 305 m (16 to 1000 ft), i from 2.5 to 254 mm/hr (0.1 to 10.0 in./h), and S_o from 0.0001% to 10%. Seven hundred and fifty Q2DWM runs were conducted. Four regression equations (Table 2.6) were developed for T_c estimation of overland flow planes for standard slopes ($S_o \geq 0.1\%$). Formulas developed in this study and by Henderson and Wooding (1964) and Morgali and Linsley (1965) for standard slopes performed poorly in predicting T_c for low slopes with R^2 from 0.17 to 0.23. However, Eq. (2.17), which resulted from the regression analysis of 200 Q2DWM-derived low-sloped T_c dataset, performed reasonably well, with an R^2 of 0.87. Eq. (2.17) was developed for overland flow on low-sloped planes using S_o+S_{lb} in place of topographic slope S_o. This equation is recommended for estimating T_c where topographic slopes are low ($S_o < 0.1\%$).

2.10 Notation

The following symbols are used in this paper:

$a_{cj,}$ a_{lj} = convective and local accelerations;

$C_{1,}$ C_2 = regression coefficients;

C_r = Courant Number;

g = acceleration due to gravity in m/s^2;

H = water surface elevation in m;

h = flow depth in m;

h_{max} = maximum flow depth in m of all cells in the domain;

h_p^{t-1}, h_p^t = flow depth at cell p in m at time step t-1 and t;

h_{vmax}= corresponding flow depth in m where v_{max} occurs in the domain;

i = rainfall intensity in m/sec or mm/hr;

j = subscript that stands for the flow direction (east, west, north, and south)

Δj = spacing in j direction;

$k_{1...}$ k_8 = regression constants for power functions of T_c estimation formulas;

k_n = 1 (SI units) or 1.49 (FPS units);

K_j = conduction parameter in j direction;

L = plot length in m;

m_j = dimensionless momentum quantity in j direction;

n = Manning roughness coefficient;

Ns = Nash-Sutcliffe coefficient;

p = arbitrary cell number;

q_j = flow rates per unit width in m^2/sec in j direction;

q_{east} , q_{north} , q_{south} , q_{west} ,= flow rates per unit width in m^2/sec in east, north, south and west direction;

Q_p = peak discharge in m^3/s or cms;

Q_{pm} = measured peak discharge in cms;

Q_{ps} = simulated peak discharge in cms;

R^2 = coefficient of determination;

RMSE = root mean square error between observed and simulated discharges in cms;

S_o = topographic slope in m/m;

S_{lb} = lower bound topographic slope in m/m;

S_{fj} = frictional slope in m/m in *j* direction;

t = time in sec;

^{t} = superscript that stands for the time step (*t-1* and *t+1* is previous and next time step)

Δt = time step in sec;

Δt_{max} = maximum time step in sec;

Δt_{min} = minimum time step in sec;

T_c = time of concentration;

T_{cm} = measured time of concentration in minutes;

T_{cs} = simulated time of concentration in minutes;

T_p = observed time to peak in minutes or hr;

T_{pm} = measured time to peak in hr;

T_{ps} = simulated time to peak in hr;

v_{hmax} = corresponding flow velocity in m/sec where h_{max} occurs in the domain;

v_j = flow velocity in m/sec in *j* direction;

v_{max} = maximum flow velocity in m/sec of all cells in the domain;

$\Delta x, \Delta y$ = spacing in x or y direction;

X = distance in m from its boundary along each j direction;

z = bottom elevation in m;

α = parameter given by $S_{fj}^{0.5} / n$;

β = 5/3;

Table 2.1. Total Rainfall Depth, Total Rainfall Duration, Maximum Rainfall Intensity, Total Runoff Volume and Runoff Coefficient for 24 Rainfall Events Measured on a Concrete Surface for the Field Study

Events	Total Rainfall Depth (mm)	Total Rainfall Duration (hr)	Maximum Rainfall Intensity (mm/hr) [a]	Total Runoff Volume (m^3)	Volumetric Runoff Coefficient
04/12/2009	8.18	1.58	34.14	2.22	0.58
04/18/2009	22.40	3.33	34.14	7.11	0.68
04/25/2009	59.39	4.58	89.61	25.55	0.93
04/27~28/2009	7.11	2.92	12.80	2.08	0.63
04/28/2009	11.38	4.42	38.40	4.20	0.79
07/20/2009	47.64	1.92	76.81	18.69	0.84
09/10/2009	14.58	1.50	68.28	3.56	0.53
09/11~12/2009	38.40	14.00	17.07	13.06	0.73
09/13/2009	76.20	1.50	102.41	12.44	0.35
09/23~24/2009	6.05	11.92	4.27	1.85	0.66
09/24/2009	6.40	1.92	12.80	2.55	0.86
10/09/2009	55.83	8.17	55.47	24.54	0.95
10/11/2009	13.16	4.17	25.60	5.63	0.92
10/13/2009	36.63	5.50	85.34	13.67	0.80
10/21~22/2009	27.74	11.83	34.14	11.94	0.93
10/26/2009	7.47	3.92	8.53	2.54	0.73
11/20~22/2009	21.34	24.67	12.80	9.55	0.96
12/01~02/2009	30.58	8.25	12.80	11.76	0.83
01/28~29/2010	70.05	5.00	81.08	30.42	0.94
02/08/2010	9.25	1.42	46.94	3.80	0.89
03/01~02/2010	13.51	16.08	29.87	5.81	0.93
03/08~09/2010	8.53	8.42	34.14	3.29	0.83
03/16~17/2010	19.91	26.83	8.53	7.96	0.86
03/24~25/2010	8.53	1.00	59.74	3.13	0.79

[a] Time interval used to compute rainfall intensity was 5 minutes.

Table 2.2. Time of Concentration (T_c) and Peak Discharge (Q_p) Estimated from Published Experimental Data and Modeled Using Q2DWM for Published Overland Flow Planes Including Q_p Estimated Using Rational Method, Input Parameters, and Model Performance Parameters

T_c (min)		Q_p ($\times 10^{-3}$ m^3/s)			Input Variables				Performance Parameters	
Expt.	Model	Rational Method	Expt.	Model	L (m)	S_o (%)	n	i (mm/hr)	*Ns*	*RMSE* ($\times 10^{-3}$ m^3/s)
3.2 [a]	3	0.091	0.09	0.091	3.7	2	0.013	49	0.87	0.008
8.0 [a]	7.9	0.518	0.518	0.518	21.9	0.1	0.013	46.5	0.99	0.022
6.3 [a]	6.5	1.045	1.048	1.045	21.9	0.1	0.013	93.7	0.99	0.031
6.7 [a]	6.4	1.096	1.099	1.096	21.9	0.1	0.013	98.3	0.98	0.059
4.6 [b]	4.1	2.439	2.435	2.438	152.4	2	0.011	189	0.98	0.116
11.7 [b]	10.8	0.648	0.663	0.649	152.4	0.5	0.011	50.3	0.98	0.031
22.6 [b]	21.3	0.656	0.658	0.655	152.4	0.5	0.035	50.8	0.99	0.024
16.9 [b]	14.9	0.278	0.28	0.279	152.4	0.5	0.011	21.6	0.95	0.024

Note: Input (controlling) variables for the experimental overland flow planes are L = Length in m, S_o = Slope in percent, n = Manning's Roughness Coefficient, and i = Rainfall Intensity in millimeters/hr. Model performance parameters are *Ns* = Nash-Sutcliffe coefficient and *RMSE* = Root Mean Square Error.
[a] Experimental data from Izzard & Augustine (1943).
[b] Experimental data from Yu & McNown (1964).

Table 2.3 Peak Discharge (Q_p) and Time to Peak (T_p) Measured and Simulated Using Q2DWM and Nash-Sutcliffe coefficient (*Ns*) and Root Mean Square Error (*RMSE*) for 24 Rainfall Events Observed on the Concrete Plot

Events	Measured		Simulated		*Ns*	*RMSE*
	Q_{pm} [a] ($\times 10^{-3}$ m^3/s)	T_{pm} (hr)	Q_{ps} [b] ($\times 10^{-3}$ m^3/s)	T_{ps} (hr)		($\times 10^{-3}$ m^3/s)
04/12/2009	0.720	0.33	0.729	0.42	0.95	0.045
04/18/2009	0.615	2.67	0.795	0.50	0.77	0.109
04/25/2009	2.447	2.92	3.553	2.83	0.51	0.535
04/27-28/2009	0.301	0.58	0.326	0.58	0.83	0.030
04/28/2009	0.718	4.00	1.108	4.00	0.82	0.071
07/20/2009	2.721	1.67	4.161	1.67	0.76	0.360
09/10/2009	1.813	0.50	1.149	0.58	0.83	0.198
09/11-12/2009	0.718	6.00	0.678	6.00	0.96	0.037
09/13/2009	2.411	1.08	3.458	1.00	0.86	0.262
09/23-24/2009	0.218	1.25	0.188	1.42	0.76	0.019
09/24/2009	0.385	1.42	0.505	1.42	0.87	0.037
10/09/2009	1.798	0.58	2.372	0.75	0.93	0.137
10/11/2009	0.493	1.08	0.766	0.33	0.86	0.044
10/13/2009	2.194	5.33	3.458	5.33	0.70	0.267
10/21-22/2009	0.974	11.00	1.136	11.00	0.92	0.079
10/26/2009	0.374	0.75	0.366	0.67	0.86	0.031
11/20-22/2009	0.414	20.83	0.521	21.00	0.80	0.045
12/01-02/2009	0.658	6.67	0.884	6.67	0.85	0.076
01/28-29/2010	3.262	3.50	3.831	3.67	0.69	0.453
2/08/2010	0.724	0.83	0.996	0.50	0.78	0.107
03/01-02/2010	0.710	3.00	0.878	3.00	0.86	0.057
03/08-09/2010	0.670	8.17	1.200	8.08	0.64	0.074
03/16-17/2010	0.534	13.08	0.577	12.67	0.86	0.049
03/24-25/2010	0.718	0.33	1.160	0.33	0.72	0.098

[a] subscript *m* stands for measured values.
[b] subscript *s* stands for simulated values.

Table 2.4. Dimensionless Low-Slope Bound (S_{lb}) where “Low-Slope" Behavior is in Effect, Which is Recommended in Published Literature and Current Study

S_{lb} (%)	Methods	Reference(s)
0.1	Classification of data	Yates and Sheridan (1973)
0.5	Observed data analysis	Capece et al. (1988)
0.5	Physical model experiments	De Lima and Torfs (1990)
0.1	Classification of data	Sheridan (1994)
0.2	Numerical model experiments	Van der Molen et al. (1995)
0.05	Numerical model experiments	Su and Fang (2004)
0.5	Physical model experiments	Li et al. (2005), and Li and Chibber (2008)
0.2	Numerical model experiments	Cleveland et al. (2008)
0.3	Observed data analysis	Cleveland et al. (2011)
0.1	Numerical model experiments	Current Study

Table 2.5. Parameter Estimates for the Independent Variables of Time of Concentration (T_c) Estimation Formula Eq. (2.15) for Standard Slopes ($S_o \geq 0.1\%$).

Parameter	Parameter estimate	95% confidence limits		Standard error	t-value	*p*-value
$Ln(C_1)$	2.160	2.103	2.217	0.029	74.6	<0.0001
k_1 *for* L	0.542	0.533	0.551	0.005	119.8	<0.0001
k_2 *for* S_o	-0.359	-0.366	-0.352	0.003	-105.0	<0.0001
k_3 *for* n	0.649	0.642	0.655	0.003	198.9	<0.0001
k_4 *for* i	-0.391	-0.399	-0.384	0.004	-100.7	<0.0001

Table 2.6 Statistical Error Parameters for T_c Estimation Formulas Previously Published and Developed in Current Study for Standard Slopes ($S_o \geq 0.1\%$)

Source or Function	Formula	R^2	*RMSE* [a] (min)	*p*-value [b]
Henderson and Wooding (1964)	$T_c = 6.98\ L^{0.60} n^{0.60} / \left(i^{0.40}\ S_o^{0.3} \right)$	0.936	14.9	-
Morgali and Linsley (1965)	$T_c = 7.05\, L^{0.593} n^{0.605} / \left(i^{0.388}\ S_o^{0.38} \right)$	0.962	11.3	-
T_c = f (L, S_o, n, i), Eq. (2.15)	$T_c = 8.67\, L^{0.541} n^{0.649} / \left(i^{0.391} S_o^{0.359} \right)$	0.974	6.4	<0.0001
T_c = f (nL, S_o, i)	$T_c = 5.89 (nL)^{0.617} / \left(i^{0.400}\ S_o^{0.358} \right)$	0.953	8.7	<0.0001
T_c = f ($L/\sqrt{S_o}$,n,i)	$T_c = 9.84\, n^{0.659} \left(L/\sqrt{S_o} \right)^{0.596} / i^{0.392}$	0.946	8.9	<0.0001
T_c = f ($n\,L/\sqrt{S_o}$, i)	$T_c = 6.82 \left(nL/\sqrt{S_o} \right)^{0.633} / \ i^{0.398}$	0.939	10.5	<0.0001

[a] Statistical parameter R^2 and *RMSE* were developed against T_c data generated from 550 Q2DWM model runs for the parametric study.

[b] The *p*-value reported herein was developed between T_c and all input variables in each regression equation.

Table 2.7. Parameter Estimates for the Independent Variables of Time of Concentration (T_c) Estimation Formula Eq. (2.17) for Low Slopes (S_o < 0.1%)

Parameter	Parameter estimate	95% confidence limits		Standard error	t-value	*p*-value
$Ln(C_2)$	-9.310	-10.288	-8.331	0.496	-18.77	<0.0001
k_5 *for* L	0.563	0.517	0.609	0.023	24.08	<0.0001
k_6 *for* (S_o+S_{lb})	-2.139	-2.281	-1.997	0.072	-29.74	<0.0001
k_7 *for* n	0.612	0.575	0.648	0.019	32.77	<0.0001
k_8 *for* i	-0.304	-0.354	-0.254	0.025	-11.98	<0.0001

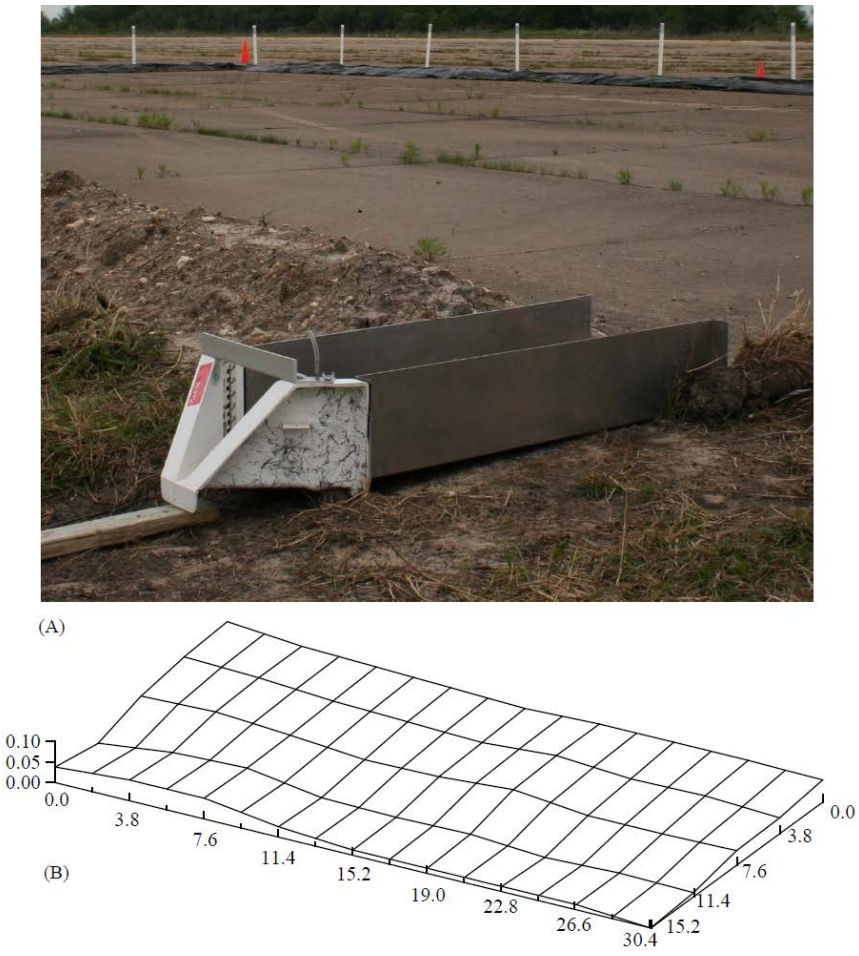

Fig. 2.1. Field study test site; the z-axis scale is magnified 20 times in comparison to the scale of x- or y-axis for better visualization of elevation changes: (A) Airfield concrete runaway plot of 30.5 m by 15.2 m with *H*-flume at the outlet and tipping bucket rain gauge near the plot located at the Texas A&M University Riverside Campus; (B) Digital elevation model of the concrete runaway plot

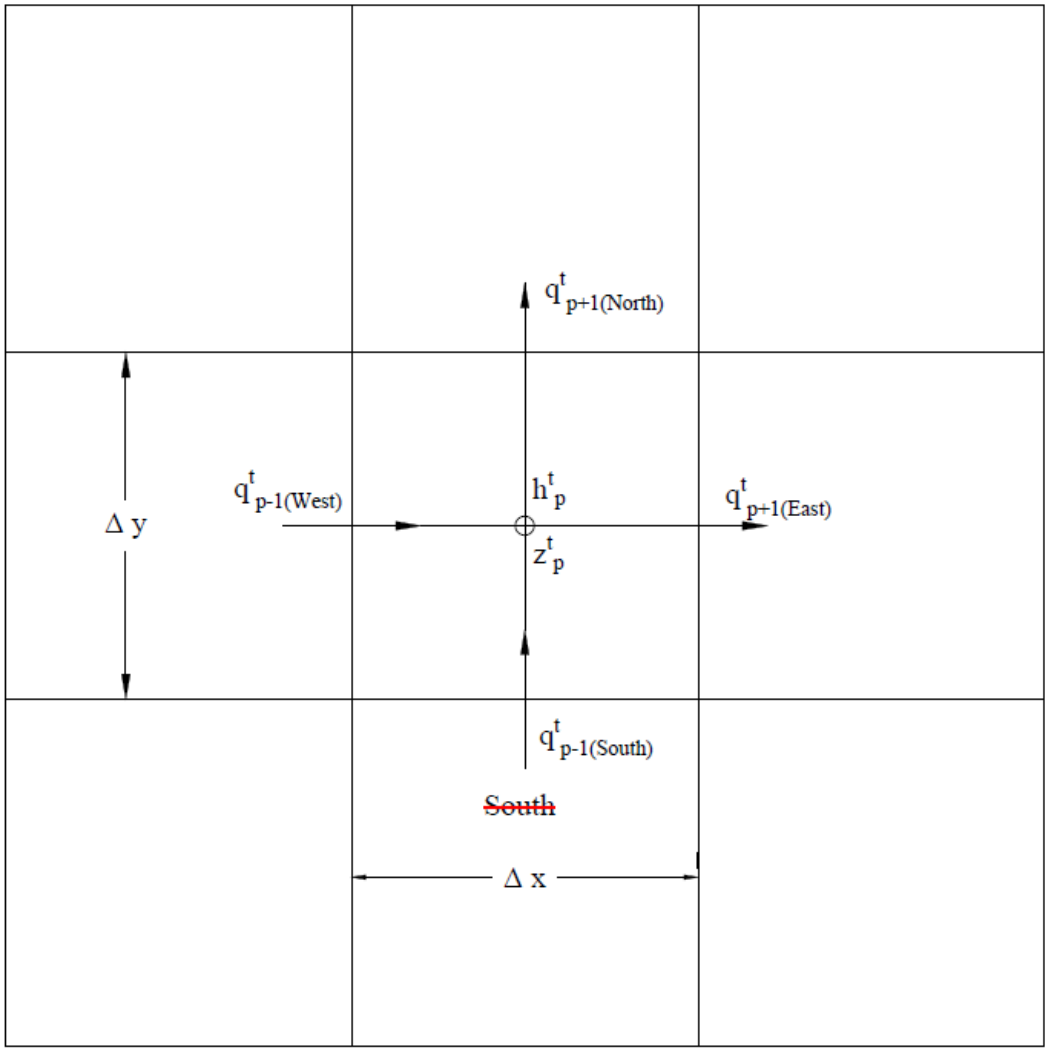

Fig. 2.2. Two-dimensional Q2DWM finite difference grids surrounding the cell *j, k* in the Cartesian computational domain, where *q* is flow rate (flux) between adjacent cells, *h* and *z* are water depth and bottom elevation for the cell

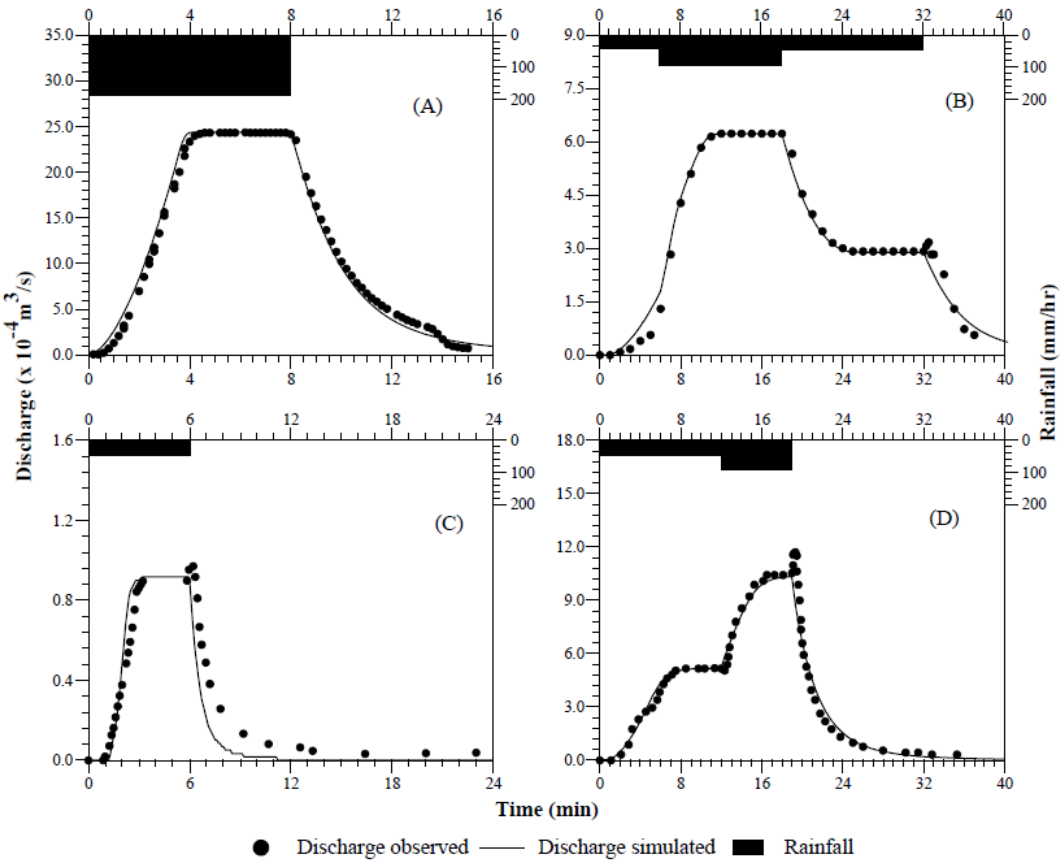

Fig. 2.3. Observed rainfall hyetographs and observed and simulated hydrographs for (A) concrete surface of 152.4 m long and 0.3 m wide with slope of 2%; (B) concrete surface of 76.8 m long and 0.9 m wide with slope of 0.5%; (C) asphalt pavement of 3.7 m long and 1.8 m wide with slope of 2%; and (D) concrete surface of 21.9 m long and 1.8 m wide with slope of 0.1% (observed data presented in (A) and (B) are from Yu and McNown 1963 and in (C) and (D) from Izzard and Augustine 1943)

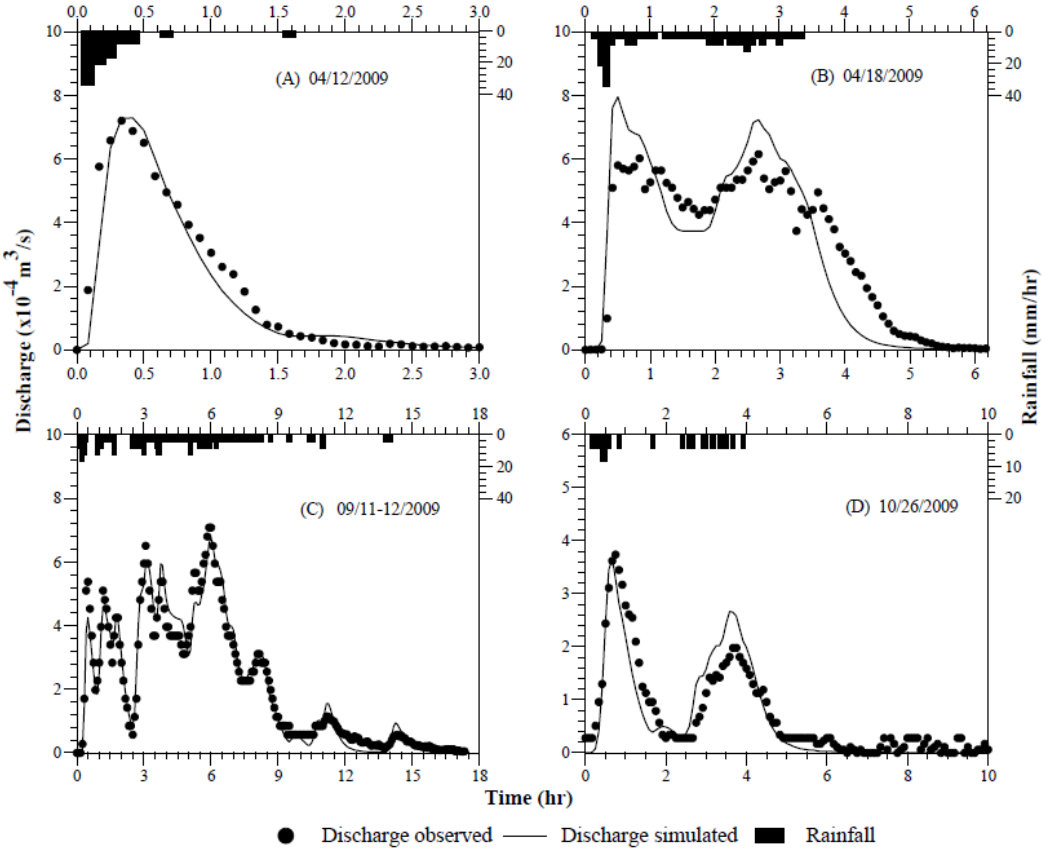

Fig. 2.4. Observed rainfall hyetographs and observed and simulated hydrographs on the concrete plot located at the Texas A&M University for the events on (A) April 12, 2009; (B) April 18, 2009; (C) September 11-12, 2009; (D) October 26, 2009

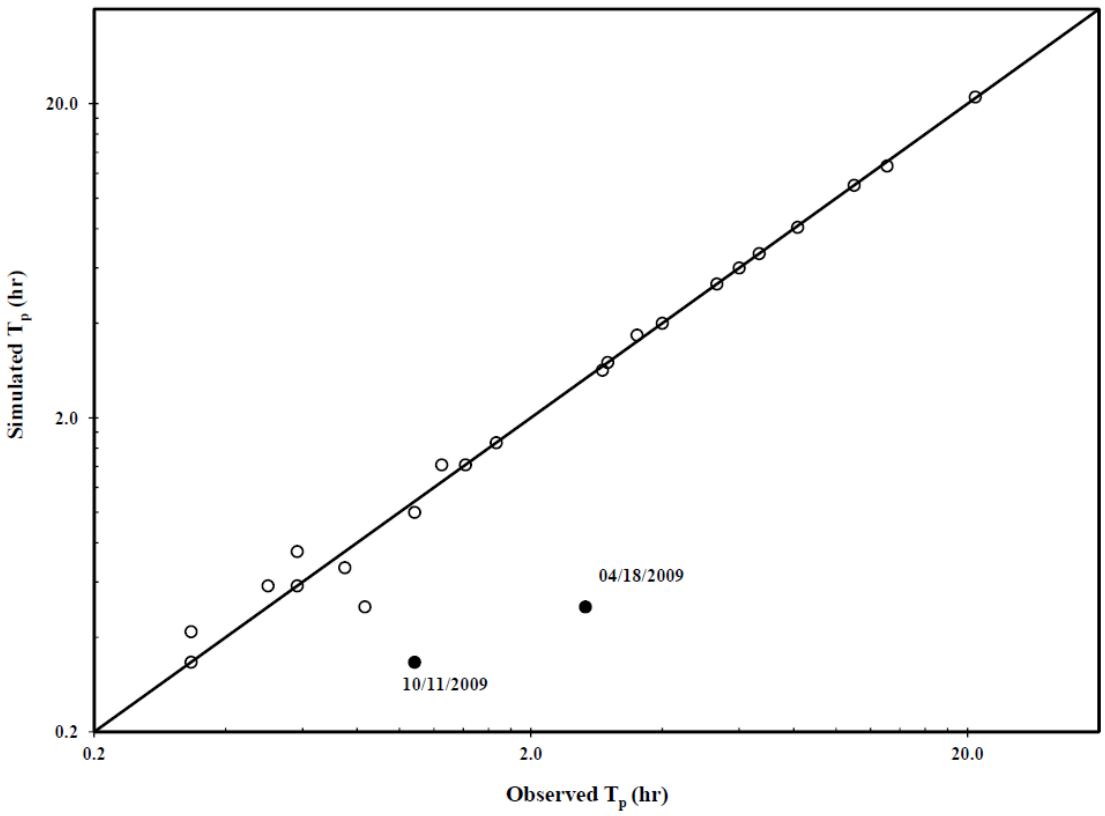

Fig. 2.5. Simulated time to peak (T_p) using Q2DWM versus observed T_p for 24 rainfall events on the concrete plot (Fig. 2.1)

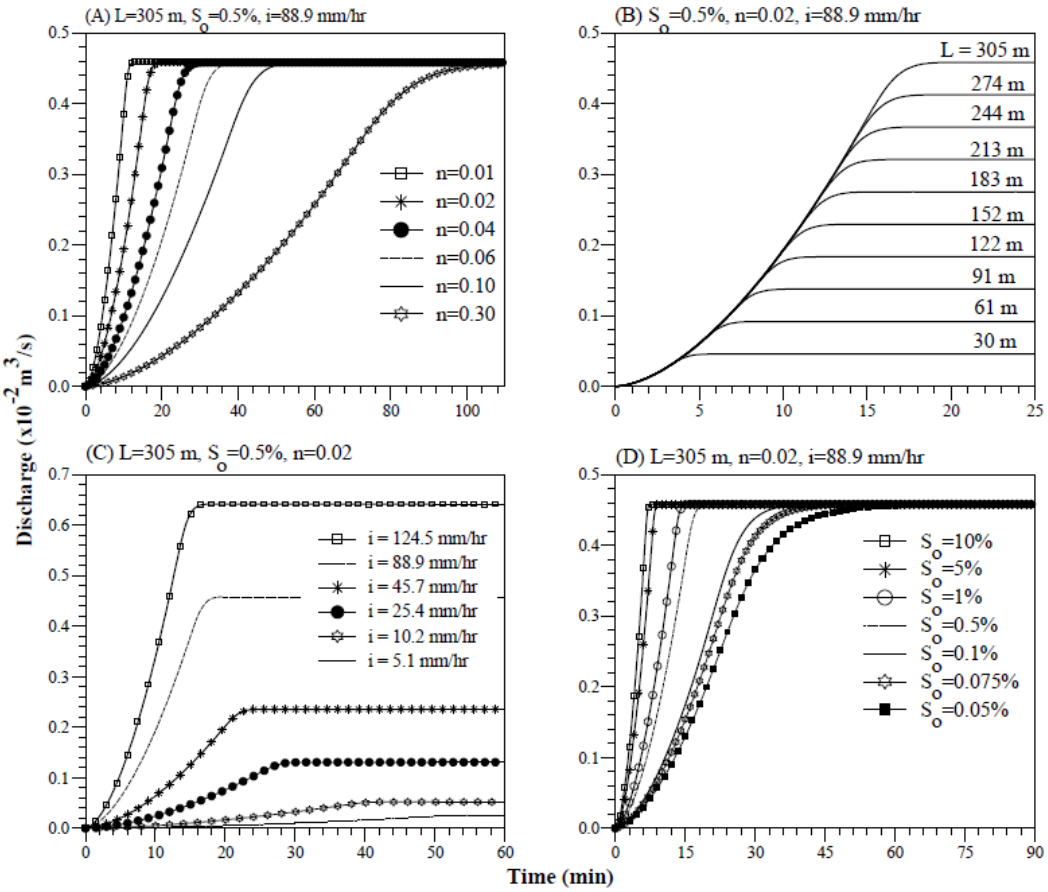

Fig. 2.6. Equilibrium S-hydrographs simulated using Q2DWM on impervious overland flow planes with (A) constant L, S_o, and i, and varying n; (B) constant n, S_o and i, and varying L; (C) constant L, S_o and n, and varying i; (D) constant L, n, and i and varying S_o

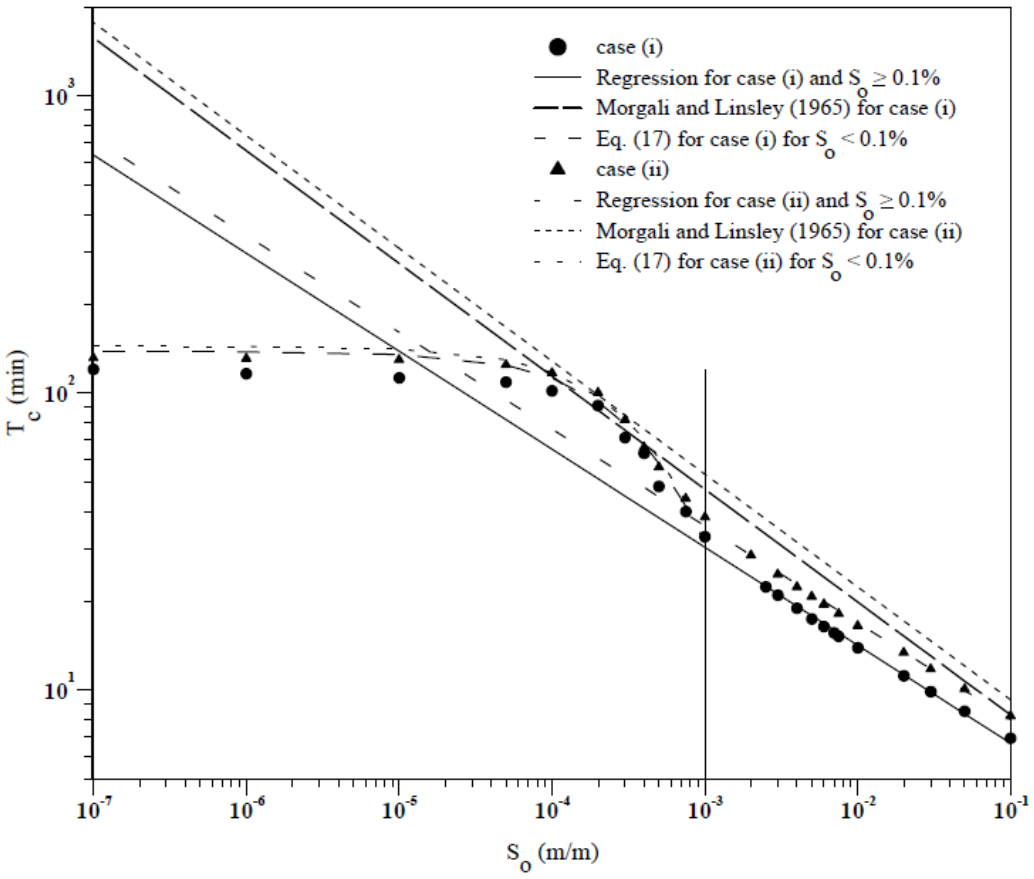

Fig. 2.7. Time of concentration (T_c) estimated using Q2DWM for overland flow planes at different slopes: case (i) L = 305 m, n = 0.02, i = 88.9 mm/hr; and case (ii) L = 90 m, n = 0.035, i = 24.4 mm/hr; linear regressions were developed for T_c data for planes with slope ≥ 0.1% (or S_o = 0.001); T_c predicted using Eq. (2.17) and the formula of Morgali and Linsley (1965) for cases (i) and (ii) are displayed for comparison

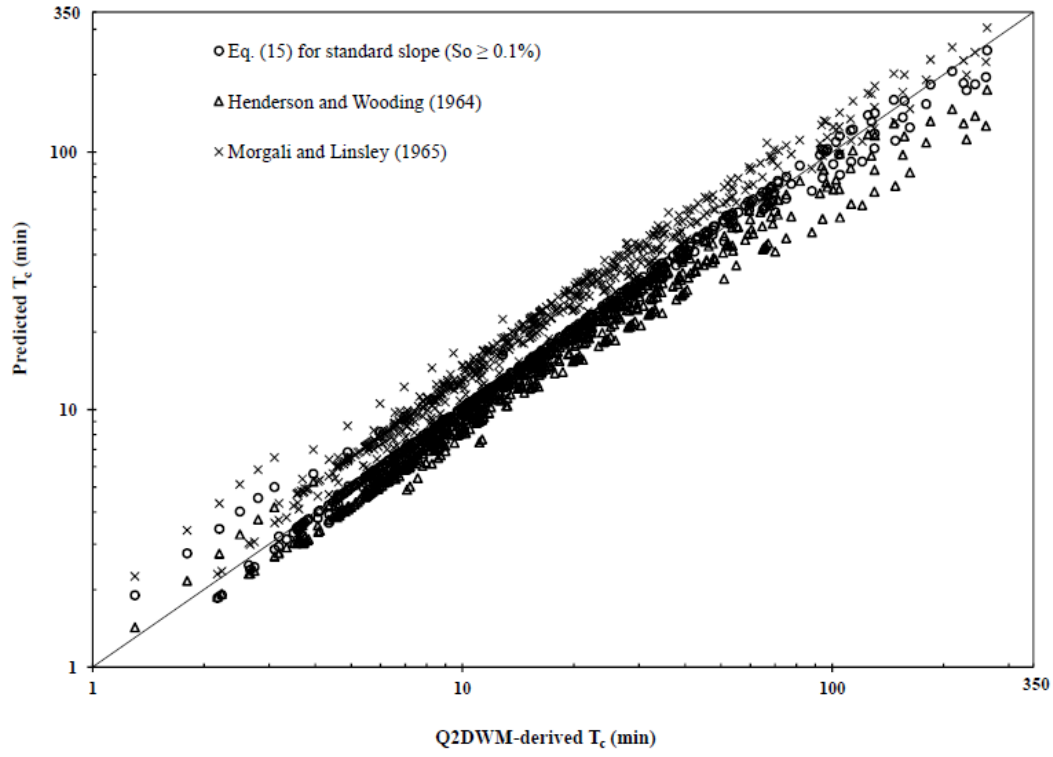

Fig. 2.8. Time of concentration (T_c) of overland flow planes predicted using regression Eq. (2.15) and the formulas of Henderson and Wooding (1964) and Morgali and Linsley (1965) versus T_c developed from numerical experiments using Q2DWM for standard slopes ($S_o \geq 0.1\%$)

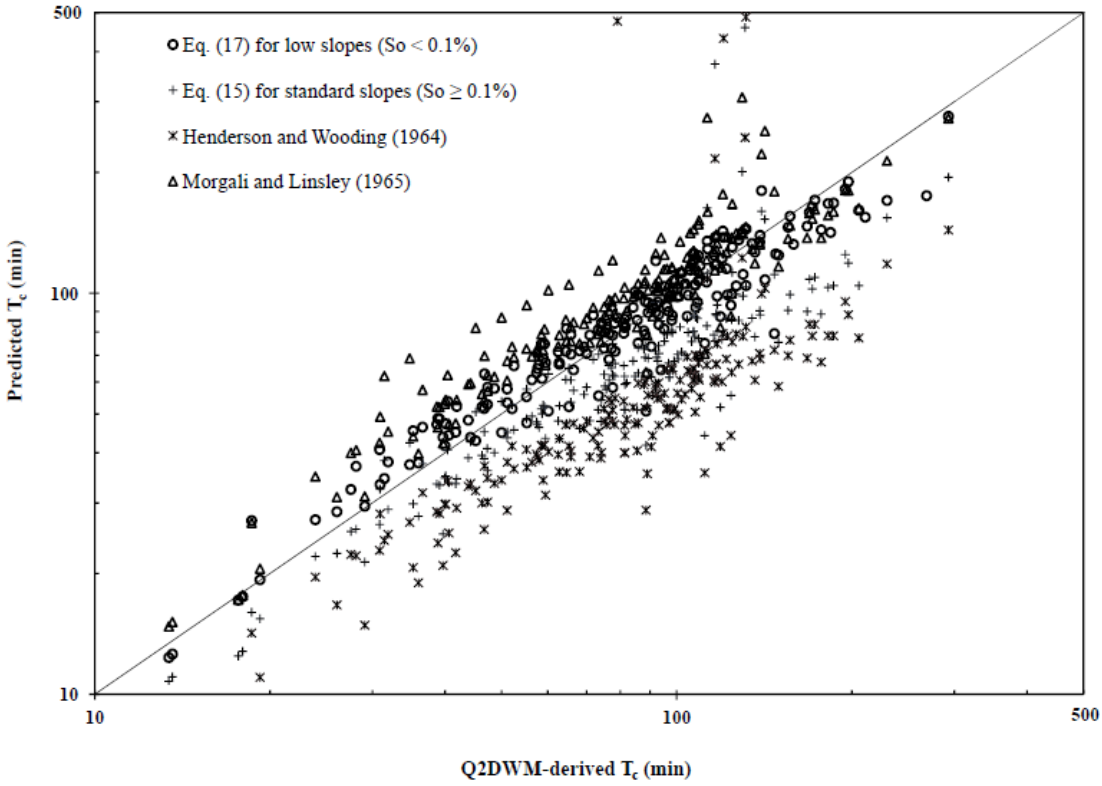

Fig. 2.9. Time of concentration (T_c) of overland flow planes predicted using regression Eqs. (2.17) and (2.15) and the formulas of Henderson and Wooding (1964) and Morgali and Linsley (1965) versus T_c developed from numerical experiments using Q2DWM for low slopes (S_o < 0.1%)

Chapter 3 Estimating Time Parameters of Overland Flow on Impervious Surfaces by the Particle Tracking Method

3.1 Abstract

Travel time and time of concentration T_c are important time parameters in hydrologic designs. Although T_c is the time for the runoff to travel to the outlet from the most remote part of the catchment, most researchers have used an indirect method such as hydrograph analysis to estimate T_c. A quasi-two dimensional diffusion wave model with particle tracking for overland flow was developed to determine the travel time and validated for runoff discharges, velocities, and depths. Travel times for 85%, 95% and 100% of particles arrival at the outlet of impervious surfaces (i.e., T_{t85}, T_{t95}, and T_{t100}) were determined for 530 model runs. The correlations between these travel times and T_c estimated from hydrograph analysis showed a significant agreement between T_c and T_{t85}. All the travel times showed non-linear relations with the input variables (plot length, slope, roughness coefficient, and effective rainfall intensity) but showed linear relations with each other.

3.2 Introduction

The problem of estimating travel velocities and thus travel time from digital elevation model (DEM) is still an open topic. The contribution of Maidment (1993) is just one of the first attempts to relate travel velocities to geomorphic properties, such as contributing area and slope. However, to specify travel speed for each particle along the travel path

was challenging and Maidment (1993) used DEM for overland flow routing based on constant velocity. Similarly, Olivera and Maidment (1999) developed a raster-based, spatially distributed routing technique based on a first-passage-time response function. Smedt et al. (2000) and Liu et al. (2003) proposed flow routing method along flow paths determined by the topography depending upon slopes, flow velocities, and dissipation characteristics along the flow paths. Luo and Harlin (2003) derived simplified theoretical travel time based on watershed hypsometry ignoring friction and stated that the theoretical travel time is not equal to the real measured time to peak discharge. Admiraal et al. (2004) used particle tracking routine in their two-dimensional flow model to release particles (water parcels) at the inlet and computed their paths and travel times through the wetland from the velocity field. Noto and La Loggia (2007) computed travel time of two watersheds implementing a cell-to-cell flow path through the landscape determined from a DEM. Cleveland et al. (2008) used a particle tracking model based on DEM to derive synthetic unit hydrographs for 126 Texas watersheds. The velocity of each particle was calculated using an equation similar to Manning's equation with resistance coefficient and mean flow depth as watershed calibration parameters. Grimaldi et al. (2010) improved the Width Function Instantaneous Unit Hydrograph based on travel time function and tested it in eleven case studies. Froehlich (2011) developed overland flow travel time formula based on rainfall intensity-duration relations using the kinematic wave approximation. Niri et al. (2012) derived semi analytical travel time formula for time-area model applications. Travel time often closely linked to another time parameter, time of concentration T_c commonly used in hydrologic designs and analyses (Kent 1972; Pilgrim 1976; McCuen et al. 1984; Saghafian and Julien 1995).

Most of the empirical formulas developed for T_c are based on estimation of T_c from observed or simulated hydrographs.

Even though T_c is commonly defined as the time it takes runoff to travel from the most distant point along a hydraulic pathway in the watershed to the outlet, many researchers have used the indirect method such as hydrograph analysis to estimate T_c instead of measuring or determining travel time for particles to reach the outlet. Kull and Feldman (1998) assumed the travel time of runoff from each cell in a watershed is proportional to the T_c scaled by the ratio of travel length of the cell over the maximum travel length. This method is implemented in HEC-GEOHMS (Doan 2000). However, this means that the average runoff velocity traveling from any point to the outlet is assumed uniform and constant (Saghafian et al. 2002). This assumption of uniform velocity gives incorrect estimate of both travel time and T_c. Since overland flow is both unsteady and non-uniform, the spatial variability in flow characteristics both across and down the slope makes it difficult to obtain reliable estimates of all the velocities in the flow (Abrahams et al. 1986).

Another alternative to obtain the travel time is to measure the time required for the passage of dye between prespecified distance. There are studies by Emmett (1970b), Dunne and Dietrich (1980), Roels (1984), Govers (1992), and Rouhipour et al. (1999) which recorded travel time of the front of the dye. However, they measured the travel time for the fastest fronts of flow while neglecting the slower-moving parts of the flow. Consequently, their measurements of surface velocity were overestimated (Emmett 1970b; Dunne and Dietrich 1980). Moreover, the larger the fraction in a flow that is outside the measured fast flowing front, the more severe will be the overestimation

of the velocity (Abrahams et al. 1986). Similarly, coarse space and time resolutions of such data have limited their usability (Grimaldi et al. 2012). Similarly, while there is an increasing availability of high resolution DEM for river basins, there is often lack of adequate hydrologic data for small and ungauged catchments (Grimaldi et al. 2010). As a result, travel time estimation for such small and poorly monitored catchments is a topic of increasing interest.

Hence, a direct approach of determining travel time of both fast and slow moving particles to reach the outlet of impervious surfaces is presented in this paper. Even though, the travel of particles in a watershed may occur on the surface or below it or in a combination of both; however, only the travel of particles on the surface (impervious) is considered in this study. A quasi-two dimensional diffusion wave model with particle tracking (DWMPT) was developed from the diffusion hydrodynamic model (DHM) (Hromadka and Yen 1986) and validated extensively using observed discharge, flow depth and velocity data from published studies. The travel times of all particles consisting of both slow moving particles at the upstream and fast moving particles at the downstream are consolidated into representative time parameters. Based on the percentage of particles reaching the outlet, travel times for 85%, 95% and 100% particles arrival at the outlet are defined as T_{t85}, T_{t95} and T_{t100}, respectively. A total of 530 DWMPT runs were performed to determine travel times on impervious surfaces using diverse combinations of the four physically based input variables: length (L), slope (S_o), Manning's roughness coefficient (n) of the surfaces, and effective rainfall intensity (i). The dataset of travel times were generated using particle tracking method with simulated velocities from validated DWMPT for conducting a parametric study. Finally, relations

between these travel times and input variables were developed for impervious overland flow planes, and relations between these travel times were investigated. Relations between T_c estimated from hydrograph analysis and these travel times were developed and presented.

3.3 Diffusion Wave Model With Particle Tracking

Hydrological models are the numerical models, which attempt to mimic the physical processes within a watershed. Both the kinematic and diffusion wave models have been used to simulate these physical processes of surface water movement (Kazezyılmaz-Alhan and Medina Jr. 2007b; López-Barrera et al. 2012a) in hydrologic-hydraulic models. This study deals with numerical simulations of overland flows to investigate direct estimation of travel times of particles on impervious surfaces. Overland flow has been simulated using one- and two-dimensional (1D or 2D) kinematic or diffusion wave models (Henderson and Wooding 1964; Woolhiser and Liggett 1967; Singh 1976; Yen and Chow 1983; Abbott et al. 1986; Chen and Wong 1993; Wong 1996; Jia et al. 2001; Ivanov et al. 2004) and dynamic wave models (Morgali and Linsley 1965; Yeh et al. 1998; Su and Fang 2004). The kinematic wave model is frequently used for the development of T_c formulas (Wong 2005). McCuen and Spiess (1995) suggested that the kinematic wave assumption should be limited to the kinematic wave number $nL/\sqrt{S_o}$ < 100. Hromadka and Yen (1986) developed the quasi-2D diffusion hydrodynamic model (DHM) to incorporate the pressure effects neglected by the kinematic wave approximation. The diffusion wave approximation is generally accurate for the most of the overland flow conditions (Singh and Aravamuthan 1995; Moramarco

and Singh 2002; Singh et al. 2005). It is to understand that DHM is inaccurate for cases in which the inertial terms play prominent roles such as when the slope of the surface is small (Yeh et al. 1998), and studying overland flows on low-sloped planes was presented elsewhere (KC et al. 2014) and beyond the scope of this study.

In this study, a quasi-2D diffusion wave model (DWM) that includes the particle-tracking (PT) capability, called DWMPT, was developed by modifying the quasi-2D DHM (Hromadka and Yen 1986) for simulating overland flow on impervious surfaces/planes. The quasi-2D DWMPT solves the momentum and continuity equations (Akan and Yen 1984). Detailed information of governing equations and numerical solution method used in DHM is described by Hromadka and Yen (1986). A number of modifications have been made in DWMPT over DHM. DWMPT has an efficient numerical stability criteria using Courant number, checks for mass and momentum conservation errors, incorporates detailed rainfall loss models (fractional loss model for impervious surface), and sub-module for determining time of concentration from outflow hydrograph. These modifications and improvements were described in details by KC et al. (2014). The 1D particle tracking model (PTM), a new sub-module of DWMPT, is presented below.

3.3.1 Particle Tracking Model

The fundamental idea of PTM is to introduce discrete particles (or parcels) in the simulation domain that move according to some kinematics. Various approaches of particle tracking are employed in tracking the flow and pollutants in different fields of computational fluid dynamics. Particle-in-cell approach for particle tracking in fluid

dynamics was used earlier by Harlow (1963) and Amsden (1966). Since then, a number of different approaches have been used for tracking particles like the random walk method (Ahlstron et al. 1977; Prickett et al. 1981), method of characteristics (Konikow and Bredehoeft 1978) and marker-and-cell method (Harlow and Welch 1966; Taylor 1983). Similarly, there are many measurement studies of particle tracking that often involve the use of tracers such as dyes (Emmett 1970b; Dunne and Dietrich 1980; Roels 1984; Abrahams et al. 1986), electrolytes (Planchon et al. 2005; Tingwu et al. 2005; Lei et al. 2010), magnetic materials (Ventura Jr et al. 2001; Hu et al. 2011), isotopes (Gardner and Dunn III 1964; Berman et al. 2009), buoyant and fluorescent objects (Bradley et al. 2002; Dunkerley 2003; Meselhe et al. 2004; Tauro et al. 2010; Tauro et al. 2012a). Among these, particle tracking velocimetry (PTV) and particle image velocimetry (PIV) are well suited for measurements of surface velocity of particles in physical models (Admiraal et al. 2004). The credit for initial development of PTV and PIV goes to Chang et al. (1985), Liu et al. (1991), and Landreth et al. (2004) who contributed primarily with their laboratory experimental studies of turbulent flows. Particularly, PIV is a powerful technique to perform velocity measurements for a large number of flows (Adrian 1991; Raffel et al. 1998) and has been used in the velocity measurements for shallow flows (Weitbrecht et al. 2002; Meselhe et al. 2004; Tauro et al. 2012b). However, development of physically based regression equations to calculate travel times using particle tracking in hydrology for small and ungaged catchments has not been attempted.

In this study, the travel time of each particle in the experimental watershed is computed using PTM sub-module that uses flow velocities simulated by DWMPT at each

time step (Fig. 3.1). Over each computational time step, the particle travels over a distance determined by the product of the appropriate velocities and the time interval. The PTM is integrated within the framework of the DWMPT model to simulate the travel time required by the particle at the farthest cell (or designated cells) to arrive at the outlet. Thus, the travel time estimated can be used to define T_c for the watershed because it is the time required by the farthest particle to reach the outlet. The algorithm used to calculate the travel time using PTM is summarized below:

1. Flow velocities such as v_N and v_S in Fig. 3.1 at the inter-cell faces are calculated by the DWMPT by solving the flow equations. The PTM sub-module is activated at the desired time (at the beginning of the rainfall event for impervious surfaces). A single particle at each cell of the discretized domain is initialized.
2. Check the location of the particle; if the particle is at the outlet cell, it is removed out of the domain; and PTM counts number of particles arrival at the outlet. Find the direction of steepest gradient to determine the direction of the flow. The direction of the flow can also be designated in the input file if the travel time at a defined path (e.g., along a stream) has to be determined.
3. Find the first estimate of the particle velocity v_1 (Fig. 3.1) by linear interpolation. Based on the current position of the particle, its velocity is interpolated using modeled velocities of the two opposite inter-cell faces such as v_N and v_S in Fig. 3.1 in the direction of the flow.
4. Calculate the distance Δd that is travelled by the particle using the velocity v_1 during the time interval Δt.

5. Find the second estimate of particle velocity v_2 at the new location d+Δd by linear interpolation. Using an average of the velocities at current (v_1) and new location (v_2), a new estimate of Δd is calculated. This process is iterated until the error between the old and the new estimate of Δd is reduced to pre-specified tolerance. The Courant condition ($C_r \leq 1$) is implemented in DWMPT, and the particle does not travel more than a cell length during a computational time interval.
6. Check whether or not the particle crosses the cell boundary. If the particle travels to the next cell, a new velocity is interpolated using the new particle cell location. The distance travelled for the remaining time interval with the new velocity is calculated similar to above steps.
7. The travel path length and travel time of the particle are updated along with the particle position.
8. The above steps are iterated for the next time step with updated velocities simulated by DWMPT until all the particles in the discretized domain reach the outlet.

Before PTM was used to determine the particle travel time, DWMPT was validated using observed velocity, flow depth, and discharge measurements published in the literature.

3.4 Model Validation

3.4.1 Model Validation using Discharge Hydrographs

The DWMPT was first validated using observed discharge hydrographs published by Chow (1967) and Ben-zvi (1984), who conducted experiments in the Watershed Experimentation System of the University of Illinois. The experiments were conducted

on a 12.2 × 12.2 m (40 × 40 ft) masonite and aluminum-surfaced watershed. The rainfall intensities of the experiments varied from 51 to 305 mm hr^{-1} (2 to 12 in. hr^{-1}), and the rainfall durations from 0.5 to 8 min. The longitudinal slope of the watersheds varied from 0.5% to 3% and cross slope was fixed at 1%. Areas exposed to the rainfall had nine different configurations (Ben-zvi 1984); the configuration called lot 3, which had rainfall in the entire watershed, was modeled using DWMPT in this study. Simulated discharge hydrographs at the outlet for four rainfall events on different slopes selected from lot 3 data of aluminum surface from Ben-zvi (1984) experiments were compared with observed ones (Fig. 3.2). Observed and simulated hydrographs along with rainfall hyetographs for a longitudinal slope of 0.5%, 1.0%, 1.5%, and 2.0% are shown in Figs. 3.2(a)– 3.2(d), respectively. The hyetographs with durations of 8 minutes of the experiments presented in Figs. 3.2(a)– 3.2(d) are uniform rainfall intensities of 215 mm hr^{-1} (8.45 in. hr^{-1}), 291 mm hr^{-1} (11.46 in. hr^{-1}), 220 mm hr^{-1} (8.65 in. hr^{-1}), and 221 mm hr^{-1} (8.72 in. hr^{-1}), respectively. DWMPT simulated hydrographs were generated using calibrated Manning's roughness coefficient of 0.02 for aluminum surface. The agreement between observed and simulated peak discharges and hydrographs is excellent (Fig. 3.2 and Table 3.1).

Yu and McNown (1963) measured runoff and depth hydrographs for different combinations of slope, roughness, and rainfall intensity at the airfield drainage in Santa Monica, California. Table 3.1 lists four rainfall events from Yu and McNown (1963), and four events from Ben-zvi (1984), along with input variables (L in m, S_o in percent, n, and i in mm hr^{-1}), peak discharge Q_p in $m^3 s^{-1}$ estimated using rational method, observed and simulated Q_p values, and model performance parameters. The goodness of fit

between modeled and observed quantities was measured using Nash-Sutcliffe coefficient *Ns* (Legates and McCabe 1999) and root mean square error *RMSE*. For a hydrograph simulation, a good agreement between simulated and measured discharges is achieved when *Ns* exceeds 0.7 (Bennis and Crobeddu 2007). The average *Ns* was 0.97 (ranged from 0.94 to 0.99), and average *RMSE* was 0.04×10^{-3} $m^3 s^{-1}$ (ranged from $0.02–0.09\times10^{-3}$ $m^3 s^{-1}$) for eight simulated hydrographs (Table 3.1). The Q_p estimates from the rational method agreed well with measured and simulated Q_p values (Table 3.1). The average error between the rational method Q_p and observed Q_p was 2.5% (ranged from 0.2% to 7.4% in Table 3.1), and average error between simulated Q_p and observed Q_p was also 2.5% (ranged from 0.1% to 7.5% in Table 3.1). These statistics indicate close agreement between measured and simulated hydrographs.

3.4.2 Model Validation using Depth Hydrographs

The DWMPT was also validated using observed depth hydrographs from Yu and McNown (1963). They measured observed depth to the accuracy of a few ten-thousandths of a foot. Figures 3.3(a) and 3.3(b) show simulated and observed depth hydrographs from concrete surfaces of 152.4 m (500 ft) by 0.3 m (1 ft) with a slope of 2% and 0.5%, respectively, and Fig. 3.3(c) for a turf surface of the same dimension with a slope of 0.5%. Depth hydrographs are reported at 142.3 m (467 ft) from the upstream boundary in Figs. 3.3(a) and 3.3(c) but at 101.5 m (333 ft) for Fig. 3.3(b). The hyetographs for the experiments are effective rainfall intensities of 189 mm hr^{-1} (7.44 in. hr^{-1}) with duration of 8 minutes, 49 mm hr^{-1} (in. hr^{-1}) with duration of 16 minutes, and 49 mm hr^{-1} (in. hr^{-1}) with duration of 28 minutes in Figs. 3.3(a), 3.3(b), and 3.3(c),

respectively. Depth hydrographs simulated using DWMPT matched well with the observed ones (Fig. 3.3). The average *Ns* was 0.96, and average *RMSE* was 0.63 mm for three simulated depth hydrographs. These statistics indicate close agreement between measured and simulated depth hydrographs.

3.4.3 Model Validation using Velocity Observations

The DWMPT was also validated using calculated and observed velocity data from Yu and McNown (1963), Izzard and Augustine (1943), and Mügler et al. (2011). Yu and McNown (1963) used an ogee-shaped weir to measure the runoff at the outlet. Since the critical flow condition was created for the measurement of the observed discharge hydrograph, the calculated velocity can be obtained from observed discharge hydrograph using critical flow equation. Four example comparisons using calculated velocity data from Yu and McNown (1963) are shown in Figs. 3.4(a)–3.4(d). Calculated and simulated runoff velocity hydrographs at the outlet for a 152.4 m (500 ft) long and 0.3 m (1 ft) wide concrete surface with slopes of 2%, 0.5%, and 0.5% are shown in Figs. 3.4(a), 3.4(b), and 3.4(d), respectively, and for a turf surface with a slope of 0.5% are shown in Fig. 3.4(c). The hyetographs for the experiments presented in Figs. 3.4(a)–3.4(d) were uniform effective rainfall intensities of 189 mm hr^{-1} (7.44 in. hr^{-1}) with duration of 8 minutes, 50 mm hr^{-1} (1.98 in. hr^{-1}) with duration of 16 minutes, 51 mm hr^{-1} (2.0 in. hr^{-1}) with duration of 28 minutes, and 22 mm hr^{-1} (0.85 in. hr^{-1}) with duration of 22 minutes, respectively. Even though turf surface is a pervious surface, it was simulated by DWMPT as an impervious surface. The rainfall in the experiment was applied for a longer time to make the rainfall loss uniform. The rainfall input to the DWMPT was the

effective rainfall intensity. DWMPT simulated velocity hydrographs were generated using calibrated Manning's roughness coefficient of 0.011–0.013 for concrete and 0.035 for turf surfaces (Table 3.2). The calculated velocities compared well with the simulated velocities at the outlet having the critical flow condition (Fig. 3.4).

Izzard and Augustine (1943) collected rainfall and runoff data from paved and turf surfaces for the Public Roads Administration in 1942. Runoff was measured by a 0.4 ft wide HS flume with head measured by a point gauge. The calculated velocity hydrograph was obtained similarly from observed discharge hydrograph using critical flow equation. Table 3.2 lists four rainfall events from Yu and McNown (1963) and four events from Izzard and Augustine (1943), along with input variables L, S_o, n, and i; and model performance parameters (*Ns* and *RMSE*) developed between simulated and calculated velocity hydrographs. The average *Ns* was 0.89 (ranged from 0.66 to 0.98), and average *RMSE* was 2.0 cm s^{-1} (ranged from 1.1–2.5 cm s^{-1}) for eight simulated velocity hydrographs (Table 3.2). These statistics indicate a strong agreement between measured and simulated velocity hydrographs.

Mügler et al. (2011) collected velocity measurements to compare different roughness models in a 10 m (32.8 ft) long by 4 m (13.1 ft) wide sandy soil surface with a 1% longitudinal slope. The rainfall simulator provided a constant average intensity of 69 mm hr^{-1} (Esteves et al. 2000). Rainfall was applied for more than 2 hours to maintain steady runoff before the flow velocity measurements were performed. The steady state discharge was 0.5×10^{-3} m^3 s^{-1} (0.018 ft^3 s^{-1}). The flow velocities were measured at 60 monitoring points on the surface using the salt velocity gauge technology, an automated, miniaturized device based on the inverse modeling of the propagation of a

salt plume (Tatard et al. 2008). The observed flow velocities ranged from 0.006 m s^{-1} to 0.27 m s^{-1} and provided a valuable dataset for comparison with DWMPT simulated velocities. Figure 3.5 shows observed versus simulated velocities at 60 locations within the plot. The *Ns* for velocity data pairs is 0.76, and *RMSE* is 0.03 m s^{-1}. All above statistics derived between velocity observations from Yu and McNown (1963), Izzard and Augustine (1943), and Mügler et al. (2011) and simulations by DWMPT indicate that the flow model can predict runoff velocities with an acceptable accuracy and, therefore, can be used for particle tracking to determine travel times of the particles.

3.5 Computation of Travel Times and Time Of Concentration

3.5.1 Flow Velocity of Overland Flow

Previous studies (Abrahams et al. 1986; Maidment 1993; Kull and Feldman 1998; Grimaldi et al. 2012) have acknowledged the difficulty of measuring the runoff speed of overland flow in the whole study domain with fine spatial resolution. Hence some researchers have assumed constant velocity to compute travel time of the overland flow (Maidment 1993; Kull and Feldman 1998). However, the flow characteristics (such as flow depth in Fig. 3.2 and flow velocity in Figs. 3.4, 3.5 and 3.6) of the overland flows are spatially varied (non-uniform) and can be unsteady before reaching equilibrium condition and after the cease of rainfall event. Figure 3.6 shows simulated velocity distributions from the upstream boundary to the downstream outlet at different simulation times for a concrete surface of 152.4 m (500 ft) by 0.3 m (1 ft) with a slope of 2% under a constant effective rainfall intensity of 189 mm hr^{-1} (7.44 in h^{-1}) with duration of 8 minutes. The length of the plot was discretized into 500 cells, and the x-axis represents

the distance of each cell (grid) center from the outlet (152.2 m for the upstream boundary cell and 0.2 m for the outlet cell). Before surface runoff reaches equilibrium condition (time t = 1, 2, and 3 minutes), flow velocity increases from the upstream cell (near zero velocity) towards downstream cells up to a certain distance and then becomes uniform. Therefore, before reaching equilibrium, there is a downstream portion with the front of fast moving particles and an upstream portion with slow moving particles trailing behind. At about 4 minutes, the uniform flow portion disappears, and it indicates the fast moving particles (front) from the upstream have arrived at the outlet. From 4 to 8 minutes, velocity distribution remains more or less the same and is spatially varied. When the rainfall stops at 8 minutes (Fig. 3.6), runoff velocities at all cells begin to decrease with time. The velocity distributions after the cease of the rainfall event (t > 8 minutes) are spatially varied over the whole plot length and are different from ones before reaching equilibrium (t < 4 minutes). In comparison to the velocity distributions for a steady rainfall event, velocity distributions of an overland flow under unsteady rainfall intensities would be highly unsteady and spatially varied and are not graphically illustrated here.

3.5.2 Travel Times

Based on spatially varied velocity distributions (an example on Fig. 3.6), pollutant particles released at different locations of the plot would have different travel times reaching the outlet. The particles near the upstream boundary of the plot travel slowly until they travel to a certain distance away where they gradually start picking up velocity. Therefore, the travel time of a particle released or washed-off by the runoff near the

upstream boundary would be significantly larger than the travel time of other particles released at the other middle locations of the plot. Hence, to correctly estimate the overall travel time of runoff/pollutant particles on a plot under a rainfall event, both the travel times of the slow-moving particles at the upstream boundary area and the fast-moving particles at the moving front should be considered. In this study, one particle is assigned for each computational cell and initiated when the rainfall begins, for example, the simulation domain of the plot for Fig. 3.6 has 500 cells with 500 virtual particles used for PTM, i.e., 500 particles were tracked by DWMPT to determine the percent of particles exiting the outlet in order to study various characteristic travel times for overland flow.

Including these slower particles near the upstream boundary makes the overall travel time of the plot longer. Similar argument also applies to discharge when it approaches equilibrium under a constant rainfall. It takes much longer time for discharge to reach equilibrium when the time rate of change of discharge near equilibrium is very small (KC et al. 2014). Hence, to avoid this sensitivity of travel time to computational equilibrium (McCuen 2009), T_c is usually computed at the time less than 100% contribution of the watershed to peak discharge (Su and Fang 2004; Wong 2005; KC et al. 2014). Following similar arguments, characteristic travel times for 85%, 95% and 100% particles arrival at the outlet were computed and were defined as T_{t85}, T_{t95}, and T_{t100}, respectively, based on the time when specified percentage of particles have arrived at the outlet of the plot. It should be noted that authors intend to choose some percentages less than 100%; however, the exact selection of T_{t85} and T_{t95} is arbitrary.

3.5.3 Time of Concentration

Another commonly used hydrologic time parameter (McCuen 2009), closely linked to travel time is T_c. In spite of frequent use, T_c lacks universally accepted definition and method to quantify it. Several definitions of T_c can be found in the literature along with several related estimation methods for each definition. Grimaldi et al. (2012), using their case studies, have demonstrated that available approaches for the estimation of T_c may yield numerical predictions that differ from each other by up to 500%.

McCuen (2009) divided multiple definitions of T_c into two broad categories; travel time for runoff particles reaching the watershed outlet and lag time related to the distribution of rainfall and runoff. McCuen then divided the latter definition into six more computational methods for estimating T_c. However, the estimation of T_c by latter definition requires the knowledge of distribution of rainfall hyetograph and runoff hydrograph, which are not available for ungauged watersheds. Hence, T_c defined as travel time of runoff is often used in many previous studies and this study. Even though researchers as early as Mulvany (1851) and Kuichling (1889a) to McCuen (2009) defined T_c similarly as the time it takes for runoff to travel from the most distant point along a hydraulic pathway in the watershed to the outlet, their computational implementation of estimating T_c differed. An indirect method such as hydrograph analysis is often used to estimate T_c and then develop T_c regression formulas with respect to certain independent variables.

Several researchers (Kuichling 1889a; Hicks 1942a; Muzik 1974) estimated T_c as the time until discharge from a given drainage area reaches equilibrium. Izzard and Hicks (1946) defined T_c from the beginning of a rainfall until the runoff reaches 97% of

the rainfall input rate. Wong (2005) considered T_c as the time from the beginning of effective rainfall to the time when flow reaches 95% of the equilibrium discharge. Su and Fang (2004) and KC et al. (2014) determined T_c as the time from the beginning of effective rainfall to the time when the flow reaches 98% of the peak discharge, and the same method is also used in this study to compute T_c.

Figure 3.7 shows an example how three characteristic travel times (T_{t85}, T_{t95} and T_{t100}) and T_c were computed from either the percent of particles arrival at the outlet or outflow hydrograph. Both observed and simulated hydrographs are shown in Fig. 3.7 for an asphalt pavement of 21.9 m long and 1.83 m wide with a slope of 0.1% and a rainfall of 98.3 mm hr^{-1} for 11 minutes (Izzard and Augustine 1943). The occurrence times of 98% of peak discharges (Q_p) and 100% Q_p in the discharge hydrograph are shown in Fig. 3.7 with three characteristic travel times (T_{t85}, T_{t95}, and T_{t100}). Table 3.2 lists three T_c estimates (in minutes) using observed and simulated hydrographs and using empirical equation from KC et al. (2014) for non-low slopes, and travel times T_{t85}, T_{t95} and T_{t100} (in minutes) derived from DWMPT for four rainfall events from Yu and McNown (1963) and four events from Izzard and Augustine (1943). Three T_c estimates agree well with each other. The estimates of travel times T_{t85}, T_{t95}, and T_{t100} are different from T_c because travel times and T_c are computed using two separate methods. Figure 3.7 shows that T_{t100} occurs when the discharge is near the equilibrium discharge and travel times T_{t95} and T_{t85} occur when the discharge approaches the equilibrium discharge. The time rate of change of discharge near equilibrium is very small as shown in Fig. 3.7. However, the time rate of change of discharge near equilibrium also depends on input parameters. The discharge approaches the equilibrium faster when the

plot length is shorter, the slope is steeper, the surface roughness is smaller, and the rainfall intensity is larger. Figure 3.7 as an example and Table 3.2 for eight experiments show that T_c may correlate to T_{t85} and T_{t95}, which will be further explored at the next step.

In this study, the travel times are computed based on the percentage of particles arrival at the outlet using PTM coupled with DWM velocity simulation, which is to directly compute the travel time of particles through the simulation domain. However, T_c is computed from the discharge hydrograph as the time from the beginning of effective rainfall to the time when the flow reaches 98% of the peak discharge. Therefore, T_c directly depends on the flow depth of a single cell at the outlet. However, the travel times T_{t85}, T_{t95} and T_{t100} are consolidated time parameters synthesizing the arrival times of most or all particles at the outlet cell and are more representative time parameters to describe the movement of runoff/pollutant particles inside the simulation domain. To develop regression equations for estimating travel times (T_{t85}, T_{t95} and T_{t100}), based on physically based input parameters, provides a simple and easy method to determine the overall travel time characteristics of the overland flows. The parametric study to find the relations between the travel times and the input variables (L, S_o, n, and i) is given in the next section.

3.6 Parametric Study of the Travel Time of Overland Flow

Several authors (Morgali and Linsley 1965; Woolhiser and Liggett 1967; Su and Fang 2004; KC et al. 2014) have derived estimation formulas using the four physically based input variables: L, S_o, n, and i. Hence, same input variables are chosen for parametric study computing travel times of overland flows. More than 530 separate values of each

time parameter (T_c, T_{t85}, T_{t95} and T_{t100}) were determined from numerical experiments using DWMPT by varying input variables, L, S_o, n, and i to extend the dataset available for regression analysis. The input variable L was varied from 5 to 305 m (16 to 1000 ft), S_o from 0.1% to 10%, n from 0.01 to 0.80, and i from 2.5 to 254 mm hr^{-1} (0.1 to 10.0 in. h^{-1}). The numerical experiments were simulated holding the three variables constant and varying the fourth one by 10–20%.

A generalized power relation, equation (3.1) was chosen for developing the regression equations,

$$T_{t85} = C_1 \, L^{k_1} \, S_o^{k_2} \, n^{k_3} \, i^{k_4} \, , \tag{3.1}$$

where L is in m, S_o is in m m^{-1} (dimensionless), i is in mm hr^{-1}, C_1, k_1, k_2, k_3, and k_4 are regression parameters. Equation (3.1) was log-transformed and non-linear regression was used to estimate parameter values. The resulting equation for T_{t85} is

$$T_{t85} = 9.25 \frac{L^{0.599} n^{0.609}}{i^{0.399} S_o^{0.303}} \, , \tag{3.2}$$

where T_{t85} is in minutes, and other variables are as previously defined. Regression results are presented in Table 3.3. Statistical results indicate that the input variables L, S_o, n, and i have a high level of significance with the p-value < 0.0001 (Table 3.3) and are critical variables in the determination of T_{t85}. The regression parameters (C_1, k_1, k_2, k_3, and k_4) have small standard errors and small ranges of variation at the 95% confidence interval (Table 3.3). Predicted values from equation (3.2) compare well with the estimates from DWMPT numerical experiments (Fig. 3.8).

Similar regression analysis resulted following equations for T_{t95}:

$$T_{t95} = 10.66 \frac{L^{0.599} n^{0.615}}{i^{0.399} S_o^{0.305}}, \quad (3.3)$$

and for T_{t100}:

$$T_{t100} = 12.23 \frac{L^{0.594} n^{0.632}}{i^{0.398} S_o^{0.318}}. \quad (3.4)$$

The estimation equations for T_{t85}, T_{t95} and T_{t100} along with the statistical parameters: coefficient of determination R^2, *RMSE*, and *p*-values are summarized in Table 3.4. The R^2 and *RMSE* were developed against respective time parameter (T_{t85}, T_{t95}, and T_{t100}) data generated from 530 DWMPT model runs for the parametric study. The estimation equations have an excellent average R^2 of 0.99 and low average *RMSE* of 1.06 min. The *p*-values reported herein were developed between respective time parameters and all four input variables (L, S_o, n, i) and are < 0.0001 showing the high level of statistical significance for each estimation equation (Table 3.4). The regression equations for three travel time parameters have the same or almost the same exponents for each of input variables L, S_o, n, and i (Table 3.4). Travel times are directly proportional (non-linearly) to L and n, and inversely proportional (non-linearly) to S_o and i. Saghafian et al. (2002) also showed that for spatially uniform yet temporal variable excess rainfall intensity, the travel time is inversely proportional to the rainfall intensity raised to a power of 0.4. Designers can use the estimating equations (Table 3.4) to determine the overall travel times of 85%, 95% and 100% particles arriving at the outlet of an impervious plot by simply using physically based input parameters.

The time parameters T_c, T_{t95}, and T_{t100} show a linear variation with T_{t85} (Fig. 3.9). This is because regression equation for T_c developed by KC et al. (2014) has similar exponents to four input variables as equations in Table 3.4 do. Hence, the time

parameters T_c, T_{t95}, and T_{t100} can also be expressed in linear relations with T_{t85} (Table 3.5). The equation for T_c in terms of T_{t85} is

$$T_c = 0.97 T_{t85} \tag{3.5}$$

Similarly the equations for T_{t95} and T_{t100} in terms of T_{t85} are

$$T_{t95} = 1.17 T_{t85} \tag{3.6}$$

and

$$T_{t100} = 1.43 T_{t85} \tag{3.7}$$

Equation (3.5) shows that T_{t85} estimated using the particle-tracking method could be used to compute T_c with acceptable accuracy, which was estimated from outflow hydrograph analysis. Equations (3.6) and (3.7) show T_{t95} and T_{t100} are about 17% and 43% larger than T_{t85}, respectively. The equations for T_c, T_{t95}, and T_{t100} in terms of T_{t85} along with R^2, *RMSE* are given in Table 3.5. The R^2 and *RMSE* were developed against respective time parameters (T_c, T_{t95}, and T_{t100}) from DWMPT and predicted using corresponding equation (Table 3.5) for 530 data points. The linear equations have an excellent average R^2 of 0.98 and average *RMSE* of 5.78 min (Table 3.5). Estimations of three travel times were useful to check the inter-relations between these travel times. From Tables 3.4 and 3.5, it can be seen that T_{t95} can be approximately expressed as an average of T_{t85} and T_{t100}. Even though, all the travel times (T_{t85}, T_{t95}, and T_{t100}) show the non-linear relations with the input variables L, S_o, n, and i; the characteristic time parameters showed linear relations between each other (T_{t85}, T_{t95}, and T_{t100}, and T_c).

3.7 Summary and Conclusions

A quasi-two dimensional diffusion wave model with particle tracking, DWMPT was

developed from the diffusion hydrodynamic model DHM (Hromadka and Yen 1986) for calculating travel time of all the particles in the discretized domain of the impervious overland surface. A comprehensive validation of the model was performed using discharge, velocity and depth data from four different sources (Izzard and Augustine 1943; Yu and McNown 1963; Ben-zvi 1984; Mügler et al. 2011). The travel times of all particles in the domain consisting of both slow moving particles at the upstream and fast moving particles at the downstream are considered in DWMPT, and consolidated representative time parameters T_{t85}, T_{t95}, and T_{t100} are extracted. Based on the percentage of particles that have arrived at the outlet, travel times for 85%, 95% and 100% particles arrival at the outlet are defined as T_{t85}, T_{t95}, and T_{t100}, respectively. A total of 530 DWMPT runs were performed to determine travel times on impervious surfaces using diverse combinations of the four physically based input variables L, S_o, n, and i; and were used to develop estimation equations for T_{t85}, T_{t95} and T_{t100}. All the travel times (T_{t85}, T_{t95}, and T_{t100}) showed non-linear relations with the input variables (L, S_o, n, and i) in equations (3.2), (3.3), and (3.4); and are directly proportional to L and n (both raised approximately to a power 0.6) and inversely proportional to S_o (raised approximately to a power 0.3) and i (raised approximately to a power 0.4). Similarly, T_c was estimated from hydrograph analysis as the time when outflow discharge reaches 98% of Q_p, and T_{t85} showed a close correlation with T_c as shown in equation (3.5) and can be used to estimate T_c. Even though, all the travel times showed non-linear relations with the input variables, they showed linear relations with each other in equations (3.6) and (3.7), and T_{t95} can be approximately expressed as an average of T_{t85} and T_{t100}.

Table 3.1. Input variables, peak discharges Q_p estimated using the rational method, from experimental data, and modeled using DWMPT, and corresponding model performance parameters calculated between observed and modeled discharge hydrographs for impervious overland flow planes.

L (m)	S_0 (%)	n	i (mm hr^{-1})	Q_p ($\times 10^{-3}$ m^3 s^{-1})			Ns	$RMSE$ ($\times 10^{-3}$ m^3 s^{-1})
				Rational Method	Observed	Modeled		
152.4 [a]	2.0	0.013	189	0.086	0.086	0.086	0.98	0.116
152.4 [a]	0.5	0.011	50	0.023	0.023	0.023	0.98	0.031
152.4 [a]	0.5	0.035	51	0.023	0.023	0.023	0.99	0.024
152.4 [a]	0.5	0.011	22	0.010	0.010	0.010	0.95	0.024
12.2 [b]	0.5	0.020	215	0.313	0.338	0.313	0.94	0.895
12.2 [b]	1.0	0.020	291	0.425	0.439	0.425	0.97	0.831
12.2 [b]	1.5	0.020	220	0.321	0.334	0.320	0.98	0.497
12.2 [b]	2.0	0.020	221	0.323	0.331	0.323	0.97	0.733

Note: Input variables for the experimental overland flow planes are L = length in m, S_o = slope in percent, n = Manning's roughness coefficient, and i = effective rainfall intensity in mm hr^{-1}. Model performance parameters are Ns = Nash-Sutcliffe coefficient and $RMSE$ = Root Mean Square Error.

[a] Experimental data from Yu & McNown (1964)

[b] Experimental data from Ben-Zvi (1984)

Table 3.2. Input variables, model performance parameters for simulated velocity hydrographs, time of concentration T_c, travel times (T_{t85}, T_{t95} and T_{t100}) for impervious overland flow planes.

L (m)	S_0 (%)	n	i (mm hr^{-1})	Ns	$RMSE$ (cm s^{-1})	T_c (min)			Travel Times (min)		
						Experiment	Model	KC et al. (2014)	T_{t85}	T_{t95}	T_{t100}
152.4 [a]	2.0	0.013	189	0.98	1.6	4.6	4.1	4.1	4.7	5.4	6.2
152.4 [a]	0.5	0.011	50	0.97	1.1	11.7	10.8	10.2	12.0	13.9	16.2
152.4 [a]	0.5	0.035	51	0.97	1.2	22.6	21.3	21.5	24.4	28.1	33.1
152.4 [a]	0.5	0.011	22	0.96	1.1	16.9	14.9	14.2	16.8	19.5	22.7
3.7 [b]	2	0.013	49	0.66	2.5	3.2	2.0	0.9	0.9	1.0	1.3
21.9 [b]	0.1	0.013	46	0.96	1.6	8.0	8.1	7.3	7.0	8.2	9.6
21.9 [b]	0.1	0.013	94	0.97	1.6	6.3	6.5	5.6	5.4	6.4	7.6
21.9 [b]	0.1	0.013	98	0.96	2.2	6.7	6.5	5.5	5.2	6.3	7.5

Note: Input variables for the experimental overland flow planes are L = length in m, S_o = slope in percent, n = Manning's roughness coefficient, and i = effective rainfall intensity in mm hr^{-1}. Travel times for 85%, 95% and 100% particles arrival at the outlet are T_{t85}, T_{t95}, and T_{t100}, respectively. Model performance parameters are Ns = Nash-Sutcliffe coefficient and $RMSE$ = Root Mean Square Error.

[a] Experimental data from Yu & McNown (1964)

[b] Experimental data from Izzard and Augustine (1943)

Table 3.3. Parameter estimates of the regression equation (3.2) for the independent variables of travel time for 85% of particles arrival at the outlet (T_{t85}) for impervious overland flow surfaces.

Parameter	Parameter estimate	95% confidence limits		Standard error	t-value	*p*-value
$Ln(C_2)$	2.225	2.209	2.240	0.008	284.42	<0.0001
k_1 *for L*	0.599	0.597	0.602	0.001	473.66	<0.0001
k_2 *for So*	-0.303	-0.304	-0.301	0.001	-331.74	<0.0001
k_3 *for n*	0.609	0.607	0.611	0.001	699.21	<0.0001
k_4 *for i*	-0.399	-0.401	-0.397	0.001	-381.35	<0.0001

Table 3.4. Statistical error parameters for regression equations of three time parameters (T_{t85}, T_{t95}, and T_{t100}) developed for impervious overland flow surfaces.

Function, Equation	Formula	R^2	*RMSE* [a] (min)	*p*-value [b]
T_{t85} = f (L, S_o, n, i), Equation (3.2)	$T_{t85} = 9.25 L^{0.599} n^{0.609} / \left(i^{0.399} S_o^{0.303} \right)$	0.999	1.1	<0.0001
T_{t95} = f (L, S_o, n, i), Equation (3.3)	$T_{t95} = 10.66 L^{0.599} n^{0.615} / \left(i^{0.399} S_o^{0.303} \right)$	0.998	1.0	<0.0001
T_{t100} = f (L, S_o, n, i), Equation (3.4)	$T_{t100} = 12.23 L^{0.594} n^{0.632} / \left(i^{0.398} S_o^{0.303} \right)$	0.996	1.1	<0.0001

[a] Statistical parameter R^2 and *RMSE* were developed against respective time parameters (T_{t85}, T_{t95}, and T_{t100}) generated from 530 DWMPT model runs for the parametric study.
[b] The *p*-values reported herein were developed between respective time parameters and all four input variables (L, S_o, n, i) in each regression equation.

Table 3.5. Statistical error parameters for linear regression equations between three time parameters (T_c, T_{t95}, and T_{t100}) and T_{t85} developed for impervious overland flow surfaces.

Equation	Formula	R^2	$RMSE$ [a] (min)
Equation (3.5)	$T_c = 0.97T_{t85}$	0.949	7.83
Equation (3.6)	$T_{t95} = 1.17T_{t85}$	0.998	1.55
Equation (3.7)	$T_{t100} = 1.43T_{t85}$	0.996	7.97

[a] Statistical parameter R^2 and $RMSE$ were developed against respective time parameters (T_c, T_{t95}, and T_{t100}) derived from DWMPT and predicted using the corresponding equation for 530 data points for the parametric study.

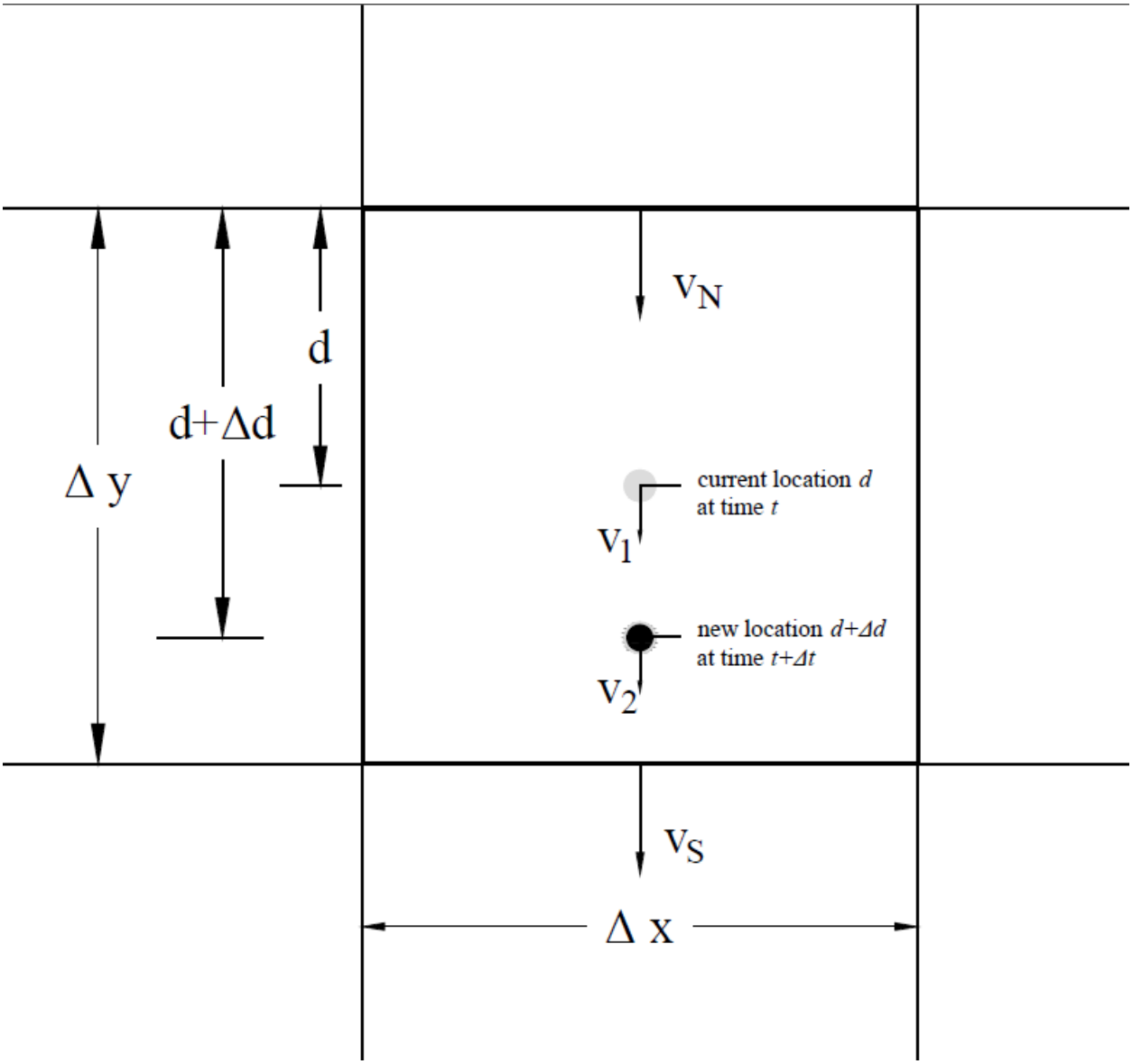

Fig. 3.1. Two-dimensional DWMPT finite difference grids illustrating the movement of particle *i* from the old location *d* at time *t* to new location $d+\Delta d$ at time $t+\Delta t$. The grid size Δx and Δy are the same for DWMPT.

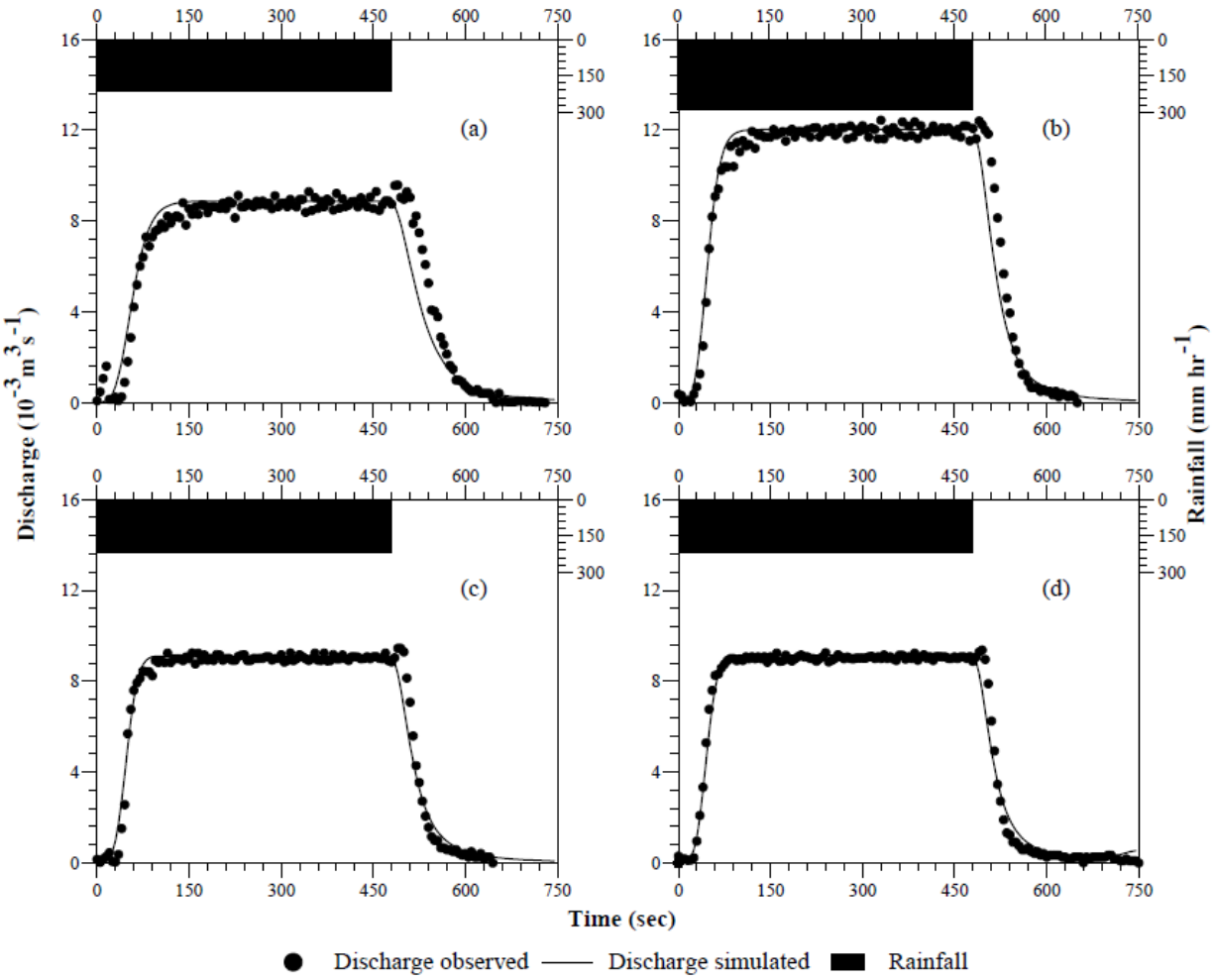

Fig. 3.2 Observed effective rainfall hyetographs and observed and simulated hydrographs for an aluminum surface of 12.2 m long and 12.2 m wide with a cross slope of 1% and longitudinal slope of: (a) 0.5%, (b) 1.0%, (c) 1.5%, and (d) 2.0%. Observed data presented above are from the lot 3 of Ben-Zvi (1984).

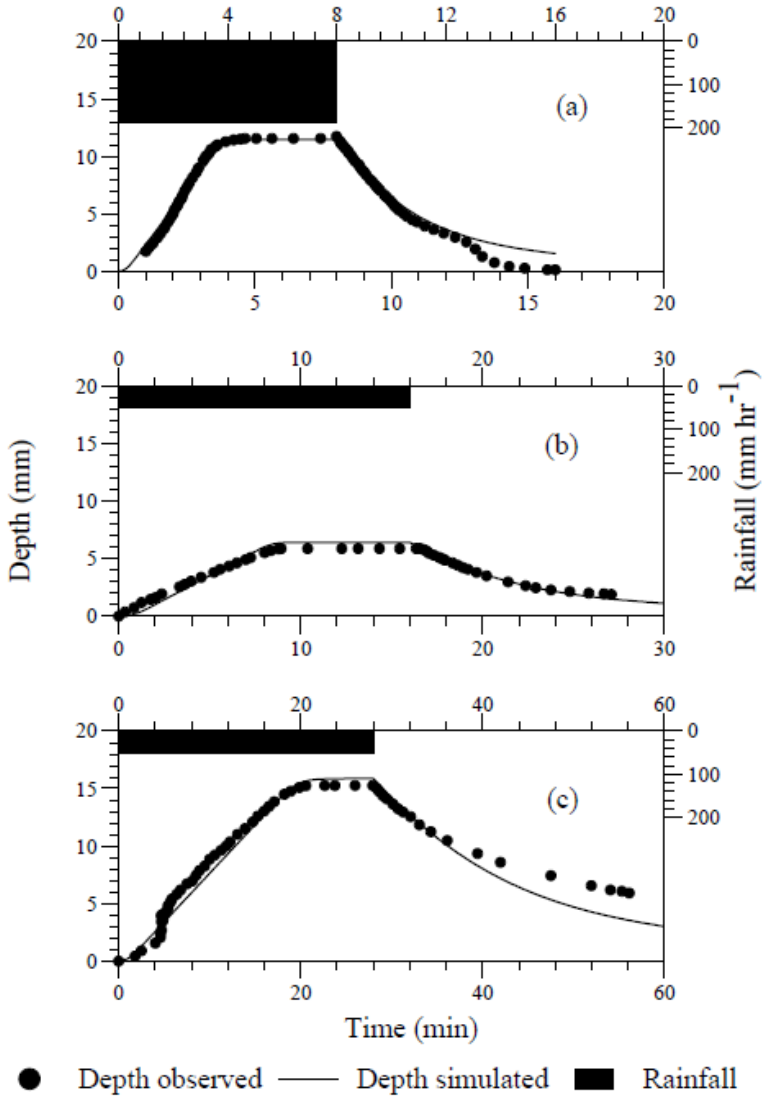

Fig. 3.3 Observed effective rainfall hyetographs and observed and simulated runoff depth hydrographs for a 152.4 m long and 0.3 m wide plot with a slope of: (a) 2% at 142.3 m from upstream, (b) 0.5% at 101.5 m from upstream, and (c) 0.5% at 142.3 m from upstream. Observed data presented in (a) and (b) are for concrete surfaces, and (c) for turf surface from Yu and McNown (1963).

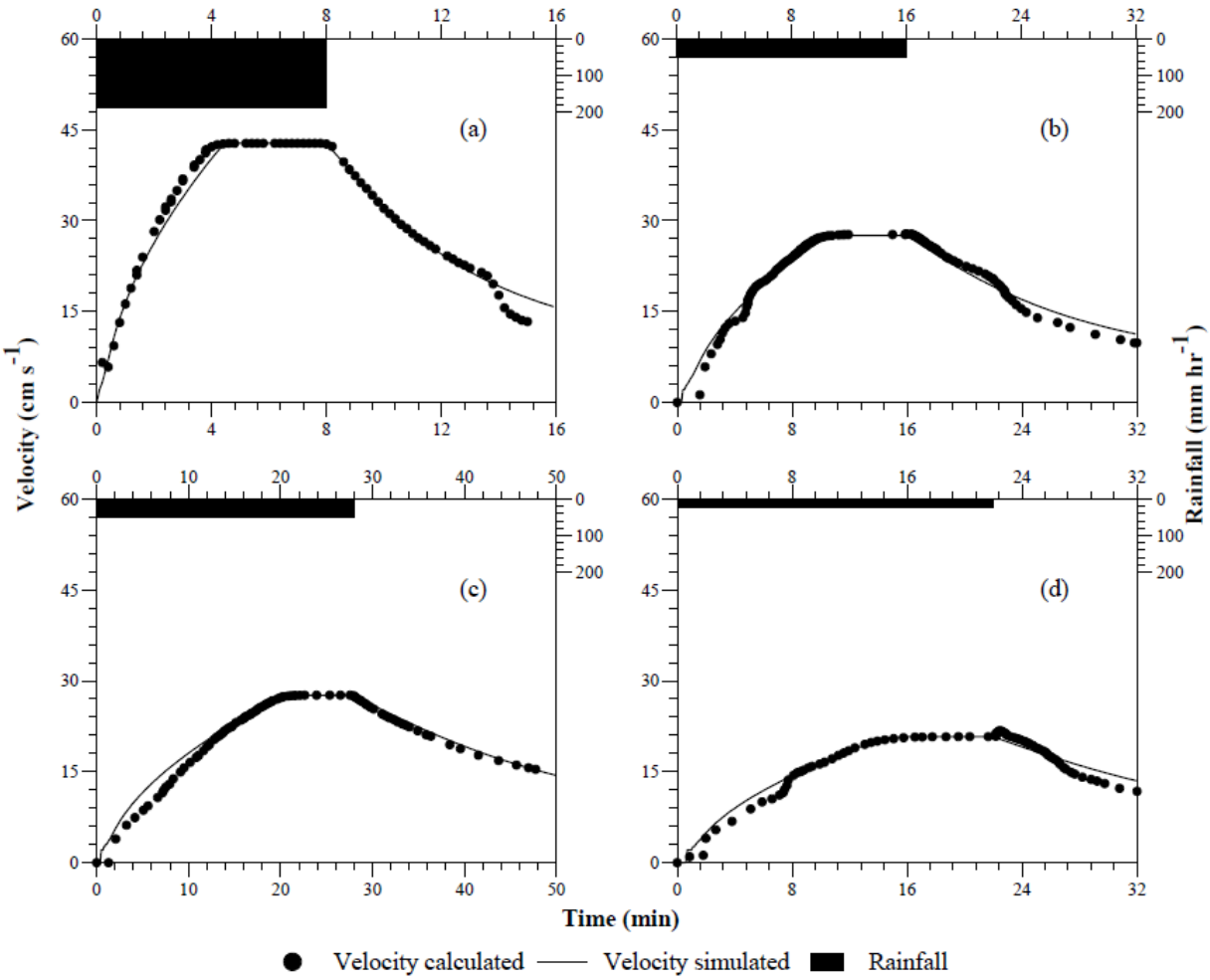

Fig. 3.4. Observed effective rainfall hyetographs and calculated and simulated runoff velocity hydrographs at the outlet for a 152.4 m long and 0.3 m wide plot with a slope of: (a) 2%, (b) 0.5%, (c) 0.5%, and (d) 0.5%. Calculated data presented in (a), (b), and (d) are for concrete surfaces, and (c) for turf surface from Yu and McNown (1963) based on the critical flow condition at the outlet.

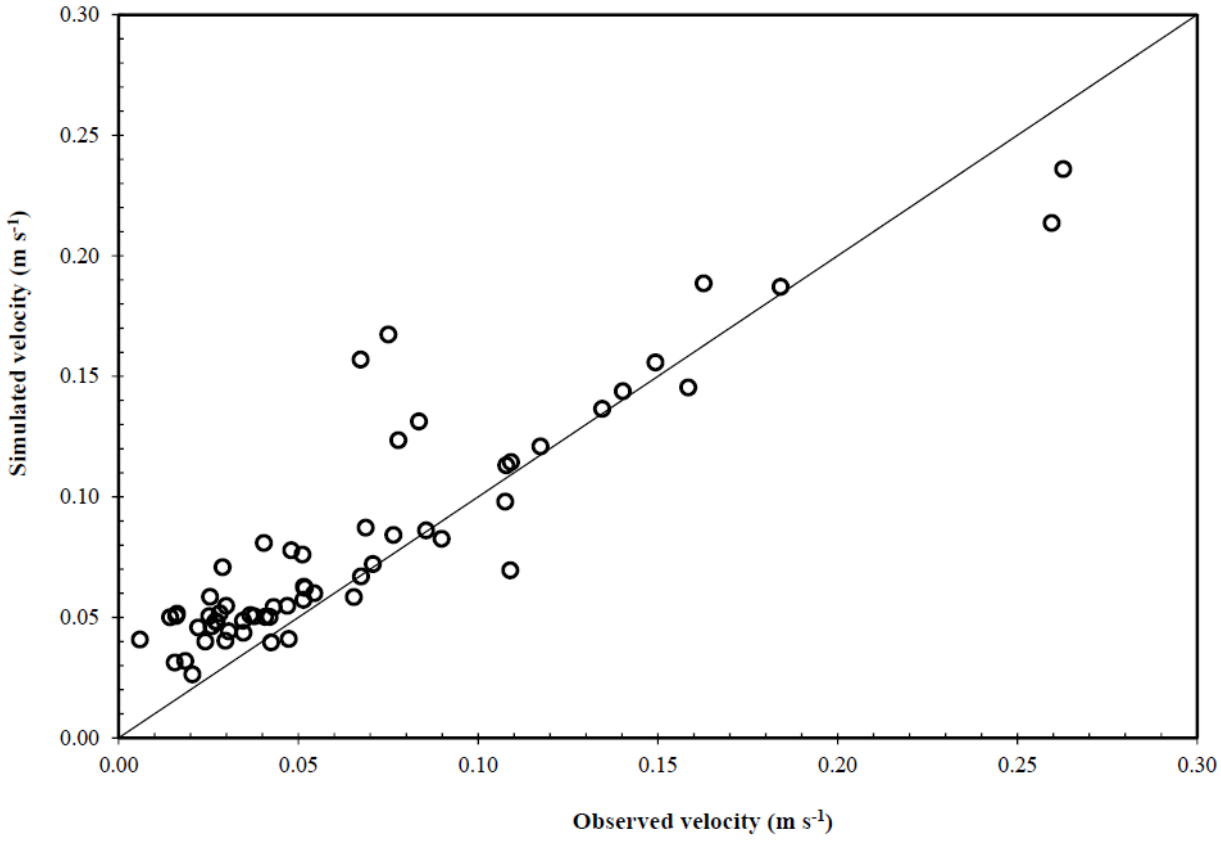

Fig. 3.5. Observed and simulated velocities for a 10 m long and 4 m wide plot of sandy soil surface with a slope of 1.0% and constant average rainfall intensity of 70 mm hr^{-1}. Observed data are from Mügler et al. (2011).

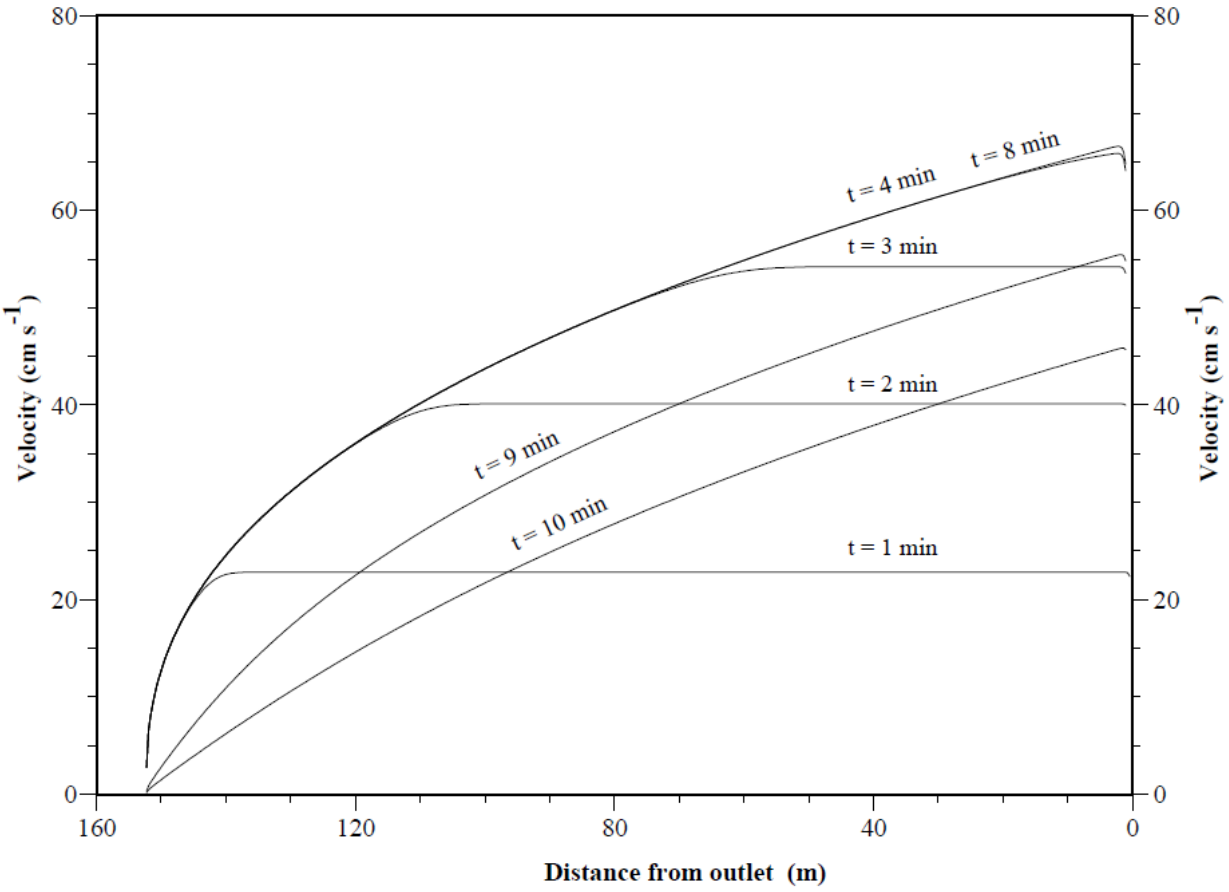

Fig. 3.6. Simulated runoff velocity at different times (t = 1, 2, 3, 4, 8, 9, and 10 minutes) at each cell from upstream to downstream for a 152.4 m long and 0.3 m wide plot with a slope of 2%. The length of the plot is discretized into 500 cells.

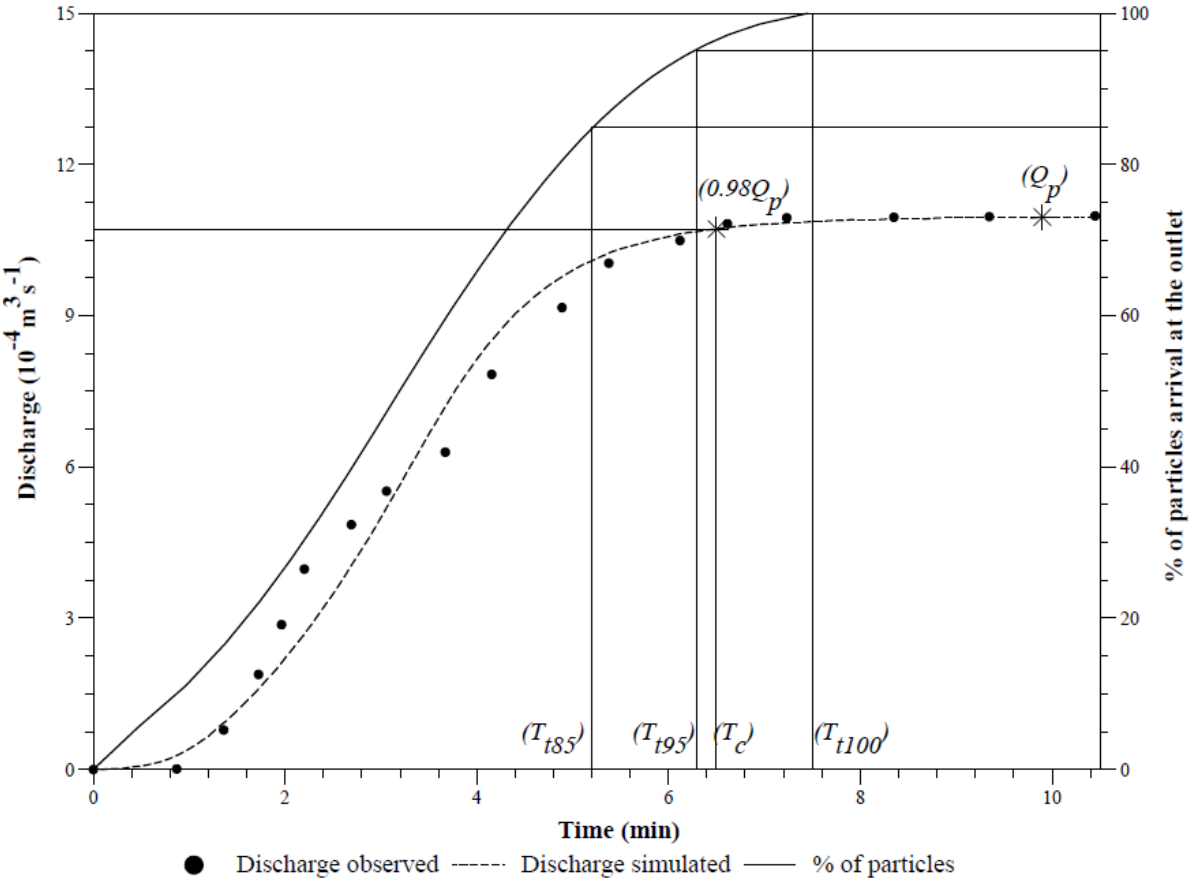

Fig. 3.7 Observed and simulated hydrographs, percentage of particles arrival at the outlet out of total particles, and time of concentration (T_c), and travel times for 85% (T_{t85}), 95% (T_{t95}) and 100% (T_{t100}) particles arrival for an asphalt pavement of 21.9 m long and 1.83 m wide with a slope of 0.1% and an effective rainfall of 98.3 mm hr^{-1}. The occurrence times of 98% of peak discharge (Q_p) and 100% of Q_p in the discharge hydrograph are also shown. Observed hydrograph was from Izzard and Augustine (1943).

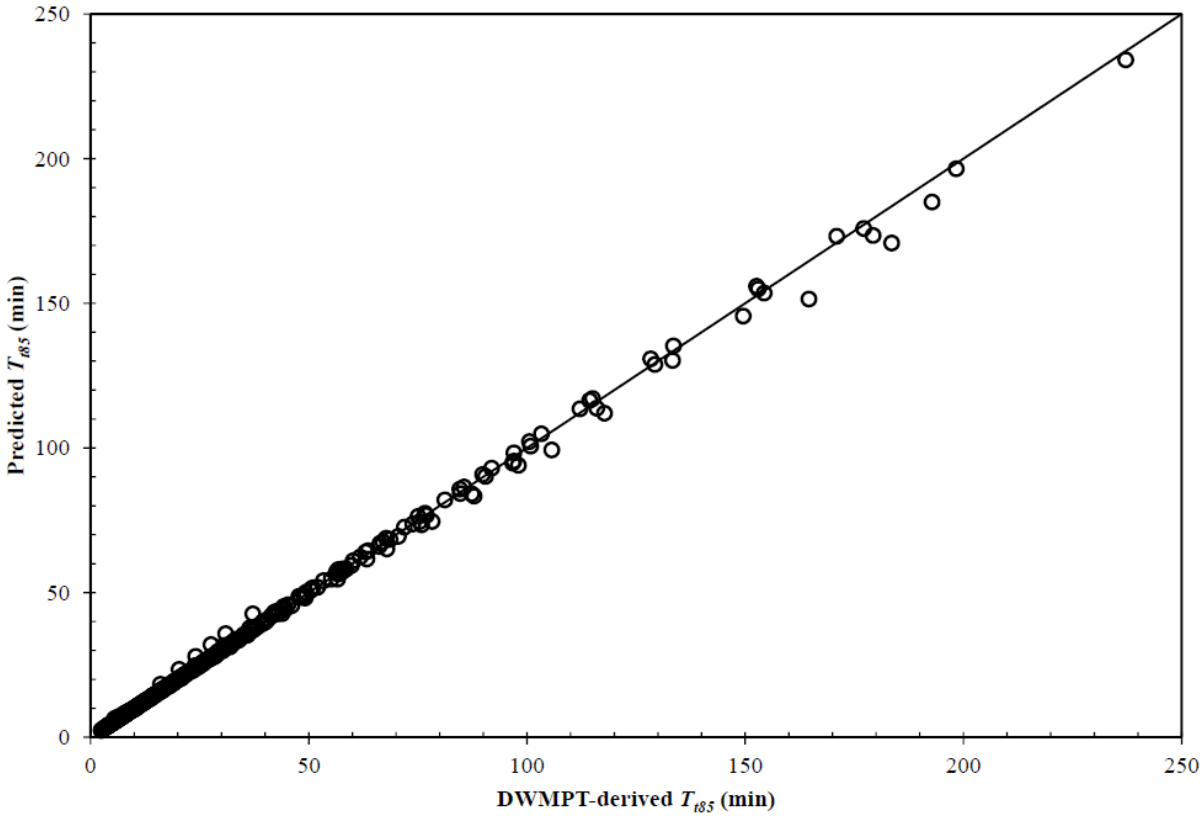

Fig. 3.8. Travel time for 85% of particles arrival at the outlet (T_{t85}) predicted using regression equation (3.2) versus T_{t85} derived from numerical experiments using DWMPT for impervious overland flow planes.

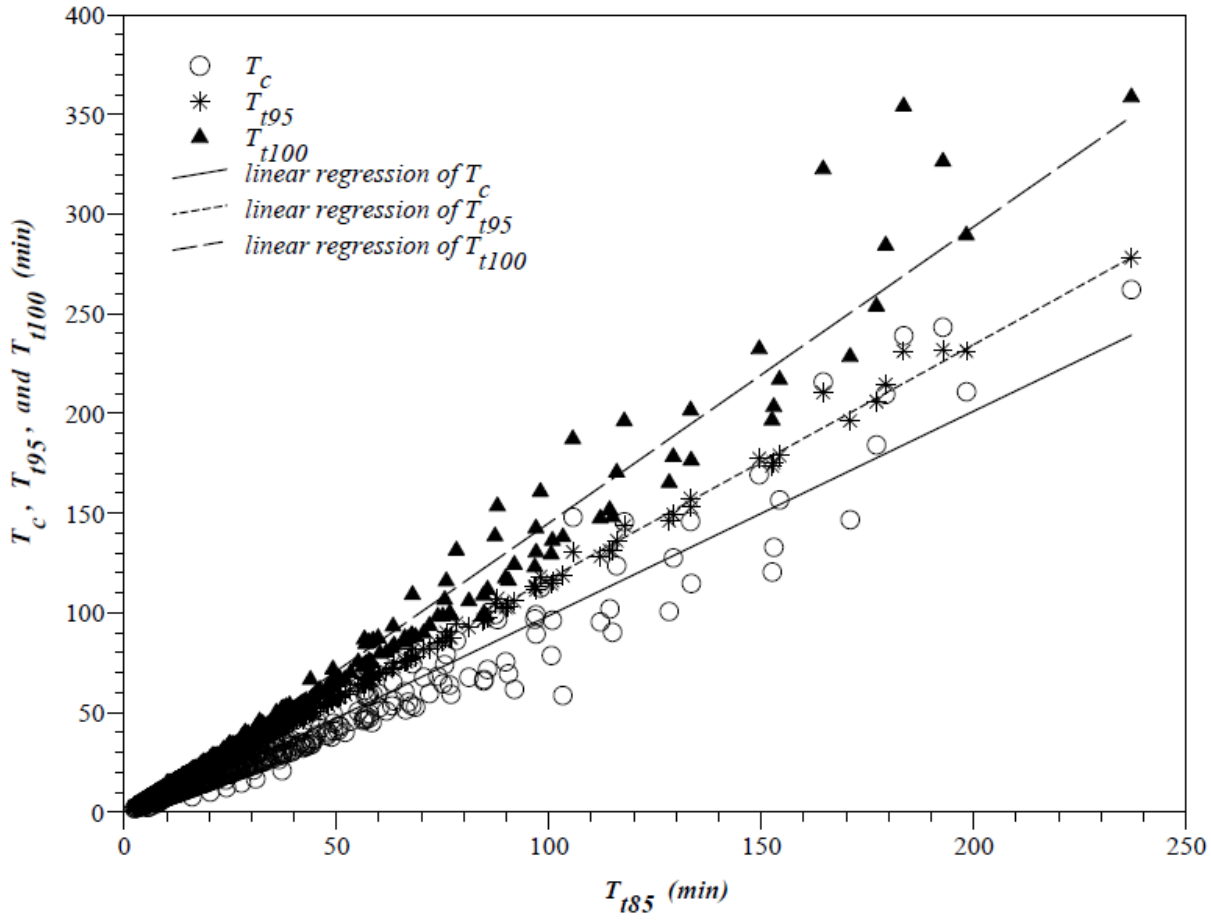

Fig. 3.9. Time of concentration (T_c), travel times for 95% (T_{t95}) and 100% (T_{t100}) of particles arrival at the outlet versus travel time for 85% of particles arrival at the outlet (T_{t85}) developed from numerical experiments using DWMPT for impervious overland flow planes. Three linear regression lines between three time parameters (T_c, T_{t95}, and T_{t100}) and T_{t85} are also shown.

Chapter 4 Estimation of the Equilibrium Velocity of Overland Flows Induced by Constant Rainfalls on Impervious Surfaces

4.1 Abstract

Stormwater with velocity equal or close to the equilibrium velocity can cause more soil erosion and transport significant amounts of particulate materials to downstream receiving waters. A quasi-two dimensional diffusion wave model was validated using observed discharges and calculated velocities at the outlet and then used to simulate overland flows on impervious surfaces using diverse combinations of the four physically based input variables: length, slope, roughness coefficient of the surfaces, and effective rainfall intensity. The equilibrium velocity V_{eq} for overland flow, defined as the maximum velocity attained under the constant rainfall, was determined for each model run. Simulation results show when and where V_{eq} occurs under constant rainfall. A dataset of 530 V_{eq} estimates was developed; the relation between V_{eq} and input variables was developed in which V_{eq} is found to be directly but nonlinearly proportional to the rainfall intensity and the length and slope of the flow plane and inversely proportional to the surface roughness. Similarly, the relation between the time to equilibrium velocity T_{veq} and the input variables is also presented.

4.2 Introduction

During a rainfall event, a part of the rainfall is lost to interception, evaporation, and

infiltration, and remaining part becomes surface runoff that starts as overland (sheet) flow first. The runoff at the upstream of an overland flow surface travels slowly until it begins picking up velocity. As the water speeds up, it starts picking up dissolved and particulate materials and becomes a pollutant carrier. In fact, stormwater runoff from urban areas is noted as a major source of water pollution (Shaw et al. 2006). Along with transporting dissolved materials from impervious surfaces, stormwater also isolate and transport significant amounts of particulate materials (Sartor et al. 1974; Sansalone et al. 1998). Similarly, the high velocity waters are equally responsible for causing severe hydraulic scour and erosion along the soil slope on pervious surfaces. The runoff with high velocity decreases the stability of the soil by removing protective surface covers and reduces the productivity of top soil in agricultural areas. Erosion rates in the hilly areas are high which often cause pollution and sedimentation downstream as well as reduce the depth of soil available for future agricultural production (Nezu and Rodi 1986). Similarly, the overland flow velocity is an important parameter in number of physically based soil erosion models such as the water erosion prediction project (WEPP) (Laflen et al. 1991), the European soil erosion model (EUROSEM) (Morgan et al. 1998), the Griffith University erosion system template (GUEST) (Rose 1993; Rose et al. 1997; Tilahun et al. 2012), and the saturation excess erosion model (SEEModel) (Tilahun et al. 2013). Thus, determination of surface runoff velocity is important in the overland flow study.

There are many studies on the physical measurements of flow velocity in a laboratory or a natural environment. Abrahams et al. (1986) classified the standard procedures for measuring velocity into two categories: discharge (indirect) and tracer

(direct) methods. The first method involves dividing discharge by the cross-sectional area of the flow while the second method involves timing the passage of a tracer or object. The measurement of flow velocity often involves the use of tracers such as dyes (Emmett 1970a; Dunne and Dietrich 1980; Roels 1984; Abrahams et al. 1986), electrolytes (Planchon et al. 2005; Tingwu et al. 2005; Lei et al. 2010), magnetic materials (Ventura Jr et al. 2001; Hu et al. 2011), isotopes (Gardner and Dunn III 1964; Berman et al. 2009), buoyant and fluorescent objects (Bradley et al. 2002; Meselhe et al. 2004; Tauro et al. 2010; Tauro et al. 2012b). However, many factors can be responsible to cause errors in measured velocities using the tracer method. The duration of the dye injection, the correct timing for the tracer to travel pre-specified length, dispersion of the dye in the flow, human and instrumental errors, are all possible factors for error accumulation (Lei et al. 2013). Moreover, field measurement is labor, time and cost intensive (KC et al. 2014). Hence, development of regression formula to estimate overland flow velocity using physically based input variables is relevant.

One of the widely used physically based velocity estimation methods is the Natural Resources Conservation Service (NRCS) velocity method (Grimaldi et al. 2012). The NRCS velocity method suggests two empirical formulas for estimating the velocity of overland flow and channel flow. Weyman (1973) classified digital elevation model (DEM) cells into “hill slope” or “channel”. The flow velocity for these two types of the cells can be respectively computed using following equations (4.1) and (4.2) (Natural Resources Conservation Service (NRCS) 1972, 1986):

$$v = a\sqrt{S_o}\,, \tag{4.1}$$

$$v = \frac{R^{2/3}}{n}\sqrt{S_o}\,, \tag{4.2}$$

where v is the flow velocity in m s^{-1} in a DEM cell, S_o is the cell slope (dimensionless), a is a soil use coefficient in m s^{-1} (McCuen 1998), n is Manning's roughness coefficient, and R is hydraulic radius. However, use of equation (4.1) is limited to the physical location that was used for developing the calibration coefficient a. Similarly, Grimaldi et al. (2012) pointed out the several uncertainties in using equation (4.2) that is Manning's equation for the estimation of flow velocity. They stated several geometrical hypotheses are required to define the hydraulic radius of the channel section, which in turn induces several relevant uncertainties. Similarly, it is also not clear whether to implement this method cell by cell or segment by segment (Grimaldi et al. 2012).

Moreover, most of the studies dealing with the tracer and pollutant transport have been confined to erosion with erodible boundary (agricultural erosion) and little research has been focused to sediment transport by overland flow over a non-erodible impervious surface (Smith 1991). Moreover, pollutant transport by overland flow across parking lots, airfields, and other paved areas into groundwater, streams, and rivers has been increasing and requires more attention (Smith 1991). Recent increased interest in implementing pollutant management practices in urban areas requires predictive modeling of movement and transportation of pollutants (Shaw et al. 2006). Nezu and Rodi (1986) insisted that the design strategies to control pollution associated with runoff requires knowledge of what happens in individual rainstorms.

Most of the above studies are focused on the estimation of mean velocity (Lei and Nearing 2000; Dunkerley 2001; Myers 2002). However, fast moving water is usually responsible for movement and transportation of pollutants in urban areas and erosion on

disturbed surfaces of a construction site. Govers (1992) stated that measured velocities are expected to be equal or close to equilibrium values when stormwater causes maximum changes in surface elevations (erosion or scour). Hence, estimation of the fastest velocity for a storm will provide useful and valuable information for engineers, managers, and decision makers to better understand on erosion potentials and pollutant transport.

In this study, an equilibrium velocity V_{eq} for the overland flow on an impervious surface under specific rainfall event was determined from numerical simulation results of overland flow on the surface. The equilibrium velocity is defined as the maximum velocity attained under a constant effective rainfall over an impervious plane. The model used is a quasi-two dimensional (2D) diffusion wave model (DWM) that was previously enhanced and modified (KC et al. 2014) from the diffusion hydrodynamic model (DHM) (Hromadka and Yen 1986). The model was further validated extensively in this study using observed discharges and calculated velocities at the outlet of overland flow planes from three different published studies. Simulation results were used to understand and identify when and where V_{eq} occurs during and after a constant rainfall event. Five hundred and thirty DWM runs were performed to determine V_{eq} on impervious surfaces using diverse combinations of the four physically based input variables: length (L), slope (S_o), Manning's roughness coefficient (n) of the surfaces, and effective rainfall intensity (i). A relation between V_{eq} and the input variables was developed for impervious overland flow planes. Similarly, a relation between the time to equilibrium velocity (T_{veq}) and the four physically based input variables is also presented.

4.3 Methods – Diffusion Wave Model

The quasi-2D DWM was used for estimating V_{eq} for simulated overland flows on impervious surfaces. The DWM was developed from DHM (Hromadka and Yen 1986) that solves the momentum and continuity equations for overland flows (Akan and Yen 1984). Detailed description of governing equations and numerical method employed in DHM is described by Hromadka and Yen (1986). The DHM was modified and enhanced to a quasi-2D dynamic wave model for simulating overland flows on small slopes by KC et al. (2014), which incorporated inertial terms in the flow momentum equations. The model developed by KC et al. (2014) has the option to neglect the inertial terms and then becomes DWM, a diffusion wave approximation model. The diffusion wave approximation is found to be accurate for most overland flow conditions (Gonwa and Kavvas 1986; Singh and Aravamuthan 1995; Moramarco and Singh 2002; Singh et al. 2005) and is used in the present study to determine V_{eq} and T_{veq} on the overland flow surfaces with the slope at or greater than 0.1%. When the slope is very small (flat planes), both upstream and downstream boundary conditions in addition to plane parameters (L, S_o, and n) and rainfall intensity can affect when and where V_{eq} occurs during and after a constant rainfall event, and V_{eq} possibly occurs at multiple locations. The study of V_{eq} on small slopes is beyond the scope of the study.

A number of modifications and enhancements made from DHM for the dynamic wave model (KC et al. 2014) are inherited into DWM. DWM incorporates an efficient numerical stability criterion using Courant number, checks for mass and momentum conservation errors, and consists of two rainfall loss models. The rainfall loss model

used in this study is a fractional loss model (FRAC) (Thompson et al. 2008) which assumes that the catchment converts a constant fraction of each rainfall input into an effective rainfall using volumetric runoff coefficient (Dhakal et al. 2012). Moreover, DWM was further validated using observed discharges and calculated velocities published in three independent studies before additional numerical simulations were performed to determine V_{eq} in this study. For the model validation using observed data, an initial abstraction was used to remove a short period of rainfall that did not yield runoff, and then FRAC was used to calculate effective rainfall input (McCuen 1998). However, for the numerical simulations to develop a dataset of V_{eq} and T_{veq}, effective rainfall was directly inputted into the model for each model run.

4.3.1 Model Validation using Discharge Hydrographs

The DWM model was first validated using observed discharge hydrographs from three different studies: Chow (1967) and Ben-zvi (1984), Yu and McNown (1963), and Izzard and Augustine (1943). Chow (1967) and Ben-zvi (1984) conducted rainfall-runoff experiments on a 12.2 × 12.2 m (40 × 40 ft) masonite and aluminum-surfaced watershed (laboratory scale). The rainfall duration of the experiments lasted from 0.5 to 8 minutes with the intensities varying from 51 to 305 mm hr^{-1} (2 to 12 in. hr^{-1}). The longitudinal slope of the experimental watersheds varied from 0.5% to 3% and cross slope was fixed at 1%. Figures 4.1(a) and 4.1(b) show observed and simulated discharge hydrographs at the outlet along with rainfall hyetographs for two rainfall events on an aluminum surface with longitudinal slopes of 0.5% and 1.0% from lot 3 data from Ben-zvi (1984). The hyetographs with durations of 8 minutes of the experiments presented in Figs. 4.1(a) and

1(b) are constant rainfall intensities of 214.6 mm hr^{-1} (8.5 in. hr^{-1}), and 223.3 mm hr^{-1} (8.8 in. hr^{-1}), respectively. DWM simulated hydrographs were generated using calibrated Manning's roughness coefficient of 0.02 for the aluminum surface.

Yu and McNown (1963) published runoff and depth hydrographs for different combinations of slope, roughness, and rainfall intensity at the airfield drainage in Santa Monica, California. They conducted experiments on 152.4 m (500 ft) by 0.3 m (1 ft) plot with slopes ranging from 0.5% to 2%. Figure 4.1(c) shows observed and simulated discharge hydrographs along with observed rainfall hyetograph on a turf surface of 152.4 m (500 ft) by 0.3 m (1 ft) with a slope of 0.5%. The experiment had a constant effective rainfall intensity of 50.8 mm hr^{-1} (2.0 in. hr^{-1}) with a duration of 28 minutes as shown in Fig. 4.1(c). The rainfall in the experiment was applied for a longer time to make the rainfall loss uniform and steady (Yu and McNown 1963). Even though turf surface is a pervious surface, it was simulated as an impervious surface using the effective rainfall hyetograph as the rainfall input to the DWM.

Izzard and Augustine (1943) also published runoff data from paved and turf surfaces collected by the Public Roads Administration in 1942. The measurements were conducted in three phases on plots of 3.6 m (12 ft) to 21.9 m (72 ft) with slopes of 1% to 6%. Figure 4.1(d) shows observed and simulated discharge hydrographs along with observed rainfall hyetograph from an asphalt surface of 21.9 m (72 ft) by 1.8 m (6 ft) with a slope of 0.1%. The experiment used a variable effective rainfall intensity of 93.7 mm hr^{-1} (3.7 in. hr^{-1}) for the first 10 minutes that was then decreased to 49.0 mm hr^{-1} (1.9 in. hr^{-1}) for the next 16 minutes as shown in Fig. 4.1(d).

Table 4.1 lists eight overland-flow surfaces under different rainfall events that were used for hydrograph validation. Observed rainfall hyetographs on the surfaces and hydrographs measured at the outlets were obtained from experiments performed by Ben-zvi (1984), Yu and McNown (1963), and Izzard and Augustine (1943). Table 4.1 lists input variables L, S_o, n, and i used for experiments and DWM, peak discharges (Q_p) estimated using the rational method, from experimental data and modeled using DWM, and model performance parameters (Nash-Sutcliffe coefficient *Ns* and root mean square error *RMSE*) developed between observed and simulated hydrographs. Observed rainfall hyetographs and observed and simulated hydrographs for the first four rainfall events listed in Table 4.1 are shown in Fig. 4.1. The agreement between observed and simulated peak discharges and hydrographs is excellent as shown in Figs. 4.1(a) – 4.1(d) and Table 4.1. For Fig. 4.1(d) with variable rainfall intensities, the comparison of Q_p listed in Table 4.1 is for the first 8-minute rainfall intensity of 93.7 mm hr $^{-1}$ (3.7 in. hr^{-1}). The average *Ns* was 0.96 (ranged from 0.87 to 0.99), and average *RMSE* was 0.38×10^{-3} $m^3 s^{-1}$ (ranged from 0.01–0.89×10^{-3} $m^3 s^{-1}$) for eight rainfall events simulated in Table 4.1. These statistics indicate a strong agreement between measured and simulated discharge hydrographs.

4.3.2 Model Validation using Calculated Velocity Data

Flow velocities and the maximum velocity of an overland flow are typically not measured in the laboratory and field experiments. For above three studies that were used to validate hydrographs, the critical flow conditions were created for the measurement of discharge hydrographs at the outlets, therefore, the velocities at the

outlets for these experiments can be calculated from observed discharge hydrographs using critical flow equation. Therefore, the DWM model was validated using calculated velocity data at the outlets of eight experimental plots from the three different studies. Figure 4.2 shows calculated and simulated runoff velocity hydrographs at the outlets along with rainfall hyetographs for the last four of the eight experiments listed in Table 4.1 and Table 4.2 from the three studies. Calculated and simulated velocity hydrographs of two aluminum surface plots with longitudinal slopes of 1.5% and 2.0% from lot 3 data from Ben-zvi (1984) are shown in Figs. 4.2(a) and 4.2(b), respectively. Constant rainfalls with durations of 8 minutes were used for the experiments presented in Figs. 4.2(a) and 4.2(b) and had intensities of 219.7 mm hr^{-1} (8.65 in. hr^{-1}), and 221.5 mm hr^{-1} (8.72 in. hr^{-1}), respectively. Figure 4.2(c) shows calculated and simulated runoff velocity hydrographs at the outlet of a concrete surface with slope of 0.5% under a 16-minute constant effective rainfall intensity of 50.3 mm hr^{-1} (1.98 in. hr^{-1}) from Yu and McNown (1963). Figure 4.2(d) shows calculated and simulated runoff velocity hydrographs at the outlet of a 3.7 m (12 ft) by 1.8 m (6 ft) asphalt surface with a slope of 2% under a 6-minute constant rainfall intensity of 49.0 mm hr^{-1} (1.93 in. hr^{-1}) from Izzard and Augustine (1943). The agreement between the calculated and the simulated peak velocities and velocity hydrographs as shown in Figs. 4.2(a) – 4.2(d) is very good.

Table 4.2 lists maximum outlet velocity calculated from experimental data and modeled using DWM under the eight rainfall events on different surfaces for velocity validation along with model input variables: L, S_o, n, and i; and model performance parameters (*Ns* and *RMSE*) developed between calculated and simulated velocity hydrographs. The average *Ns* was 0.90 (ranged from 0.66 to 0.97), and average *RMSE*

was 2.6 cm s^{-1} (ranged from 1.1–4.2 cm s^{-1}) for the eight rainfall events in Table 4.2. These statistics indicate a strong agreement between calculated and simulated velocity hydrographs, therefore, it was concluded that DWM could be used to accurately simulate V_{eq} for the overland flow on impervious surfaces.

4.4 Results – Equilibrium Velocity

Valdes et al. (1979) concluded that overland flow velocity under steady rainfall increases with time at the beginning until it reaches a maximum value at equilibrium, remains constant until the rainfall ends, and then starts to decrease. Figure 4.2 shows such phenomena for four different events from three independent experimental studies. It is also important to understand when and where the maximum velocity occurs on an impervious surface under a constant rainfall input. Figure 4.3 shows a 3-D plot of simulated maximum velocities (in z-axis) over the simulation period (in x-axis) on a concrete surface of 152.4 m long and 0.3 m wide plot with a longitudinal slope of 2% under a constant rainfall intensity of 189 mm/hr that lasts 8 minutes. The location where the maximum velocity occurs is shown through the y-axis of Fig. 4.3 – the distance of the cell center from the outlet. In the early period of the rainfall event, the maximum velocity is quite low and occurs on the upstream of the plot, as the rainfall continues the maximum velocity increases as well as its location moves to the downstream towards the outlet. The maximum velocity finally reaches an equilibrium value V_{eq} and stays at that magnitude until the rainfall stops. Figure 4.3 shows that V_{eq} occurs near to the outlet (0.38 m or about two to three cells upstream from the outlet), but the location of V_{eq} is not exactly at the outlet due to the boundary effect (the critical flow

boundary is used). When the rainfall stops the maximum velocity decreases with time and but its occurrence remains near to the outlet (Fig. 4.3).

When Akan (1986) studied the time of concentration of overland flow, he suggested that physically based formulas are suitable for practical use, and the assumptions involved in the formulation can be clearly stated. Previous studies on overland flow (Morgali and Linsley 1965; Su and Fang 2004; KC et al. 2014) also used four physically based input parameters L, S_o, n, and i to simulate overland flows on different surfaces. Even though Manning's n is an empirical coefficient, it can be considered as a physically based parameter since it is a well-established coefficient for a large number of surface types (Engman 1986). Moreover, Rouhipour et al. (1999) tested Manning's, Darcy-Weisbach, and Chezy equations against observed data for overland flow velocity estimation and concluded Manning's equation best estimated the velocity. Similarly, most of the existing erosion models using the Universal Soil Loss Equation (USLE) claim that rainfall intensity and steep slopes are important driving forces and factors for runoff causing erosion (Tilahun et al. 2013). Therefore, these four input parameters L, S_o, n and, i were chosen as independent variables for the development of an estimation equation for V_{eq}. Five hundred and fifty values of V_{eq} were derived from numerical experiments using DWM by varying input variables: L, S_o, n, and i to develop the dataset for regression analysis. The input variable L was varied from 5 to 305 m (16 to 1000 ft), S_o from 0.1% to 10%, n from 0.01 to 0.80, and i from 2.5 to 254 mm hr^{-1} (0.1 to 10.0 in. h^{-1}). The cell sizes varied from 0.03 m (0.1 ft) to 0.61 m (2 ft) and were selected in such a way that the criteria: $0.1\, m^3 s^{-1}/m^2 < Q_p/A_s < 0.3\, m^3 s^{-1}/m^2$ (O'Brien 2009) was satisfied for balance between model simulation time and accuracy, where A_s is

the surface area of the grid element. The numerical experiments were simulated holding the three variables constant and varying the fourth one by 10–20% for different model runs. A generalized power relation, Eq. (4.3) was chosen for developing the regression equation,

$$V_{eq} = C_1 \, L^{k_1} \, S_o^{k_2} \, n^{k_3} \, i^{k_4} \, , \tag{4.3}$$

where L is in m, S_o is in m m^{-1} (dimensionless), i is in mm hr^{-1}, C_1, k_1, k_2, k_3, and k_4 are regression parameters. Equation (4.1) was log-transformed and non-linear regression was used to estimate parameter values. Using the DWM dataset for V_{eq}, the resulting regression equation is

$$V_{eq} = 0.33 \frac{L^{0.359} \, i^{0.402} S_o^{0.045}}{n^{0.326}} \tag{4.4}$$

where V_{eq} is in cm s^{-1}, and input variables and their units are as previously defined. Regression results are shown in Table 4.3. Statistical results indicate that the input variables L, S_o, n, and i have a high level of significance with the p-value < 0.0001 (Table 4.3) and are critical variables in the determination of V_{eq}. The regression parameters (C_1, k_1, k_2, k_3, and k_4) have smaller standard errors and small ranges of variation at the 95% confidence interval (Table 4.3). Predicted V_{eq} values from Eq. (4.4) compare well with the estimates from DWM numerical experiments as shown in Fig. 4.4(a) with R^2 of 0.78, *Ns* of 0.81 and *RMSE* of 6.9 cm s^{-1}. From Eq. (4.4), V_{eq} is directly but nonlinearly proportional to rainfall intensity and length of the flow plane and inversely proportional to the slope and roughness of the flow. However, Eq. (4.4) shows that the slope is less significant because of the small exponent. This result infers that the slope plays a less important role in the magnitude of equilibrium velocity and equilibrium discharge. This

is most likely because V_{eq} occurs near the outlet (Fig. 4.3) where the critical flow condition exists; it means V_{eq} is associated or closely linked to the critical flow condition. As one knows, the critical flow is independent of the slope and depends on the water depth that is controlled by L, S_o, n, and i. However, the slope plays a significant role when the equilibrium velocity occurs (i.e., T_{veq}) as shown in the subsequent section. The rainfall intensity, length and roughness of the surface are significant to both V_{eq} and T_{veq}.

4.4.1 Time to Equilibrium Velocity

Time to equilibrium velocity T_{veq} for an impervious overland flow is defined as the time required for the velocity to attain an equilibrium value under the influence of constant effective rainfall over a flow plane, i.e., time required for the velocity to reach V_{eq}. Hence, estimation of T_{veq} for the flow plane will provide useful information for hydrologists and analysts to understand when V_{eq} is expected to occur during a rainfall event. Moreover, T_{veq} is essentially the same as the time to equilibrium discharge T_e, which is the time associated with the maximum steady-state runoff discharge from a watershed under constant effective rainfall (Niri et al. 2012). T_e has been studied by Henderson and Wooding (1964), Butler (1977), Singh (1996), Aryal et al. (2005) and Niri et al. (2012) in the past. Saghafian and Julien (1995) stated T_e as the indicative of the length of response time of a basin under a given storm. They even suggested that time of concentration T_c is the same as T_e for the kinematic condition when the rainfall lasts longer than T_c.

Using kinematic wave approximation Henderson and Wooding (1964) derived T_e

equation for turbulent flow on a rectangular runoff plane as

$$T_e = 6.98 \frac{L^{0.6} n^{0.6}}{i^{0.4} S_o^{0.3}} \tag{4.5}$$

where T_e is in min, and input variables and their units are the same as previously defined. However, Ponce (1991) realized that all problems related to overland flow could be resolved with acceptable accuracy by using diffusion wave approximation instead of kinematic wave approximation. Niri et al. (2012) derived integral T_e equation for a rectangular plane under constant rainfall using diffusion wave approximation, however, the equation is complex and has no analytical solution. Hence, development of the regression equation of T_e based on physically based parameter using diffusion approximation will provide easy and accurate estimation method for hydrologists.

To develop the estimation formula of T_{veq} for overland-flow plots, a dataset of T_{veq} was obtained from the same 530 DWM runs for surfaces with slopes $S_o \geq 0.1\%$. The generalized power relation, Eq. (4.3) with new regression parameters (C_2, k_5, k_6, k_7, and k_8), was chosen for developing the regression equation for T_{veq}. Using the DWM dataset for T_{veq} in minutes, the resulting regression equation is

$$T_{veq} = 5.54 \frac{L^{0.555} n^{0.672}}{i^{0.352} S_o^{0.450}} \tag{4.6}$$

Regression results for Eq. (4.6) are shown in Table 4.4. Statistical results indicate that the input variables L, S_o, n, and i have a high level of significance with the p-value < 0.0001 and are critical variables in the determination of T_{veq}. The regression parameters have smaller standard errors and small ranges of variation at the 95% confidence interval (Table 4.4). T_{veq} is directly proportional to the length and roughness of the flow plane and inversely proportional to the rainfall intensity and the slope of the plane. Saghafian

and Julien (1995) compared the kinematic travel times of runoff for overland and channel flows and verified that T_e varies inversely with the rainfall intensity. Predicted values from equation (4.6) compare well with the estimates from DWM numerical experiments as shown in Fig. 4.4(b) with R^2 of 0.97, *Ns* of 0.97 and *RMSE* of 8.6 min. However, predicted T_e values using equation (4.5) from Henderson and Wooding (1964) are on the average 24.5% lower than the T_{veq} estimates from DWM numerical experiments (Fig. 4.5) with R^2 of 0.87, *Ns* of 0.64 and *RMSE* of 28.9 minutes. Equation (4.5) differs from Eq. (4.6) since Eq. (4.5) was derived using kinematic wave approximation while Eq. (4.6) was developed from the regression analysis of numerical experimental data from DWM that is a diffusive wave approximation model.

4.5 Conclusions

Knowledge of the relation between overland flow discharge, velocity and depth is important in many applications of deterministic hydrology and erosion models (Govers 1992). A quasi-two dimensional diffusion wave model DWM was developed from the diffusion hydrodynamic model DHM (Hromadka and Yen 1986) and further validated extensively using observed discharge, and velocity data from three different published studies. Five hundred and thirty DWM runs were performed to determine V_{eq} on impervious surfaces using diverse combinations of the four physically based input variables: L, S_o, n, and i. A regression formula for estimating equilibrium velocity V_{eq} for the overland flow on impervious surface was developed in this study (Eq. 4.4). V_{eq} is found to be directly but nonlinearly proportional to rainfall, length and slope of the flow plane and inversely proportional to the roughness of the flow. However, the slope

is found to be less significant in the regression estimation equation. Similarly, a relation between time to equilibrium velocity T_{veq} and the four physically based input variables was also developed (Eq. 4.6). V_{eq} and T_{veq} calculated using the Eqs. (4.4) and (4.6) provide useful information on predictive modeling of movement and transport of waters/pollutants on impervious surfaces.

Table 4.1. Input variables, peak discharges (Q_p) estimated using the rational method, from experimental data, and modeled using DWM, and corresponding model performance parameters calculated between observed and modeled discharge hydrographs for impervious overland flow surfaces.

Input variables				Q_p ($\times 10^{-3} m^3 s^{-1}$)			Performance parameters	
L (m)	S_0 *(%)*	*n*	*i* (mm hr^{-1})	Rational Method	Observed	Modeled	*Ns*	*RMSE* ($\times 10^{-3} m^3 s^{-1}$)
12.2 [a]	0.5	0.200	214.6	8.88	9.58	8.86	0.94	0.89
12.2 [a]	1.0	0.200	223.3	9.23	9.61	9.21	0.94	0.85
152.4 [b]	0.5	0.035	50.8	0.66	0.66	0.65	0.99	0.02
21.9 [c]	0.1	0.013	93.7	1.04	1.05	1.04	0.99	0.03
12.2 [a]	1.5	0.200	219.7	9.09	9.45	9.07	0.98	0.50
12.2 [a]	2.0	0.200	221.5	9.16	9.37	9.14	0.97	0.73
152.4 [b]	0.5	0.011	50.3	0.65	0.66	0.65	0.98	0.03
3.7 [c]	2.0	0.013	49.0	0.09	0.09	0.09	0.87	0.01

Note: Input variables for the experimental overland flow surfaces are *L* = length in m, S_o = slope in percent, *n* = Manning's roughness coefficient, and *i* = effective rainfall intensity in mm hr^{-1}. Model performance parameters are *Ns* = Nash-Sutcliffe coefficient and *RMSE* = root mean square error.

[a] Experimental data from Ben-Zvi (1984)

[b] Experimental data from Yu & McNown (1964)

[c] Experimental data from Izzard and Augustine (1943)

Table 4.2. Input variables, maximum outlet velocity calculated from experimental data and modeled using DWM, and model performance parameters for velocity hydrographs for impervious overland flow surfaces.

Input variables				Velocity(cm s^{-1})		Performance parameters	
L (m)	S_0 *(%)*	*n*	*i* (mm hr^{-1})	Observed	Modeled	*Ns*	*RMSE* (cm s^{-1})
12.2 [a]	0.5	0.200	214.6	42.5	41.5	0.89	3.2
12.2 [a]	1.0	0.200	223.3	42.6	42.0	0.93	3.4
152.4 [b]	0.5	0.035	50.8	27.7	27.6	0.97	1.2
21.9 [c]	0.1	0.013	93.7	34.8	32.8	0.96	2.2
12.2 [a]	1.5	0.200	219.7	42.4	41.8	0.95	2.6
12.2 [a]	2.0	0.200	221.5	42.2	41.9	0.90	4.2
152.4 [b]	0.5	0.011	50.3	27.8	27.5	0.97	1.1
3.7 [c]	2.0	0.013	49.0	14.6	14.9	0.66	2.5

Note: Input variables for the experimental overland flow surfaces are *L* = length in m, S_o = slope in percent, *n* = Manning's roughness coefficient, and *i* = effective rainfall intensity in mm hr^{-1}. Model performance parameters are *Ns* = Nash-Sutcliffe coefficient and *RMSE* = root mean square error.

[a] Experimental data from Ben-Zvi (1984)

[b] Experimental data from Yu & McNown (1964)

[c] Experimental data from Izzard and Augustine (1943)

Table 4.3. Parameter estimates of the regression Eq. (4.4) for the independent variables of the equilibrium velocity (V_{eq}) for impervious overland flow surfaces.

Parameter	Parameter estimate	95% confidence limits		Standard error	*t*-value	*p*-value
$Ln(C_1)$	-1.101	-1.213	-0.990	0.057	-19.4	<.0001
k_1 *for L*	0.359	0.341	0.377	0.009	39.1	<.0001
k_2 *for So*	0.045	0.032	0.058	0.007	6.8	<.0001
k_3 *for n*	-0.326	-0.339	-0.314	0.006	-51.7	<.0001
k_4 *for i*	0.402	0.387	0.417	0.008	52.9	<.0001

Table 4.4. Parameter estimates of the regression Eq. (4.6) for the independent variables of the time to equilibrium velocity (T_{veq}) for impervious overland flow surfaces.

Parameter	Parameter estimate	95% confidence limits		Standard error	*t*-value	*p*-value
$Ln(C_2)$	1.712	1.621	1.803	0.046	37.0	<0.0001
k_5 *for L*	0.555	0.540	0.570	0.008	74.1	<0.0001
k_6 *for So*	-0.450	-0.460	-0.439	0.005	-83.3	<0.0001
k_7 *for n*	0.672	0.662	0.682	0.005	130.2	<0.0001
k_8 *for i*	-0.352	-0.364	-0.340	0.006	-56.8	<0.0001

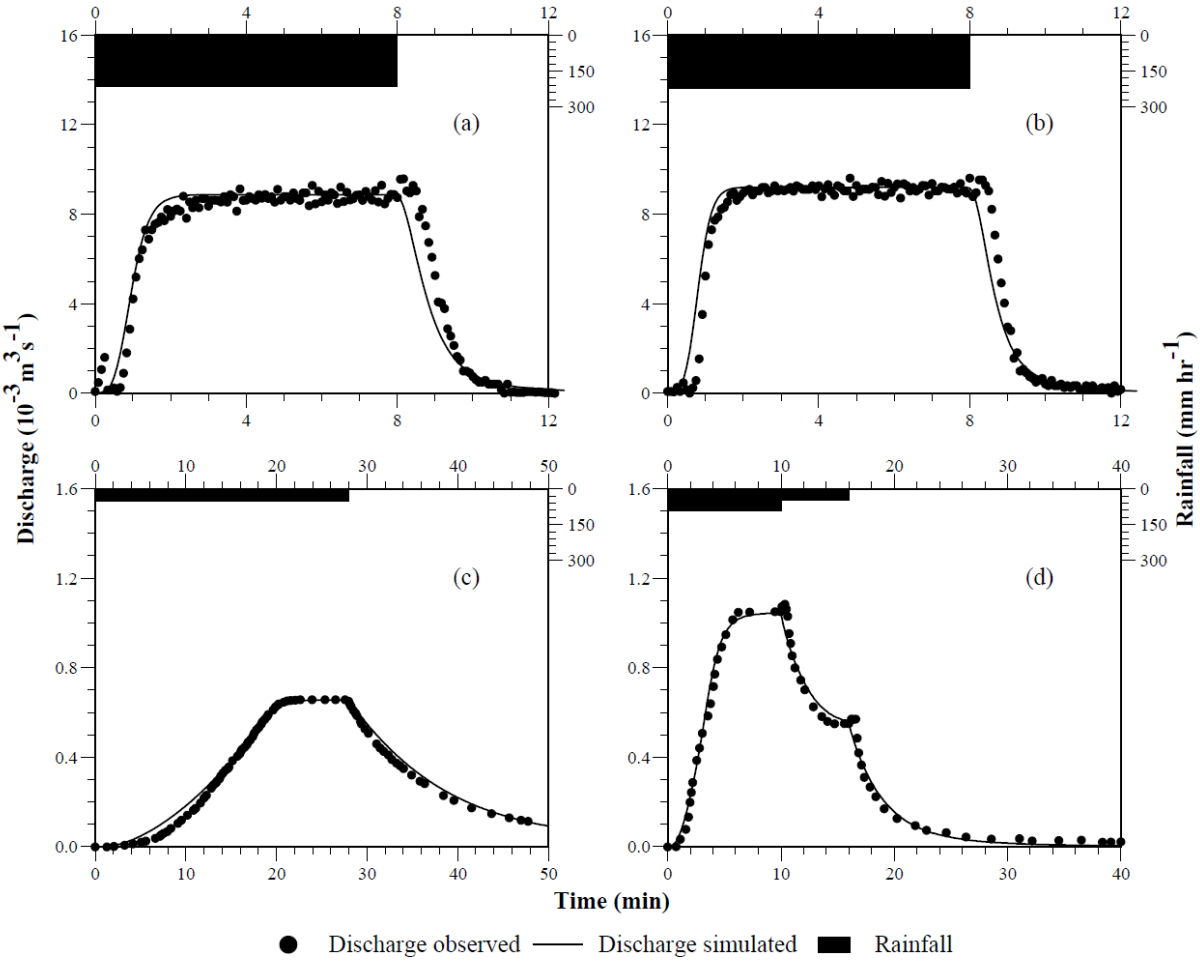

Fig. 4.1. Observed effective rainfall hyetographs and observed and simulated hydrographs for longitudinal slopes of (a) 0.5%; (b) 1.0% aluminum surface (12.2 × 12.2 m) with a cross slope of 1%; (c) 0.5% turf surface (152.4 × 0.3 m), and (d) 0.1% asphalt pavement (21.9 × 1.8 m). Observed data presented in (a) and (b) are from Ben-Zvi (1984), (c) from Yu and McNown (1963), and (d) from Izzard and Augustine (1943).

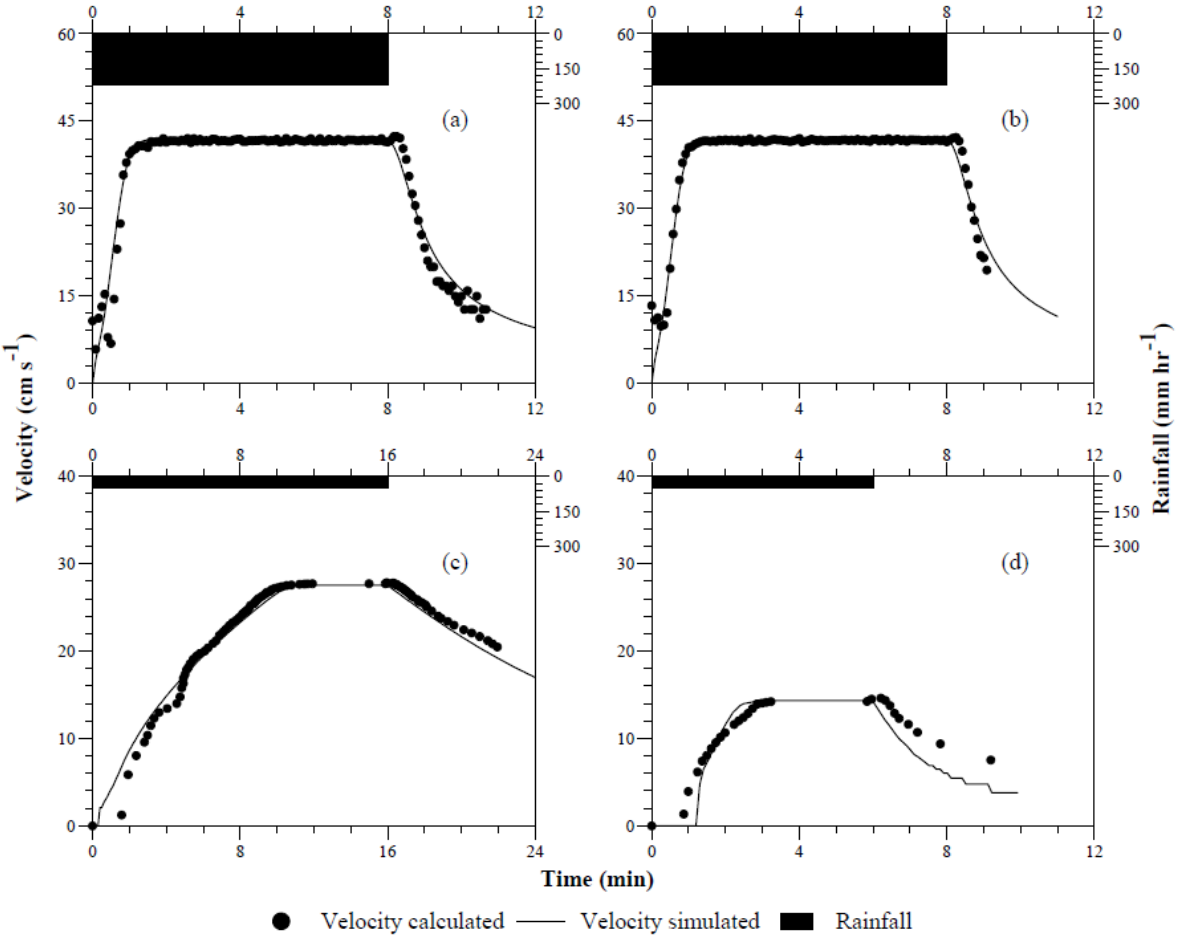

Fig. 4.2. Observed effective rainfall hyetographs and calculated and simulated runoff velocity hydrographs at the outlet for longitudinal slopes of (a) 1.5%; (b) 2.0% aluminum surface (12.2 × 12.2 m) with a cross slope of 1%; (c) 0.5% concrete surface (152.4 × 0.3 m), and (d) 2% asphalt pavement (3.7 × 1.8 m). Observed data presented in (a) and (b) are from Ben-Zvi (1984), (c) from Yu and McNown (1963), and (d) from Izzard and Augustine (1943).

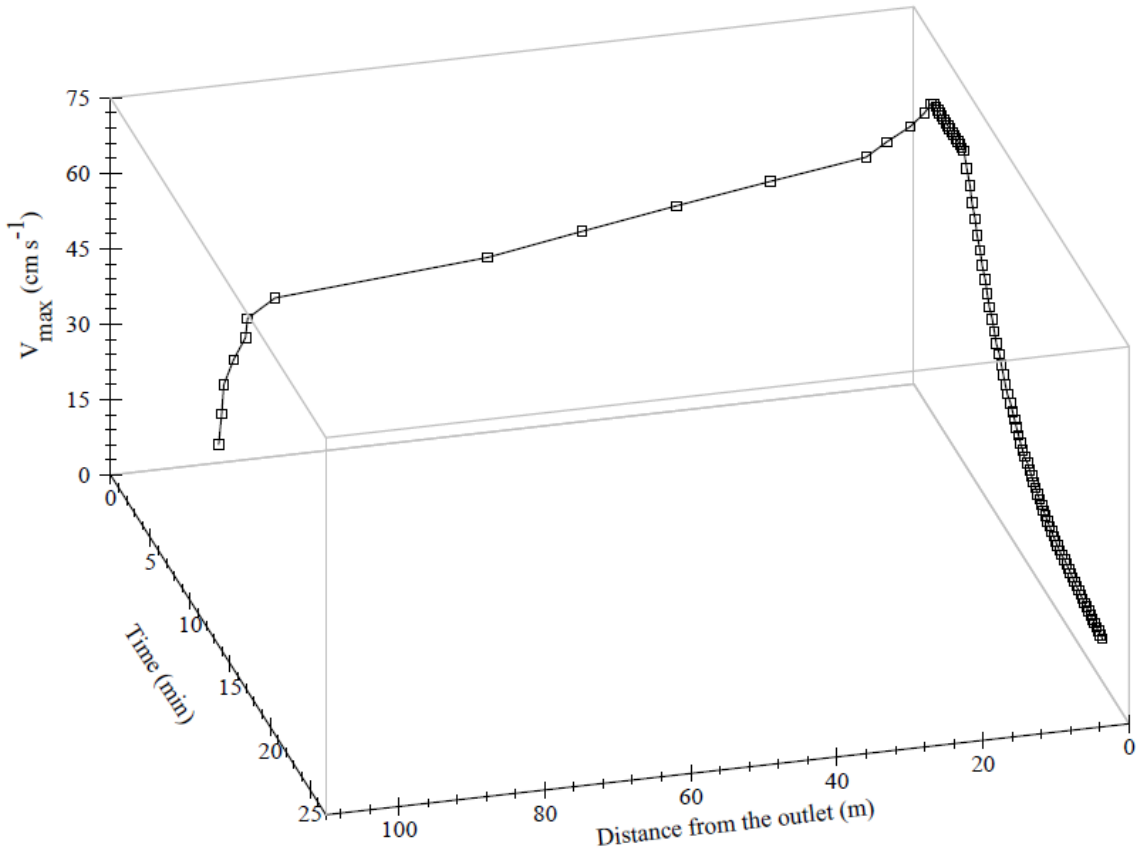

Fig. 4.3. Simulated maximum velocity on a concrete surface for a constant rainfall intensity of 189 mm hr^{-1} over the simulation period. The experimental plot (152.4 × 0.3 m plot with a longitudinal slope of 2%) is one of the plots used by Yu and McNown (1963).

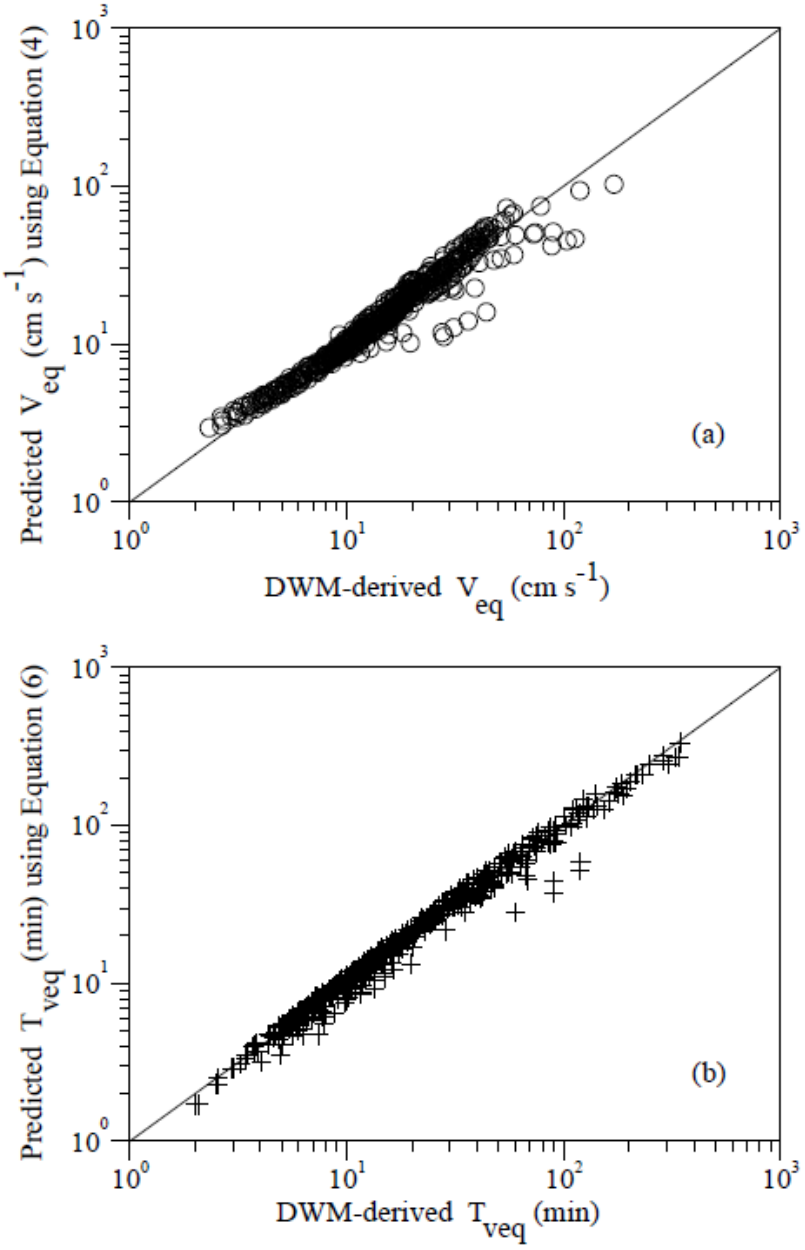

Fig. 4.4(a) Equilibrium velocity (V_{eq}) predicted using the regression Eq. (4.4) versus V_{eq} derived from numerical experiments using DWM, (b) Time to equilibrium velocity (T_{veq}) predicted using the regression Eq. (4.6) versus T_{veq} derived from DWM numerical experiments for impervious flow surfaces.

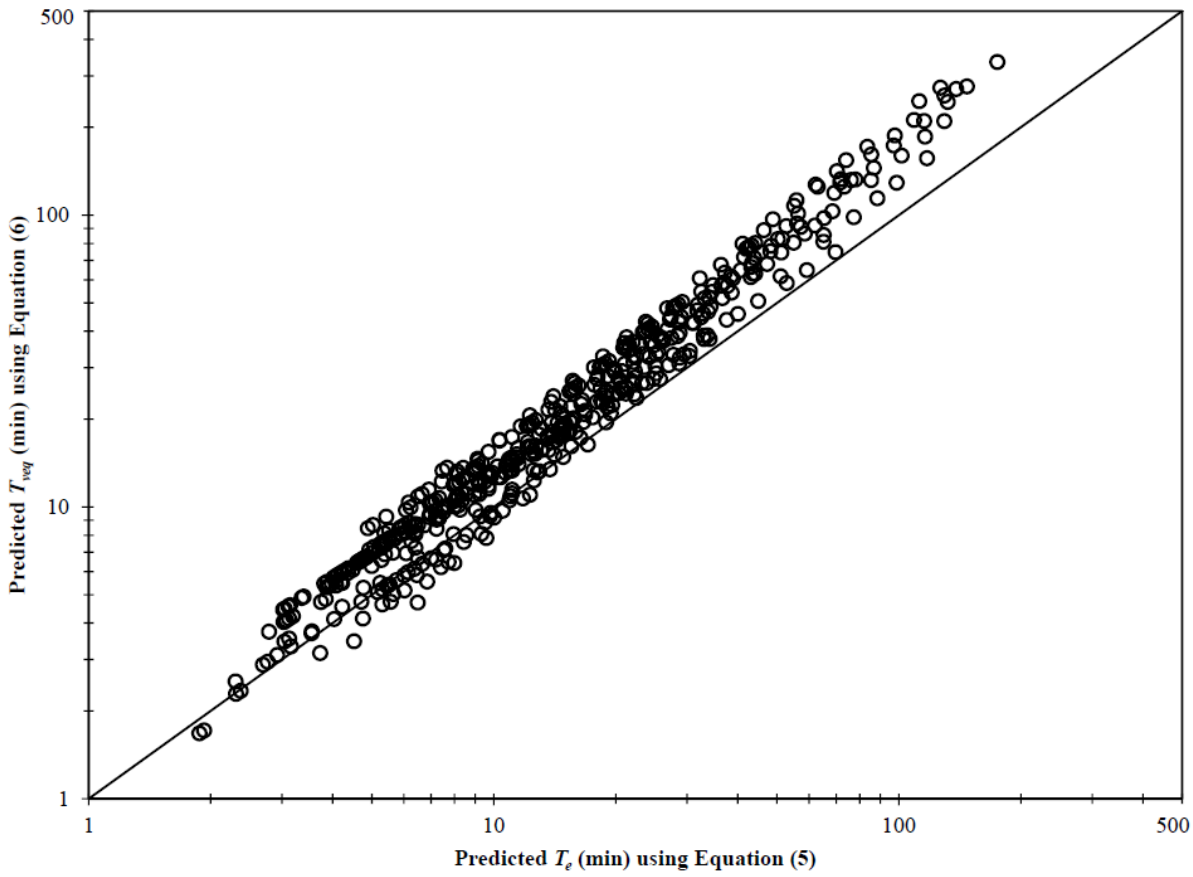

Fig. 4.5. Time to equilibrium velocity (T_{veq}) predicted using the regression Eq. (4.6) versus T_e predicted using Eq. (4.5) from Henderson and Wooding (1964) for impervious overland flow surfaces.

Chapter 5 Conclusions and Recommendations

5.1 Conclusions

Part of this research (Research Objective one and Chapter two) was conducted for Texas Department of Transportation (TxDOT) Research Project 0–6382 “Establish effective lower bounds of watershed slope for traditional hydrologic methods” funded by the TxDOT through a sub-contract from Texas Tech University. The objective of the project was the extension of research database for low-slope study, either by collection of existing data from various smaller watersheds, or by field data collection of hydrologic responses of low-slope watersheds in selected locations in Texas, to provide a research database to investigate hydrologic behavior on different slopes. The database may be analyzed in a variety of fashions by the researchers; if generic modeling is determined to be useful; such a database should be used to defend model results. An effective lower bound of the topographic slope at which the traditional hydrologic timing relationships become unreliable should be identified from literature and numerical modeling. And finally identification, suggestion, and development of alternate methods for hydrologic application in low-slope regions should be completed.

The objective was achieved through the development of overland flow model with appropriate rainfall loss models for impervious and pervious surfaces and generation of estimation equations for non-low and low slopes. The key conclusions of the first objective from Chapter two (Paper 1) are:

- The field study was conducted by researchers at Texas A&M University on a concrete plot to extend the research database for relatively low-sloped plane of 0.25%. Rainfall and runoff data were recorded for 27 events from April 2009 to March 2010. The data collected were used for the model validation in this study.
- Based on the literature review and simulation results from current study, slope at 0.1% was decided to be the lower-bound slope, S_{lb}. Slopes less than S_{lb} are defined as low slopes; those equal to or greater than S_{lb} are defined as non-low or standard slopes ($S_o \geq 0.1\%$) in this study.
- A quasi-two-dimensional dynamic wave model, Q2DWM was developed to simulate runoff hydrographs for standard ($S_o \geq 0.1\%$) and low-sloped planes ($S_o < 0.1\%$). The validated Q2DWM model was used in a parametric study to generate 750 T_c data for a range of slopes and other input variables (length L, roughness coefficient n, and rainfall intensity i) that were used to develop T_c regression formulas for non-low (standard) and low slopes. The Eq. (2.17) for low-slope is recommended for estimating T_c where topographic slopes are low ($S_o < 0.1\%$).

For the second objective, a quasi-two dimensional diffusion wave model with particle tracking, DWMPT was developed from the diffusion hydrodynamic model, DHM (Hromadka and Yen 1986) for calculating travel time of all the particles in the discretized domain of the impervious overland surface. The key conclusions of the second objective from Chapter three (Paper 2) are:

- The travel times of all particles in the domain consisting of both slow moving particles at the upstream and fast moving particles at the downstream are

consolidated into representative time parameters T_{t85}, T_{t95}, and T_{t100} that are based on the 85%, 95%, and 100% particles arrival at the outlet, respectively.

- A total of 530 DWMPT runs were performed to determine travel times on impervious surfaces using diverse combinations of the four physically based input variables L, S_o, n, and i; and were used to develop estimation equations for T_{t85}, T_{t95} and T_{t100}.
- All the travel times (T_{t85}, T_{t95}, and T_{t100}) showed non-linear relations with the input variables (L, S_o, n, and i); and are directly proportional to L and n (both raised approximately to a power 0.6) and inversely proportional to S_o (raised approximately to a power 0.3) and i (raised approximately to a power 0.4).
- Similarly, T_c was estimated from hydrograph analysis as the time when outflow discharge reaches 98% of peak discharge Q_p. T_{t85} showed a close correlation with T_c as shown in Eq. (3.5) and can be used to estimate T_c.
- Even though, all the travel times showed non-linear relations with the input variables, they showed linear relations with each other in Eqs. (3.6) and (3.7), and T_{t95} can be approximately expressed as an average of T_{t85} and T_{t100}.

For the third objective, 530 DWM runs were performed to determine equilibrium velocity V_{eq} on impervious surfaces using diverse combinations of the four physically based input variables: L, S_o, n, and i. The key conclusions of the third objective from Chapter four (Paper 3) are:

- A regression formula (Eq. 4.4) for estimating V_{eq} for the overland flow on impervious surface was developed in this study. V_{eq} was found to be directly but nonlinearly proportional to rainfall intensity, length and slope of the flow plane,

and inversely proportional to the roughness of the flow plane. However, the slope was found to be less significant in the regression estimation equation.

- Similarly, a relation between time to equilibrium velocity T_{veq} and the four physically based input variables was also developed (Eq. 4.6). V_{eq} and T_{veq} calculated using the Eqs. (4.4) and (4.6) provide useful information on predictive modeling of movement and transport of waters/pollutants on impervious surfaces.

5.2 Limitations of the Study

The study proposed estimation equations for important hydrologic time parameters; travel time, time of concentration T_c and time to equilibrium velocity T_{veq}. Since these equations are based on physically based input variables: length, slope, roughness coefficient of the surfaces, and effective rainfall intensity, they can be used for the estimation of time parameters in ungaged watersheds without the limitation of geographic location without any modeling tool. However, in order to develop generalized estimation equations, effective rainfall intensity was used as one of the input parameters in these estimation equations. The rainfall loss depends on a number of factors like location, weather, type of rainfall (moving or stationary), uniform or variable rainfall, antecedent conditions of the surface, wind intensity and direction, surface roughness, rainfall intensity, etc. These factors make the development of generalized equations for rainfall loss difficult. Hence, the users should apply an appropriate rainfall loss estimation method to find the effective rainfall intensity based on their watershed condition and available data before applying the estimation equations for time parameters developed in this study.

Even though Manning's *n* is an empirical coefficient, it is considered as a physically based parameter since it is a well-established coefficient for a large number of surface types (Engman 1986). For the parametric study the model uses single value of roughness for each type of surface even though the model has the capability of using unique value of roughness for each cell in the computational domain. However, in natural catchments, the roughness of the surface may vary from upstream to downstream. One way to evaluate this limitation is to use roughness values produced by random number generator within small tolerance for the cells in the simulation domain and redevelop estimation equations using OFM.

Similarly, the model uses specific slope for each run with uniform elevation variation for each cell in the computational domain from upstream to downstream. However, in natural catchments, even though the overall slope may be the same as used in the simulation, there can be small variations within the catchments. This limitation can also be evaluated using random variation in slope (elevation) produced by random number generator within small tolerance and to use different values in each cell of the domain for OFM modeling study.

Though the Overland Flow Model OFM was validated extensively using discharge, velocity and depth hydrographs, the accuracy of the simulation could be improved using more accurate method like smoothed-particle hydrodynamics (Monaghan 1992; Liu and Liu 2003) for particle tracking. However, the computational burden of the simulation should also be evaluated based on the accuracy increased.

5.3 Future Research

The three objectives of this study are for impervious surfaces. However, evaluation of travel time on pervious surface is equally or more important in hydrology. Even though previous and current studies (Morgali and Linsley 1965; Su and Fang 2004; KC et al. 2014) have proposed T_c estimation equations of overland flow on impervious surface; there has been lack of T_c estimation equations for pervious surface based on physically based input infiltration parameters. Even though using constant runoff coefficient over the entire rainfall event may provide an approximate estimate for impervious surface, it does not physically represent the infiltration process (Smith and Lee 1984). For overland flow generation, the rainfall rate has to exceed the infiltration capacity of the surface soil. Based on the surface infiltration capacity curves on a pervious surface and an impervious surface, rainfall excesses or effective rainfalls on these surfaces are different. Therefore, for the same rainfall input, T_c of overland flow on a pervious surface can be significantly different from T_c on an impervious surface (the same size plot). Hence, it is imperative to incorporate the influence of infiltration on T_c on pervious surface (Paintal 1974; Hjelmfelt 1978).

Akan (1989) developed an estimation equation for T_c on a rectangular pervious surface based on kinematic-wave overland flow and Green-Ampt infiltration, but did not couple the effect of surface roughness, slope, and rainfall intensity with infiltration parameters. Hence, development of regression formula to estimate overland flow T_c on pervious surface using all physically based input variables is relevant. However, for pervious surface even when the surface soil becomes saturated; the hydraulic conductivity allows the infiltration process to continue and the discharge continues to

increase gradually. Therefore, equilibrium or peak discharge cannot be directly used to determine T_c for pervious surface as was done for impervious surface (KC et al. 2014). Hence, the particle tracking method developed in this study becomes a more suitable method to determine T_c on pervious surface. Hence, the future studies using Overland Flow Model integrated with Green-Ampt Infiltration Loss Model (Appendix A) and Particle Tracking Model is being used for further journal publication under preparations:

- **KC, Manoj**, Fang, Xing, Yi, Young-Jae., Li, Ming-Han., Thompson, David. B., and Cleveland, Theodore. G. "Estimation of time of concentration for pervious overland flows using laboratory and numerical studies." (under preparation)
- **KC, Manoj,** and Fang, Xing "Estimating time parameters of overland flow on pervious surfaces by the particle tracking method." (under preparation)
- **KC, Manoj**, and Fang, X. "Estimation of the virtual equilibrium velocity of overland flows induced by constant rainfalls on pervious surfaces." (under preparation)

A part of study results has been accepted for a conference paper as:

- **KC, Manoj**, and Fang, Xing (2014). "Estimating time of concentration of overland flow on pervious surface." World Environmental and Water Resources Congress 2014, ASCE/EWRI, Portland, OR.

Appendix A Green-Ampt Infiltration Loss Model

A.1 Green-Ampt Infiltration Loss Model (GAIL)

Green and Ampt (1911) originally developed Green-Ampt model to derive infiltration from a ponded surface into a deep homogenous soil with uniform initial water content. Green and Ampt applied Darcy's law by assuming a sharply defined wetting front which separates soil into an upper zone that has been wetted or saturated by infiltration and a lower zone that is relative dry and at its initial water content. The transition was assumed to be a sharp wetting front as shown in the Fig. A.1. Referring to the Fig. A.1, Darcy's law can be written as

$$Q_z = A_z K_{sat} \frac{\partial H_z}{\partial z}, \tag{A.1}$$

where Q_z is the flow into the soil from the soil surface, A_z is the cross-sectional area of the soil column or a computation cell, K_{sat} is the saturated hyraulic conductivity of the soil, H_z is the total hydraulic head and z is the vertical coordinate. Dividing Q_z by A_z, the flux can be represented as potential infiltration rate f_p as,

$$f_p = K_{sat} \frac{z + \zeta + S_e}{z + \zeta}, \tag{A.2}$$

where ζ is the depth of water ponded on the surface, z is the vertical distance from the surface soil to the wetting front, and S_e is the effective suction head at the wetting front. The determination of S_e requires knowledge of wetting front, and is difficult to be determined (Parsons and Muñoz-Carpena 2009). Mein and Larson (1973) replaced S_e

by the average suction S_{av} at the wetting front that is typically considered as one of the soil characteristics.

Similarly the cumulative infiltration F is given by

$$F = (\theta_s - \theta_i)z = M_d z\,, \tag{A.3}$$

where θ_i and θ_s are initial water (soil moisture) content at t = 0 in the whole soil column and at any time in the dry zone and saturated water content in the wet zone, respectively, M_d is initial moisture deficit. Assuming the surface has just ponded i.e. $\zeta \approx 0$ and replacing f_p by the rate change of F, Eq. (A.2) becomes

$$f_p = \frac{dF}{dt} = K_{sat} + \frac{K_{sat} S_{av} M_d}{F}, \tag{A.4}$$

The variables in Eq. (A.4) can be separated and integrated to obtain an expression for cumulative infiltration as a function time (Mein and Larson 1971).

$$F = K_{sat} t + M_d S_{av} \ln\left(1 + \frac{F}{M_d S_{av}}\right), \tag{A.5}$$

Eq. (A.5) is the expression for cumulative infiltration as a function of time for ponded conditions with steady rainfall.

For non-ponded condition, all the rainfall input i_g is infiltrated hence $f_p = i_g$ and defining the cumulative infiltration at the time of ponding as $F_{p,}$ Eq. (A.4) can be written as,

$$F_p = \frac{S_{av} M_d}{i_g / K_{sat} - 1}, \tag{A.6}$$

Up to ponding $F_p = i_g t_{po}$ where t_{po} is the time to ponding, which is can be calculated by

$$t_{po} = \frac{F_p}{i_g}, \tag{A.7}$$

Rain falling on a watershed may infiltrate into the soil, flow away into the waterways, be retained upon the ground surface, or evaporate. The effect of evaporation may be considered negligible for short period of time. Hence, the water budget can be written as

$$I_g = F + S + I_e, \tag{A.8}$$

where I_g is the cumulative rainfall depth (mm or inches), S is the surface ponding, and I_e is the cumulative rainfall excess. For a given surface condition there exists a maximum amount of water which can be retained on the surface without causing runoff which is referred to as the retention capacity. The range of variation of the surface ponding is therefore limited by

$$0 \le S \le D, \tag{A.9}$$

where D is the retention capacity. Hence for steady rainfall,

$f = i_g$, for $i_g \le f_p$ or $S<D$ or (A.10)

and, if $t > t_p$, then

$$f = f_p = K_{sat} + \frac{K_{sat} S_{av} M_d}{F_p}, \quad \text{for } i_g > f_p \quad \text{or } S=D \text{ or} \tag{A.11}$$

The infiltration capacity in Eq. (A.11) is not influenced by the infiltration volume up to surface saturation (Mein and Larson 1971). Hence, Mein and Larson proposed an expression for cumulative infiltration as a function of time from the beginning of the rainfall. A new time factor t_{ps} is introduced as the equivalent time to infiltrate the volume F_p under initially ponded conditions. By replacing f_p by rate change of F, and separating variables in Eq. (A.11), Mein and Larson (1971) derive expression for

cumulative infiltration with adjusted time scale.

$$F = K_{sat}(t - t_p + t_{ps}) + M_d S_{av} \ln\left(1 + \frac{F}{M_d S_{av}}\right) \quad \text{(A.12)}$$

where t is the time from the beginning of the rainfall.

For calculating infiltration for unsteady rainfall Chu (1978) provided a simplified approach for using Green-Ampt model along with water balance. For a steady rain, infiltration starts with an un-ponded condition and later changes to a ponded condition, which lasts until the end of the rainfall event so there is only one ponding time in steady rainfall (Chu 1978). For an unsteady rainfall event, there may be several periods where the rainfall intensity exceeds the infiltration rate. The infiltration may change from ponded condition to un-ponded condition. Taking rate of change of Eq. (A.8) with respect to time,

$$i_g = f + dS/dt + i_e \quad \text{(A.13)}$$

The cumulative rainfall excess I_e is the time integral of the rainfall excess rate

$$I_e = I_e(t) = \int i_e(t)dt \quad \text{(A.14)}$$

Hence from Eqs. (A.10), (A.11), (A.13) and (A.14), the cumulative infiltration at the time of ponding is

$$F(t_p) = I_g(t) - I_e(t) = I_g(t) - I_e(t') = F_o, \quad \text{(A.15)}$$

where t' is a time during the period without surface ponding but prior to the ponding time, t_p and F_o is the cumulative infiltration at the ponding time. After the determination of t_p and t_{ps} the infiltration process during an unsteady rain can be solved analytically as follows (Chu 1978).

During no-ponding condition from time *t'* to *t*

$$I_e(t) = I_e(t') \tag{A.16}$$

$$F(t) = F_u(t) = I_g(t) - I_e(t') \tag{A.17}$$

$$f(t) = i_g(t) < f_p \tag{A.18}$$

$$i_e(t) = 0 \tag{A.19}$$

where F_u is the cumulative infiltration without surface ponding.

During ponding condition from time *t'* to *t*

$$F(t) = F_p(t) \tag{A.20}$$

where F_p is calculated by the implicit relation

$$F_p = K_{sat}(t - t_p + t_{ps}) + M_d S_{av} \ln\left(1 + \frac{F_p}{M_d S_{av}}\right) \tag{A.21}$$

$$f(t) = f_p = K_{sat} + \frac{K_{sat} S_{av} M_d}{F_p} \qquad \text{for } I_g - F - S > I_e(t) \tag{A.22}$$

$$I_e(t) = I_e(t') \qquad \text{for } I_g - F - S \le I_e(t') \tag{A.23}$$

$$i_e(t) = i_g(t) - f_p \qquad \text{for } S = D \quad i > f_p \tag{A.24}$$

$$i_e(t) = 0 \qquad \text{for } S < D \quad i \le f_p \tag{A.25}$$

The algorithm used to compute infiltration loss and excess rainfall for the GAIL is:

1. Calculate rainfall rate, i_g for the time, *t*. Then two conditions are checked; not ponded at the start of the time period or already ponded at the start of the time period.
2. For the case of not ponded at the start of the time period, first assuming to continue not ponded, then calculate time of ponding, t_p. If $t_p > t$ then it is in

non-ponded condition, calculate infiltration rate, cumulative infiltration using Eqs. (A.17) to (A.19).

3. Ponding occurs during the period: If $t_p > t$ and $t_p < t+\Delta t$; the ponding occurs during the time interval. Calculate cumulative infiltration using Eq. (A.21) using iteration by Newton-Raphson method. Calculate infiltration rate, cumulative infiltration and rainfall excess using Eqs. (A.20) to (A.25).
4. For the case of already ponded at the start of the time period, first assuming to continue ponded during the whole period, and then find equivalent time, t_{ps} to infiltrate cumulative infiltration under ponded condition using Eq. (A.21) using Newton-Raphson iteration method. Check if the ponding still continues. If the ponding still continues then calculate cumulative infiltration using Eq. (A.21) using iteration by Newton-Raphson method. Calculate infiltration rate, cumulative infiltration and rainfall excess using Eqs. (A.20) to (A.25). Calculate time of ponding, $t_{p.}$ If $t_p < t$ then it is in non-ponded condition, calculate infiltration rate, cumulative infiltration using Eqs. (A.17) to (A.19).
5. If ponding ceases during the period: calculate time at which the ponding ceases, and use non-ponded conditions to calculate infiltration rate, cumulative infiltration using Eqs. (A.17) to (A.19).
6. Repeat steps (1) to (3) for the event.

A.2 Simplified Green-Ampt Infiltration Loss Model (SGAIL)

The simplified Green-Ampt Infiltration Loss model (SGAIL) was developed using the infiltration theory of Polubarinova-Kochina (1962), but the model is structurally identical

to the independently developed Green-Ampt model with some minor conceptual differences. The model assumes Darcy's law for the propagation of infiltration front into the watershed soils, and the water content change across the front is proportional to the soil porosity. The front propagates into the soil without moisture redistribution. The difference between the gross rainfall and the loss is the excess rainfall as the event progresses.

The three soil profiles at time, $t = 0$ to time $t = t_2$ is shown in Fig. A.2. A small depth of initial wetting is assumed into the soil to prevent an infinite gradient calculation when computing the flux. The rainfall volume input is represented by the block above the second and third soil column. The second profile shows the infiltration after a pulse of rainfall. After the infiltration for that time interval is calculated, the rainfall after infiltration remaining if any becomes excess rainfall. The third profile shows the infiltration depth stacked into the soil, advancing successively.

The wetting front velocity (in second and third soil column in Fig. A.2) can be expressed as

$$\frac{\partial z}{\partial t} = \frac{f_p}{\Phi}, \tag{A.26}$$

where f_p is the potential infiltration rate, Φ is the soil porosity, and z is the infiltration front position at time t or depth of the wet (saturated) soil zone. Darcy's law relating the potential infiltration rate to the front position can be written as

$$f_p = K_{sat} \frac{h_p + h_c + z}{z}, \tag{A.27}$$

where K_{sat} is the saturated hydraulic conductivity, h_p is the ponding depth, and h_c is the suction potential. Substituting of Eq. (A.27) into Eq. (A.26),

$$\Phi \frac{\partial z}{\partial t} = K_{sat} \frac{h_p + h_c + z}{z} \qquad \text{(A.28)}$$

Above equation was simplified according to Charbeneau (2000). h_p is taken to be zero and suction potential is assumed to be constant. Since the time scale of the problem considered in this study is large enough so that this term becomes irrelevant quickly after the initial absorption of rainfall and the system behaves nearly as unit-gradient throughout each event. To avoid the intial gradient from being very large into a dry soil, a small non zero value of ponding is assumed. The simplified model is then represented as

$$\Phi \frac{\partial z}{\partial t} = K_{sat} \frac{h_c + z + \zeta}{z + \zeta} \qquad \text{(A.29)}$$

where, ζ = 0.01, h_c, K_{sat} and Φ are soil dependent parameters. The value of Φ varies from 10% to 50% with 35% being a typical value for porosity for most soil.

The algorithm used to compute infiltration loss and excess rainfall for SGAIL is:

1. Calculate potential infiltration rate, f_p using right hand side of Eq. (A.29) for the time, *t*.
2. If the infiltration loss rate is greater than gross rainfall rate, all the rainfall is lost to infiltration, *i.e.*, $i_g(t) = f_p(t)$, and the net infiltration depth for that time is calculated as $z(t+\Delta t) = z(t)+i_g(t)/\Phi$.
3. If the infiltration loss rate is less than gross rainfall rate, the loss rate is subtracted from the gross rainfall to get the effective rainfall, *i.e.*, $i(t) = i_g(t)- f_p(t)$, and the net infiltration depth for that time is calculated as $z(t+\Delta t) = z(t)+f_p(t)/\Phi$.
4. All the steps are repeated from (1) to (3) till the event lasts.

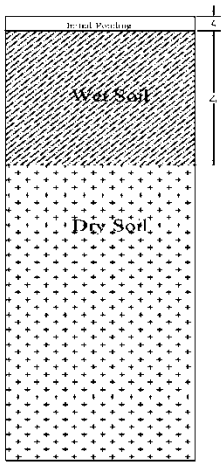

Fig. A.1. Schematic diagram for the Green-Ampt Infiltration Loss model (GAIL)

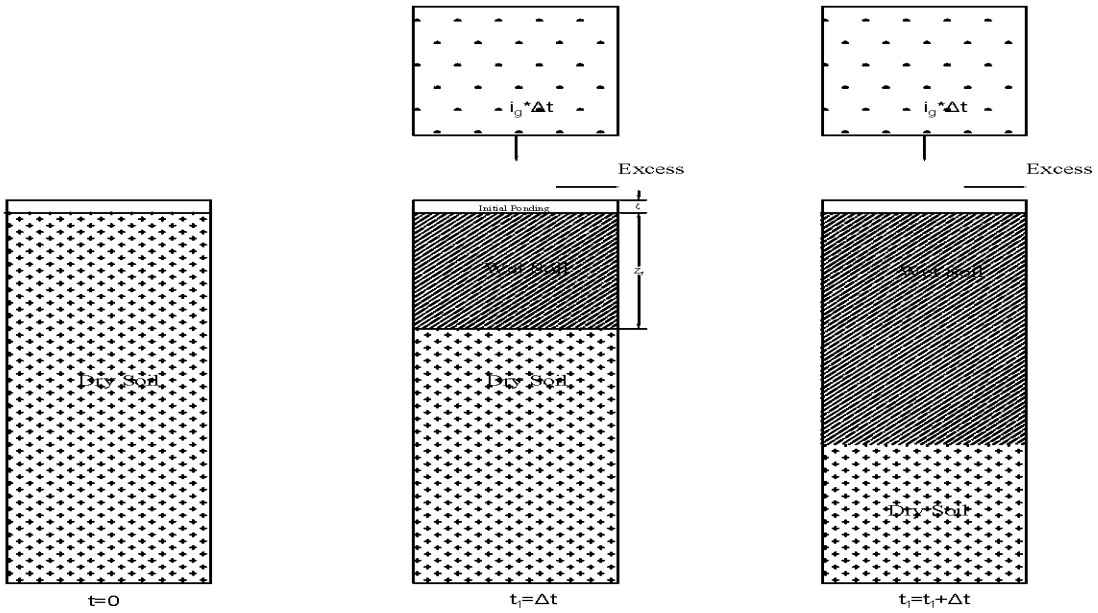

Fig. A.2. Schematic diagram for the Simplified Green-Ampt Infiltration Loss model (SGAIL)

References

Abbott, M., Bathurst, J., Cunge, J., O'connell, P., and Rasmussen, J. (1986). "An introduction to the European hydrological system—Systeme hydrologique Europeen, 'SHE', 2: Structure of a physically-based, distributed modelling system." *Journal of Hydrology*, 87(1-2), 61-77.

Abrahams, A. D., Parsons, A. J., and Luk, S. H. (1986). "Field measurement of the velocity of overland flow using dye tracing." *Earth Surface Processes and Landforms*, 11(6), 653-657.

Admiraal, D. M., Stansbury, J. S., and Haberman, C. J. (2004). "Case study: Particle velocimetry in a model of lake Ogallala." *Journal of Hydraulic Engineering*, 130(7), 599-607.

Adrian, R. J. (1991). "Particle-imaging techniques for experimental fluid mechanics." *Annual review of fluid mechanics*, 23(1), 261-304.

Ahlstron, S. W., Foote, H. P., Arnett, R. C., Cole, C. R., and Serne, R. J. (1977). "Multicomponent mass transport model: Theory and numerical implementation (discrete-parcel-random walk version." *BNWL 2127*, BNWL 2127 for ERDA, Battelle Pacific Northwest Lab., Richland, Wash., USA.

Akan, A. O., and Yen, B. C. (1981). "Diffusion-wave flood routing in channel networks." *Journal of the Hydraulics Division*, 107(6), 719-732.

Akan, A. O., and Yen, B. C. (1984). "Effect of time distribution of rainfall on overland runoff." *Proceedings of the Third International Conference on Urban Storm Drainage*, June 4-8, Goteborg, Sweden, v.1, 193-202.

Akan, A. O. (1986). "Time of concentration of overland flow." *Journal of Irrigation and Drainage Engineering*, 112(4), 283-292.

Akan, A. O. (1989). "Time of concentration formula for pervious catchments." *Journal Of Irrigation and Drainage Engineering*, 115(4), 733-735.

Amsden, A. A. (1966). "The particle-in-cell method for calculation of the dynamics of compressible fluids." *LA-3466*, Los Alamos Scientific Lab., University of California, USA.

Aryal, S. K., O'Loughlin, E. M., and Mein, R. G. (2005). "A similarity approach to determine response times to steady-state saturation in landscapes." *Advances in*

Water Resources, 28(2), 99-115.

Ben-zvi, A. (1984). "Runoff peaks from two-dimensional laboratory watersheds." *Journal of Hydrology*, 68(1–4), 115-139, doi:10.1016/0022-1694(84)90207-5.

Bennis, S., and Crobeddu, E. (2007). "New runoff simulation model for small urban catchments." *Journal of Hydrologic Engineering*, 12(5), 540-544.

Berman, E. S., Gupta, M., Gabrielli, C., Garland, T., and McDonnell, J. J. (2009). "High-frequency field-deployable isotope analyzer for hydrological applications." *Water Resources Research*, 45(10), 1-7.

Bondelid, T. R., McCuen, R. H., and Jackson, T. J. (1982). "Sensitivity of SCS models to curve number variation." *Water Resources Bulletin*, 20(2), 337-349.

Bradley, A. A., Kruger, A., Meselhe, E. A., and Muste, M. V. (2002). "Flow measurement in streams using video imagery." *Water Resources Research*, 38(12), 51-1--51-8.

Butler, S. S. (1977). "Overland-flow travel time versus reynolds number." *Journal of Hydrology*, 32(1-2), 175-182.

Capece, J. C., Campbell, K. L., and Baldwin, L. B. (1988). "Estimating runoff peak rates from flat, high-water-table watersheds." *Transactions of the ASAE*, 31(1), 74-81.

Chang, T. P. K., Watson, A. T., and Tatterson, G. B. (1985). "Image processing of tracer particle motions as applied to mixing and turbulent flow - I. The technique." *Chemical engineering science*, 40(2), 269-275.

Charbeneau, R. J. (2000). *Groundwater hydraulics and pollutant transport*, Prentice-Hall, Inc., Upper Saddle River, NJ.

Chen, C. N., and Wong, T. S. W. (1993). "Critical rainfall duration for maximum discharge from overland plane." *Journal of Hydraulic Engineering*, 119(9), 1040-1045.

Chow, V. T. (1967). "Laboratory study of watershed hydrology." Proc. Int. Hydrol. Symp., Fort Collins, Colo., 194-202.

Chow, V. T., Maidment, D. R., and Mays, L. W. (1988). *Applied hydrology*, McGraw Hill, New York.

Chu, S. T. (1978). "Infiltration during an unsteady rain." *Water Resources Research*, 14(3), 461-466.

Cleveland, T. G., Thompson, D. B., Fang, X., and He, X. (2008). "Synthesis of unit hydrographs from a digital elevation model." *Journal of Irrigation and Drainage Engineering*, 134(2), 212-221.

Cleveland, T. G., Thompson, D. B., Fang, X., and Li, M.-H. (2011). "Establish effective lower bounds of watershed slope for traditional hydrologic methods – Final Report." *Research Report 0-6382-1*, Department of Civil and Environmental Engineering, Texas Tech University Lubbock, TX.

Courant, R., Friedrichs, K., and Lewy, H. (1967). "On the partial difference equations of mathematical physics." *IBM Journal of Research and Development*, 11(2), 215-234.

Dhakal, N., Fang, X., Cleveland, G. T., Thompson, D., Asquith, W. H., and Marzen, L. J. (2012). "Estimation of volumetric runoff coefficients for Texas watersheds using land use and rainfall runoff data." *Journal of Irrigation and Drainage Engineering*, 138(1), 43-54.

Doan, J. H. (2000). "Geospatial hydrologic modeling extension HEC-GeoHMS -user's manual - version 1.0." U.S. Army Corps of Engineers Hydrologic Engineering Center, Davis, California, USA.

Dunkerley, D. (2001). "Estimating the mean speed of laminar overland flow using dye injection-uncertainty on rough surfaces." *Earth Surface Processes and Landforms*, 26(4), 363-374, doi:10.1002/esp.185.

Dunkerley, D. L. (2003). "An optical tachometer for short-path measurement of flow speeds in shallow overland flows: improved alternative to dye timing." *Earth Surface Processes and Landforms*, 28(7), 777-786, doi:10.1002/esp.468.

Dunne, T., and Dietrich, W. E. (1980). "Experimental investigation of horton overland flow on tropical hillslopes: II. Hydraulic characteristics and hillslope hydrographs." *Z. Geomorphol. Suppl.*, 35, 60-80.

Emmett, W. (1970a). "The hydraulics of overland flow on hillslopes." US Geological Survey, Professional Paper 662A.

Emmett, W. (1970b). "The hydraulics of overland flow on hillslopes ", US Geological Survey, Professional Paper 662A, 68.

Engman, E. T. (1986). "Roughness coefficients for routing surface runoff." *J. Irrig. Drain. Eng.*, 112(1), 39-53.

Esteves, M., Planchon, O., Lapetite, J. M., Silvera, N., and Cadet, P. (2000). "The 'EMIRE' large rainfall simulator: Design and field testing." *Earth Surface Processes and Landforms*, 25, 681–690.

Ferguson, B. K. (1994). *Stormwater infiltration*, I Ed., Lewis Publisher, Boca Raton, FL.

Froehlich, D. C. (2011). "NRCS overland flow travel time calculation." *Journal Of Irrigation and Drainage Engineering*, 137(4), 258-262.

Gardner, R. P., and Dunn III, J. W. (1964). "A single-sample radiotracer technique for determining stream flow rates." *The International Journal of Applied Radiation and Isotopes*, 15(6), 339-344, doi:http://dx.doi.org/10.1016/0020-708X(64)90123-1.

Gonwa, W. S., and Kavvas, M. L. (1986). "A modified diffusion equation for flood propagation in trapezoidal channels." *Journal of Hydrology*, 83(1–2), 119-136, doi:10.1016/0022-1694(86)90187-3.

Govers, G. (1992). "Relationship between discharge, velocity and flow area for rills eroding loose, non-layered materials." *Earth Surface Processes and Landforms*, 17(5), 515-528, doi:10.1002/esp.3290170510.

Graf, J. B., Garklavs, G., and Oberg, K. A. (1982). "A technique for estimating time of concentration and storage coefficient values for Illinois streams." *USGS/WRI 82-22*, Water-Resources Investigations Report, U. S. Geological Survey, 1-10.

Green, W. H., and Ampt, G. A. (1911). "Studies on soil physics. 1. The flow of air and water through soils." *J. Agric. Sci*, 4(1), 1-24.

Grimaldi, S., Petroselli, A., Alonso, G., and Nardi, F. (2010). "Flow time estimation with spatially variable hillslope velocity in ungauged basins." *Advances in Water Resources*, 33(10), 1216-1223, doi:http://dx.doi.org/10.1016/j.advwatres.2010.06.003.

Grimaldi, S., Petroselli, A., Tauro, F., and Porfiri, M. (2012). "Time of concentration: a paradox in modern hydrology." *Hydrological Sciences Journal*, 57(2), 217-228, doi:10.1080/02626667.2011.644244.

Habib, E., Krajewski, W. F., and Kruger, A. (2001). "Sampling errors of tipping-bucket rain gauge measurements." *Journal of Hydrologic Engineering*, 6(2), 159-166.

Harlow, F. E. (1963). "The particle-in-cell method for numerical solution of problems in fluid dynamics." *Proceedings of Symposia in Applied Mathematics*, 15, 269.

Harlow, F. H., and Welch, J. E. (1966). "Numerical study of large amplitude free surface motions." *Physics of Fluids*, 9(5), 842-851, doi:doi:http://dx.doi.org/10.1063/1.1761784.

Henderson, F. M., and Wooding, R. A. (1964). "Overland flow and groundwater flow from a steady rainfall of finite duration." *Journal of Geophysical Research*, 69(8), 1531-1540.

Hicks, W. I. (1942a). "Discussion of "Surface runoff determination from rainfall without using coefficients" by W. W. Horner and S. W. Jens." *Trans. ASCE*, 107, 1097-1102.

Hicks, W. I. (1942b). "Discussion of "Surface runoff determination from rainfall without

using coefficients" by W. W. Horner and S. W. Jens." *Trans. ASCE*, 107(1), 1097-1102.

Hillel, D. (2004). *Introduction to environmental soil physics*, I Ed., Academic press.

Hjelmfelt, A. T. (1978). "Influence of infiltration on overland flow." *Journal of Hydrology*, 36(1-2), 179-185.

Hromadka, T. V., and Yen, C. C. (1986). "A diffusion hydrodynamic model (DHM)." *Advances in Water Resources*, 9(3), 118-170.

Hu, G.-Q., Dong, Y.-J., Wang, H., Qiu, X.-K., and Wang, Y.-H. (2011). "Laboratory testing of magnetic tracers for soil erosion measurement." *Pedosphere*, 21(3), 328-338, doi:http://dx.doi.org/10.1016/S1002-0160(11)60133-1.

Huber, W. C., Dickinson, R. E., and Barnwell Jr, T. O. (1988). "Storm water management model; version 4." *Environmental Protection Agency, United States*.

Ivanov, V. Y., Vivoni, E. R., Bras, R. L., and Entekhabi, D. (2004). "Preserving high-resolution surface and rainfall data in operational-scale basin hydrology: a fully-distributed physically-based approach." *Journal of Hydrology*, 298(1), 80-111.

Izzard, C. F., and Augustine, M. T. (1943). "Preliminary report on analysis of runoff resulting from simulated rainfall on a paved plot." *Transactions of American Geophysical Union*, 24(2), 500-509.

Izzard, C. F. (1946). "Hydraulics of runoff from developed surfaces." *Proc.of the 26th Annual Meetings of the Highway Research Board*, 5-8 December, Washington, D.C., USA, Highway Research Board, v.26, 129-150.

Izzard, C. F., and Hicks, W. I. (1946). "Hydraulics of runoff from developed surfaces." *26th Annual Meetings of the Highway Research Board*, Highway Research Board, v.26, 129-150.

Jia, Y., Ni, G., Kawahara, Y., and Suetsugi, T. (2001). "Development of WEP model and its application to an urban watershed." *Hydrological Processes*, 15(11), 2175-2194.

Johnstone, D., and Cross, W. P. (1949). *Elements of applied hydrology*, Ronald Press, New York.

Kazezyılmaz-Alhan, C. M., and Medina Jr., M. A. (2007a). "Kinematic and diffusion waves: analytical and numerical solutions to overland and channel flow." *Journal of Hydraulic Engineering*, 133, 217.

Kazezyılmaz-Alhan, C. M., and Medina Jr., M. A. (2007b). "Kinematic and diffusion waves: analytical and numerical solutions to overland and channel flow." *Journal*

of Hydraulic Engineering, 133(2), 217-228.

KC, M., Fang, X., Yi, Y.-J., Li, M.-H., Cleveland, T. G., and Thompson, D. B. (2012). "Estimating time of concentration on low-slope planes using diffusion hydrodynamic model." World Environmental & Water Resources Congress 2012, ASCE/EWRI, Albuquerque, New Mexico.

KC, M., and Fang, X. (2014). "Estimating time parameters of overland flow on impervious surfaces by particle tracking method." *Hydrological Sciences Journal*, In Press, doi:10.1080/02626667.2014.889833.

KC, M., Fang, X., Yi, Y., Li, M.-H., Thompson, D. B., and Cleveland, T. G. (2014). "Improved time of concentration estimation on overland flow surfaces including low-sloped planes." *Journal of Hydrologic Engineering*, 19(3), 495-508.

Kent, K. M. (1972). "Travel time, time of concentration and lag." *National Engineering Hand Book - Hydrology, Section 4, Chapter 15*, U. S. Department of Agriculture, Washington, D. C., 1-16.

Kerby, W. S. (1959). "Time of concentration for overland flow." *Civil Engineering*, 29(3), 174.

Kibler, D. F., and Aron, G. (1983). "Evaluation of tc methods for urban watersheds." Frontiers in Hydraulic Engineering: Proc., Cambridge Conf., H. T. Shen, ed., ASCE, New York, 553-558.

Kirpich, Z. P. (1940). "Time of concentration of small agricultural watersheds." *Civil Engineering*, 10(6), 362.

Konikow, L. F., and Bredehoeft, J. D. (1978). *Computer model of 2-dimensional solute transport and dispersion in groundwater*, U.S.G.S. TWRI Book 7, Chapter C2, U.S. Geological Survey, Washington, D.C.

Kuichling, E. (1889a). "The relation between the rainfall and the discharge of sewers in populous areas." *Transactions, American Society of Civil Engineers* 20, 1–56.

Kuichling, E. (1889b). "The relation between the rainfall and the discharge of sewers in populous areas." *Transactions, American Society of Civil Engineers* 20(1), 1–56.

Kull, D. W., and Feldman, A. D. (1998). "Evolution of Clark's unit graph method to spatially distributed runoff." *Journal of Hydrologic Engineering*, 3(1), 9-19.

Laflen, J. M., Lane, L. J., and Foster, G. R. (1991). "WEPP: A new generation of erosion prediction technology." *Journal of Soil and Water Conservation*, 46(1), 34-38.

Landreth, C., Adrian, R., and Yao, C. (2004). "Double pulsed particle image velocimeter with directional resolution for complex flows." *Experiments in fluids*, 6(2), 119-128.

Legates, D. R., and McCabe, G. J. (1999). "Evaluating the use of “goodness-of-fit” measures in hydrologic and hydroclimatic model validation." *Water Resources Research*, 35(1), 233-241.

Lei, T., Chuo, R., Zhao, J., Shi, X., and Liu, L. (2010). "An improved method for shallow water flow velocity measurement with practical electrolyte inputs." *Journal of Hydrology*, 390(1–2), 45-56, doi:http://dx.doi.org/10.1016/j.jhydrol.2010.06.029.

Lei, T., Yan, Y., Shi, X., Chuo, R., and Zhao, J. (2013). "Measuring velocity of water flow within a gravel layer using an electrolyte tracer method with a Pulse Boundary Model." *Journal of Hydrology*, 500, 37-44, doi:http://dx.doi.org/10.1016/j.jhydrol.2013.07.025.

Lei, T. W., and Nearing, M. A. (2000). "Flume experiments of determining rill hydraulic characteristic erosion and rill patterns." *Journal of Hydraulic Engineering (in China)*, 11(2000), 49-54.

Li, M.-H., Chibber, P., and Cahill, A. T. (2005). "Estimating time of concentration of overland flow on very flat terrains." 2005 ASAE Annual International Meeting, American Society of Agricultural Engineers, Tampa, Florida.

Li, M.-H., and Chibber, P. (2008). "Overland flow time of concentration on very flat terrains." *Transportation Research Record*, 2060, 133-140, doi:10.3141/2060-15.

Linsley, R. K., Kohler, M. A., and Paulhus, J. L. H. (1958). *Hydrology for Engineers*, McGraw - Hill Publications, New York.

Liu, G. R., and Liu, M. (2003). *Smoothed particle hydrodynamics: a meshfree particle method*, World Scientific Pub Co Inc.

Liu, Y. B., Gebremeskel, S., De Smedt, F., Hoffmann, L., and Pfister, L. (2003). "A diffusive transport approach for flow routing in GIS-based flood modeling." *Journal of Hydrology*, 283(1–4), 91-106, doi:10.1016/s0022-1694(03)00242-7.

Liu, Z. C., Landreth, C., Adrian, R., and Hanratty, T. (1991). "High resolution measurement of turbulent structure in a channel with particle image velocimetry." *Experiments in fluids*, 10(6), 301-312.

López-Barrera, D., García-Navarro, P., Brufau, P., and Burguete. (2012a). "Diffusive-Wave Based Hydrologic-Hydraulic Model with Sediment Transport. I: Model Development." *Journal of Hydrologic Engineering*, 17(10), 1093-1104.

López-Barrera, D., García-Navarro, P., Brufau, P., and Burguete, J. (2012b). "Diffusive-Wave Based Hydrologic-Hydraulic Model with Sediment Transport. I: Model Development." *Journal of Hydrologic Engineering*, 17(10), 1093-1104.

Luo, W., and Harlin, J. (2003). "A theoretical travel time based on watershed hypsometry." *Journal of the American Water Resources Association*, 39(4),

785-792.

Maidment, D. R. (1993). "Developing a spatially distributed unit hydrograph by using GIS." *Proceedings of the Vienna Conf., HydroGIS93*, 181-192.

McCuen, R. H., Wong, S. L., and Rawls, W. J. (1984). "Estimating urban time of concentration " *Journal of Hydraulic Engineering*, 110(7), 887-904.

McCuen, R. H., and Spiess, J. M. (1995). "Assessment of kinematic wave time of concentration." *Journal of Hydraulic Engineering*, 121(3), 256-266.

McCuen, R. H. (1998). *Hydrologic analysis and design*, 2 Ed., Prentice-Hall, Inc., Upper Saddle River, N.J., 814.

McCuen, R. H. (2009). "Uncertainty analyses of watershed time parameters." *Journal of Hydrologic Engineering*, 14(5), 490-498.

Mein, R. G., and Larson, C. L. (1971). "Modeling the infiltration component of the rainfall-runoff process."

Mein, R. G., and Larson, C. L. (1973). "Modeling infiltration during a steady rain." *Water Resources Research*, 9(2), 384-394, doi:10.1029/WR009i002p00384

Meselhe, E., Peeva, T., and Muste, M. (2004). "Large scale particle image velocimetry for low velocity and shallow water flows." *Journal of Hydraulic Engineering*, 130(9), 937-940.

Monaghan, J. J. (1992). "Smoothed particle hydrodynamics." *Annual review of astronomy and astrophysics*, 30, 543-574.

Moramarco, T., and Singh, V. P. (2002). "Accuracy of kinematic wave and diffusion wave for spatial-varying rainfall excess over a plane." *Hydrological Processes*, 16(17), 3419-3435.

Morgali, J. R., and Linsley, R. K. (1965). "Computer analysis of overland flow." *Journal Of Hydraulics Division*, 91(HY3), 81-100.

Morgan, R., Quinton, J., Smith, R., Govers, G., Poesen, J., Auerswald, K., Chisci, G., Torri, D., Styczen, M., and Folly, A. (1998). "The European soil erosion model (EUROSEM): documentation and user guide."

Mügler, C., Planchon, O., Patin, J., Weill, S., Silvera, N., Richard, P., and Mouche, E. (2011). "Comparison of roughness models to simulate overland flow and tracer transport experiments under simulated rainfall at plot scale." *Journal of Hydrology*, 402(1–2), 25-40, doi:10.1016/j.jhydrol.2011.02.032.

Mulvany, T. J. (1851). "On the use of self-registering rain and flood gauges in making observations of the relations of rainfall and flood discharges in a given

catchment." *Proceedings of the Institution of Civil Engineers of Ireland*, 4(2), 18-33.

Muzik, I. (1974). "Laboratory experiments with surface runoff." *Journal of the Hydraulics Division*, 100(4), 501-516.

Myers, T. G. (2002). "Modeling laminar sheet flow over rough surfaces." *Water Resources Research*, 38(11), 1230.

Natural Resources Conservation Service (NRCS). (1972). *Hydrology*, National Engineering Handbook, U.S. Dept. of Agriculture, Washington D.C.,USA.

Natural Resources Conservation Service (NRCS). (1986). "Urban hydrology for small watersheds." *Technical Release 55*, Washington, D.C., USA.

Nezu, I., and Rodi, W. (1986). "Open‐channel Flow Measurements with a Laser Doppler Anemometer." *Journal of Hydraulic Engineering*, 112(5), 335-355, doi:10.1061/(ASCE)0733-9429(1986)112:5(335).

Niemelä, J., Breuste, J. H., Guntenspergen, G., McIntyre, N. E., Elmqvist, T., and James, P. (2011). *Urban ecology: patterns, processes, and applications*, Oxford University Press.

Niri, M. Z., Saghafian, B., Golian, S., Moramarco, T., and Shamsai, A. (2012). "Derivation of Travel Time Based on Diffusive Wave Approximation for the Time-Area Hydrograph Simulation." *Journal of Hydrologic Engineering*, 17(1), 85-91.

Noto, L., and La Loggia, G. (2007). "Derivation of a Distributed Unit Hydrograph Integrating GIS and Remote Sensing." *Journal of Hydrologic Engineering*, 12(6), 639-650, doi:doi:10.1061/(ASCE)1084-0699(2007)12:6(639).

O'Brien, J. S. (2009). "Flo 2-D pocket guide." Flo-2D.

Olivera, F., and Maidment, D. R. (1999). "Geographic information systems(GIS)-based spatially distributed model for runoff routing." *Water Resources Research*, 35(4), 1155-1164.

Paintal, A. S. (1974). "Time of concentration--A kinematic wave approach." *Water and Sewage Works*, R26-R30.

Parsons, J. E., and Muñoz-Carpena, R. (2009). "WinGAmpt: A Windows based teaching tool for Green-Ampt Infiltration for Unsteady Rainfall Model." Agricultural and Biological Engineering Department, University of Florida, Gainesville, FL.

Pilgrim, D. H. (1966). "Radioactive tracing of storm runoff on a small catchment II. Discussion of results." *Journal of Hydrology*, 4, 306-326.

Pilgrim, D. H. (1976). "Travel times and nonlinearity of flood runoff from tracer measurements on a small watershed." *Water Resources Research*, 12(3), 487-496, doi:10.1029/WR012i003p00487.

Planchon, O., Silvera, N., Gimenez, R., Favis-Mortlock, D., Wainwright, J., Bissonnais, Y. L., and Govers, G. (2005). "An automated salt-tracing gauge for flow-velocity measurement." *Earth Surface Processes and Landforms*, 30(7), 833-844, doi:10.1002/esp.1194.

Polubarinova-Kochina, P. (1962). "Theory of groundwater movement." Princeton University Press, Princeton, NJ.

Ponce, V. M. (1991). "Kinematic wave controversy." *Journal of Hydraulic Engineering*, 117(4), 511-525.

Prickett, T. A., Naymik, T. G., and Lonnquist, C. G. (1981). "A random walk solute transport model for selected groundwater quality evaluations." Illinois Water Survey Bulletin 65,Champaign, Illinois, USA, 68.

Raffel, M., Willert, C. E., and Kompenhans, J. (1998). *Particle image velocimetry: A practical guide*, Springer.

Richardson, J. R., and Julien, P. Y. (1994). "Suitability of simplified overland flow equations." *Water Resources Research*, 30(3), 665-671.

Riggs, H. C. (1976). "A simplified slope-area method for estimating flood discharges in natural channels." *Journal of Research of the U S Geological Survey*, 4(3), 285-291.

Roels, J. M. (1984). "Flow resistance in concentrated overland flow on rough slope surfaces." *Earth Surface Processes and Landforms*, 9(6), 541-551, doi:10.1002/esp.3290090608.

Rose, C. (1993). "Erosion and sedimentation." Hydrology and Water Management in the Humid Tropics, M. Bonnell, M. M. Hufschmidt, and J. S. Gladwell, eds., Cambridge University Press, Cambridge, 301-343.

Rose, C. W., Coughlan, K. J., Ciesiolka, C. A. A., and Fentie, B. (1997). "Program GUEST (Griffith University Erosion System Template)." A New Soil Conservation Methodology and Application to Cropping Systems in Tropical Steeplands, K. J. Coughlan and C. W. Rose, eds., ACIAR Technical Report, 34-38.

Rouhipour, H., W. Rose, C., Yu, B., and Ghadiri, H. (1999). "Roughness coefficients and velocity estimation in well-inundated sheet and rilled overland flow without strongly eroding bed forms." *Earth Surface Processes and Landforms*, 24(3), 233-245, doi:10.1002/(sici)1096-9837(199903)24:3<233::aid-esp949>3.0.co;2-t.

Rubin, H., Glass, J. P., and Hunt, A. A. (1976). "Analysis of storm water seepage basins in peninsular Florida." Publication No. 39, Florida Water Resources Research Center, University of Florida, Gainesville, FL.

Saghafian, B., and Julien, P. (1995). "Time to equilibrium for spatially variable watersheds." *Journal of Hydrology*, 172(1-4), 231-245.

Saghafian, B., Julien, P. Y., and Rajaie, H. (2002). "Runoff hydrograph simulation based on time variable isochrone technique." *Journal of Hydrology*, 261(1–4), 193-203, doi:10.1016/s0022-1694(02)00007-0.

Sansalone, J. J., Koran, J. M., Smithson, J. A., and Buchberger, S. G. (1998). "Physical characteristics of urban roadway solids transported during rain events." *Journal of Environmental Engineering*, 124(5), 427-440.

Sartor, J. D., Boyd, G. B., and Agardy, F. J. (1974). "Water pollution aspects of street surface contaminants." *Journal (Water Pollution Control Federation)*, 46(3), 458-467.

Shaw, S. B., Walter, M. T., and Steenhuis, T. S. (2006). "A physical model of particulate wash-off from rough impervious surfaces." *Journal of Hydrology*, 327(3), 618-626.

Sheridan, J. M. (1994). "Hydrograph time parameters for flatland watersheds." *Transactions of the ASAE (American Society of Agricultural Engineers)*, 37(1), 103-113.

Sheridan, J. M., Merkel, W. H., and Bosch, D. D. (2002). "Peak rate factors for flatland watersheds." *Applied Engineering in Agriculture*, 18(1), 65-69.

Singh, V. (1976). "Derivation of time of concentration." *Journal of Hydrology*, 30(1-2), 147-165.

Singh, V. P., and Aravamuthan, V. (1995). "Accuracy of kinematic wave and diffusion wave approximations for time-independent flows." *Hydrological Processes*, 9(7), 755-782.

Singh, V. P. (1996). *Kinematic wave modeling in water resources: surface-water hydrology*, Wiley-Interscience.

Singh, V. P., Jain, S. K., and Sherif, M. M. (2005). "Errors of kinematic wave and diffusion wave approximations for time-independent flows with infiltration and momentum exchange included." *Hydrological Processes*, 19(9), 1771-1790.

Smedt, D. F., Yongbo, L., and Gebremeskel, S. (2000). "Hydrologic modeling on a catchment scale using GIS and remote sensed land use information." *Risk Analysis II*, 295-304.

Smith, A. A., and Lee, K. (1984). "The rational method revisited." *Canadian Journal of Civil Engineering*(11), 854-862.

Smith, J. M. W. (1991). "Sediment transport in shallow flow on an impervious surface," University of Virginia.

Su, D. H., and Fang, X. (2004). "Estimating traveling time of flat terrain by 2-dimensional overland flow model " *Shallow Flows*, G. Jirka and W. Uijttewaal, eds., Balkema, Roterdam, The Netherlands, 623-625.

Tatard, L., Planchon, O., Wainwright, J., Nord, G., Favis-Mortlock, D., Silvera, N., Ribolzi, O., Esteves, M., and Huang, C. H. (2008). "Measurement and modelling of high-resolution flow-velocity data under simulated rainfall on a low-slope sandy soil." *Journal of Hydrology*, 348(1–2), 1-12, doi:10.1016/j.jhydrol.2007.07.016.

Tauro, F., Aureli, M., Porfiri, M., and Grimaldi, S. (2010). "Characterization of buoyant fluorescent particles for field observations of water flows." *Sensors*, 10(12), 11512-11529.

Tauro, F., Grimaldi, S., Petroselli, A., Rulli, M. C., and Porfiri, M. (2012a). "Fluorescent particle tracers in surface hydrology: a proof of concept in a semi-natural hillslope." *Hydrol. Earth Syst. Sci.*, 16(8), 2973-2983, doi:10.5194/hess-16-2973-2012.

Tauro, F., Pagano, C., Porfiri, M., and Grimaldi, S. (2012b). "Tracing of shallow water flows through buoyant fluorescent particles." *Flow Measurement and Instrumentation*, 26, 93-101, doi:http://dx.doi.org/10.1016/j.flowmeasinst.2012.03.007.

Taylor, T. D. (1983). "Computational methods for fluid flow." Springer-Verlag, New York, 358 p.

Thomas, W. O., Monde, M. C., and Davis, S. R. (2000). "Estimation of time of concentration for Maryland streams." *Transportation Research Record*, 1720, 95-99.

Thompson, D. B., Cleveland, T. G., Copula, D. B., and Fang, X. (2008). "Loss-rate functions for selected Texas watersheds." *FHWA/TX-08/0-4193-6*, Texas Department of Transportation.

Tilahun, S., Guzman, C., Zegeye, A., Engda, T., Collick, A., Rimmer, A., and Steenhuis, T. (2012). "An efficient semi-distributed hillslope erosion model for the sub humid Ethiopian Highlands." *Hydrology and Earth System Sciences Discussions*, 9(2), 2121-2155.

Tilahun, S., Mukundan, R., Demisse, B., Engda, T., Guzman, C., Tarakegn, B., Easton, Z., Collick, A., Zegeye, A., and Schneiderman, E. (2013). "A saturation excess

erosion model." *Transactions of the ASABE*, 56(2), 681-695.

Tingwu, L., Xia, W., Zhao, J., Liu, Z., and Zhang, Q. (2005). "Method for measuring velocity of shallow water flow for soil erosion with an electrolyte tracer." *Journal of Hydrology*, 301(1–4), 139-145, doi:10.1016/j.jhydrol.2004.06.025.

USACE. (2000). "HEC-HMS hydrologic modeling system, user's manual (version 2.0)." U.S. Army Corps of Engineers, Hydrologic Engineering Center, Davis, CA.

Valdes, J. B., Fiallo, Y., and Rodriguez, I. (1979). "A rainfall- runoff analysis of the geomorphologic IUH." *Water Resources Research*, 15(6), 1421-1434.

Van der Molen, W. H., Torfs, P. J. J. F., and de Lima, J. L. M. P. (1995). "Water depths at the upper boundary for overland flow on small gradients." *Journal of Hydrology*, 171(1-2), 93-102.

Ventura Jr, E., Nearing, M. A., and Norton, L. D. (2001). "Developing a magnetic tracer to study soil erosion." *CATENA*, 43(4), 277-291, doi:http://dx.doi.org/10.1016/S0341-8162(00)00149-1.

Weitbrecht, V., Kühn, G., and Jirka, G. H. (2002). "Large scale PIV-measurements at the surface of shallow water flows." *Flow Measurement and Instrumentation*, 13(5–6), 237-245, doi:http://dx.doi.org/10.1016/S0955-5986(02)00059-6.

Weyman, D. R. (1973). "Measurements of the downslope flow of water in a soil." *Journal of Hydrology*, 20(3), 267-288, doi:http://dx.doi.org/10.1016/0022-1694(73)90065-6.

Wong, T. S. W. (1996). "Time of concentration and peak discharge formulas for planes in series." *Journal of Irrigation and Drainage Engineering*, 122(4), 256-258.

Wong, T. S. W. (2005). "Assessment of time of concentration formulas for overland flow." *Journal of Irrigation and Drainage Engineering*, 131(4), 383-387.

Woolhiser, D. A., and Liggett, J. A. (1967). "Unsteady one-dimensional flow over a plane-the rising hydrograph." *Water Resources Research*, 3(3), 753-771.

Yates, P., and Sheridan, J. M. (1973). "Flow measurement of low-gradient streams in sandy soils." *Proc. of Int. Symp. on Hydrometry*, Koblez, Germany, United Nations Education Scientific and Cultural Organization--World Meteorological Organization--International Association of Hydrological Sciences, v.1, 345-352.

Yeh, G. T., Cheng, H. P., Cheng, J. R., Lin, H. C. J., and Martin, W. D. (1998). "A numerical model simulating water flow and contaminant and sediment transport in watershed systems of 1-D stream-river network, 2-D overland regime, and 3-D subsurface media (WASH123D: Version 1.0)." *Technical Report CHL-98-19*, U.S. Army Corps of Engineers.

Yen, B. C. (1982). "Some measures for evaluation and comparison of simulated models." Urban Stormwater Hydraulics and Hydrology, Proc. 2nd Int. Conf. on Urban Storm Drainage, B. C. Yen, ed., Water Resources Publications, Littleton, Colo., 341-349.

Yen, B. C., and Chow, V. T. (1983). "Local design storms: Vol III." *H 38 FHWA-RD-82/065*, U. S. Dept. of Transportation, Federal Highway Administration, Washington, D. C.

Yu, Y. S., and McNown, J. S. (1963). "Runoff from impervious surfaces." *2-66*, University of Kansas, Lawrence, Kansas, 30.

Yu, Y. S., and McNown, J. S. (1964). "Runoff from impervious surfaces " *Journal of Hydraulic Research*, 2(1), 3-24.